Protective Films on Molten Magnesium

Kari Aarstad

May 2004

Thesis submitted in partial fulfilment of the requirements for the degree Doktor Ingeniør

Norwegian University of Science and Technology
Department of Materials Technology

Preface

This work has been carried out at the Norwegian University of Science and Technology (NTNU). It has been funded by the Norwegian Research Council and Norsk Hydro.

I will express my gratitude to my supervisor, professor Thorvald A. Engh for all his enthusiasm, help and guidance through this work.

I would also like to thank Dr. Gabriella Tranell and everyone that worked with the IMA project at SINTEF for good cooperation. Dr. Martin Syvertsen has provided invaluable help far beyond the limits of the IMA project. I also take the opportunity to thank Håvard Gjestland at Norsk Hydro for giving me useful information from an industrial point of view. Jan Martin Eriksen is acknowledged for his contribution through his project work and diploma thesis.

The following persons have been of assistance in different ways: Morten Raanes for microprobe analysis, and the discussion of the results. Per Ola Grøntvedt at SINTEF for good cooperation on the hot stage, Dr. Jo Fenstad for putting at my disposal the furnace used in the solubility experiments in Chapter 4 and Dr. Ulf Södervall at Chalmers University of Technology for taking time to discuss the SIMS results with me. Dr. Kai Tang at SINTEF is thanked for assistance with the thermodynamic calculations in FactSage. Also thanks to Jan Arve Båtnes and Bjørn Olsen with team for valuable technical assistance.

My colleagues at the Department of Material Technology and SINTEF Material Technology are thanked for creating a pleasant working environment. In particular Anne Kvithyld who has become a very dear friend through these years.

I will express my gratitude to my parents, Eli and Nils, for all their help. Finally, to Ole Kristian and Torstein: Thank you so much for all the joy and support you give me.

Parts of chapters 3 and 4 have already been published:

Aarstad, K, Syvertsen, M and Engh, T A (2002) Solubility of Fluorine in Molten Magnesium *Magnesium Technology 2002*, TMS, ed. Howard I Kaplan pp. 39-42.

Aarstad, K, Tranell, G and Engh, T A (2003) Various Techniques to Study the Surface of Magnesium Protected by SF_6 *Magnesium Technology 2003* TMS, ed. Howard I Kaplan pp.5-10.

Trondheim, May 2004
Kari Aarstad

Abstract

Molten magnesium will oxidize uncontrollably in an atmosphere of air. To inhibit this, a protective gas is used to cover the melt. The gas most commonly used today is SF_6. Fluorine is known to be the active component of the gas. There is a major problem with SF_6, and that is that it has a strong Global Warming Potential (GWP). The GWP of SF_6 is 23 900 times that of CO_2.

The aim of the present work is to understand the mechanism of the protection of molten magnesium. Hopefully, this allows us to find less problematic alternatives to the use of SF_6 gas.

The present work was performed with three different experimental units:
- A furnace was especially built to expose molten magnesium to various atmospheres.
- A hot stage made it possible to study the surface of the molten or solid sample under the microscope at high temperature with SF_6 or with other gases in the atmosphere.
- Finally, the solubility of fluorine in magnesium was measured at temperatures from 700°C to 950°C.

To obtain a basic knowledge of magnesium melt protection, molten magnesium was exposed to various combinations of gases. Both SF_6 and SO_2 in air protects molten magnesium well from oxidation. It is also known that pure CO_2 has a protective effect. In these experiments, it was tested whether SF_6 and SO_2 in other carrier gases than air will be protective. Nitrogen, argon and CO_2 were used as carrier gases. Also, air was added to CO_2 to see how much air the CO_2 can contain and still be protective. An important conclusion for SF_6 and SO_2 is that air is necessary to build a protective film on the melt surface. Inert gases like nitrogen and argon will obviously not oxidize the metal, but since no film forms on the melt, the metal will keep on evaporating. A CO_2 atmosphere can contain at least 20% air, and still be protective. Problems employing CO_2, are that the metal surface gets discolored, which is at least a cosmetic problem, and that C may be introduced into the metal, which may give corrosion problems.

The hot stage placed under an optical microscope made it possible to observe the magnesium sample as it was heated under an atmosphere of SF_6 in air, pure CO_2 and 1% SO_2 in air. The samples were held at temperatures from 635°C to 705°C for varying holding times. The partial pressure of SF_6 was varied between 0.5 and 5%. The samples produced were excellent for further studies with Transmission Electron Microscope (TEM), Field Emission Scanning Electron Microscope (FE-

SEM), microprobe and Focused Ion Beam Milling (FIB). The examinations showed that a thin, dense film was formed. Magnesium fluoride particles formed on the interface between the metal and the oxide film in some cases. It is suggested that then the magnesium oxide is saturated with fluorine. The fluorine diffuses through the oxide layer and forms magnesium fluoride at the interface between MgO and Mg. In other cases, it is seen that a matrix rich in fluorine forms in between larger oxide grains. Combinations of these two situations are also seen.

Proposed explanations for the protective behavior of SF_6 are:
-the formation of a second phase, that is magnesium fluoride, which helps to give a Pilling-Bedworth ratio close to one.
-the formation of a MgO matrix containing F.

The thickness of the films formed with SF_6 is found to be proportional to the square root of time. The proportionality constant depends on temperature and the partial pressure of SF_6 in the gas.

Samples in CO_2 heated above the melting point did not keep their initial shape. The films formed with CO_2 are probably therefore not as strong as the films formed in SF_6 since these samples managed to keep their initial shape even after they had melted. The surfaces after exposure to CO_2 were black and uneven. Formation of $MgCO_3$ has not been confirmed in this work. Also thermodynamic calculations indicated that $MgCO_3$ does not form.

It was not possible to tell experimentally whether the sulphur found in the samples exposed to SO_2 is bound as magnesium sulphide or magnesium sulphate or even dissolved in MgO, although it may look like two different phases are present with a slightly different sulphur content. Thermodynamic calculations do not indicate that $MgSO_4$ should form.

It was considered to introduce fluorine directly into the melt as an alternative to the use of SF_6. In this case formation of MgF_2 would limit the content of fluorine in the molten magnesium. Therefore, the solubility of fluorine in molten magnesium has been studied by melting magnesium in a magnesium fluoride crucible. Samples were taken at various temperatures from 700°C up to 950°C. Three different analytical methods were employed to measure the fluorine content: The Sintalyzer method, Glow Discharge Mass Spectrometry (GD-MS) and Secondary Ion Mass Spectrometry (SIMS). The various analytical methods did not all give the same results. However, it is suggested that the SIMS results are the most reliable. The value for the dissolution of fluorine, $1/2\ F_2\ (g) = \underline{F}$ (in mass%) is then:

$\Delta G°_3/2 = (- 329\ 000 \pm 65\ 000) - (83 \pm 64)T$

ΔG^o for the equilibrium between magnesium and magnesium fluoride, $MgF_2 = Mg\ (l) + 2\underline{F}$ is found to be:

$\Delta G^o = (471\ 000 \pm 131\ 000) - (350 \pm 130)\ T$

Iron is found to have no effect on the solubility of fluorine in molten magnesium.

The solubility of fluorine does not seem to be sufficiently high for direct dissolution of fluorine into the melt to be an alternative to SF_6.

Contents

Chapter 1 .
Literature Survey of Protection of Molten Magnesium

MAGNESIUM

Magnesium is one of the light metals. Its density is 1.7 g/cm^3 [Aylward and Findlay, 1974]. This is low compared to other commercial metals. Commonly used metals like aluminum and steel have densities of 2.7 g/cm^3 and 7.9 g/cm^3 respectively. Pure magnesium has low strength and is therefore not used for constructional purposes [Solberg,1996]. Alloyed magnesium on the other hand, has a high strength-to-weight ratio [Leontis, 1986] compared to other metals. It is therefore possible to save weight by replacing parts made of steel or aluminum, by magnesium, without reducing the strength significantly. Of course changes regarding the design may have to be carried out to compensate for the lower strength of magnesium [Metals Handbook, 1979] and this may again lead to an increase in volume. Still, the overall result is a decrease in weight for the component. Parts that are not exposed to strain like the steering wheel on a car can be made of magnesium without changing the original design. Other examples of components that are made of magnesium are cellular phones, lap-top computers and car components like gearbox housings, dashboard mounting brackets and seat components.

Magnesium has a melting point of 650°C and is the eighth most abundant element at the earth's crust [Emley, 1966]. Seawater has a magnesium content of

0.13% which means that one liter of seawater contains 1.3 gram magnesium. Thus the magnesium industry should never experience a shortage of raw materials. Other raw materials worth mentioning are magnesite ($MgCO_3$) and dolomite ($MgCO_3 \cdot CaCO_3$) [Thonstad, 1997]. The production of magnesium in Porsgrunn, Norway was based on dolomite and seawater. From the raw materials, magnesium chloride was produced through a chlorination process. Magnesium was then produced by electrolysis of the magnesium chloride.

IMA (International Magnesium Association) and Norsk Hydro have estimated the world's demand of magnesium in the year 2000 to be 360 000 tons. Figure 1.1 shows that in 1998, 43% of the magnesium produced was used as an alloying component in aluminum. A large part, 31%, goes to die casting.

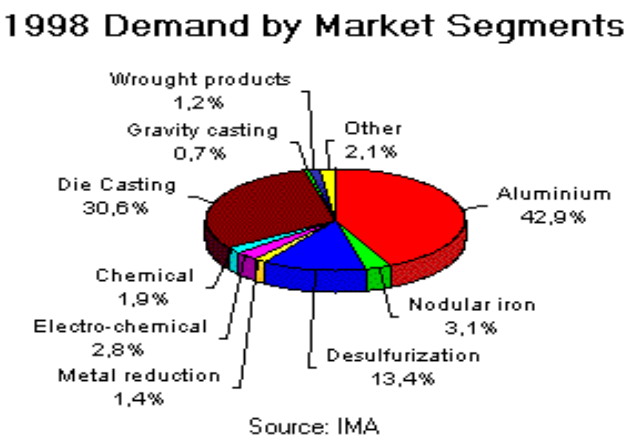

Figure 1.1 The various uses of magnesium. [Hydro Magnesium home page, 2000]

In Table 1.1, the physical properties of magnesium and various magnesium compounds are presented. The values for $\Delta G°_f$ are given for the formation of the compounds from standard states at 25°C. The values vary in different data collections, but the values presented here are taken from SI Chemical Data [Aylward and Findlay, 1974]. It would have been an advantage to give the densities at 700°C. It is possible to calculate densities by extrapolation from room temperature. However, experience indicates that such results may not represent a significant improvement. The room temperature densities have been used in the calculation of the data in Table 1.2.

Table 1.1: Physical properties of magnesium and magnesium compounds [Aylward and Findlay, 1974, Emley*, 1966]. d=decompses

Compound	Molar mass (g/mole)	Melting point (°C)	Density (g/cm^3) 25°C	$\Delta H°_f$ (kJ/ mol)	$\Delta G°_f$ (kJ/ mol)	ΔH_m (kJ/ mol)
Mg (s)	24.3	650	1.7	0	0	9
Mg (l)			1.58*			
MgF_2	62.3	1396	3.0	-1123	-1070	58
MgO	40.3	2800	3.6	-601	-570	77
$MgSO_4$	120.4	d1124	2.7	-1288	-1171	15
MgS	56.4	d>2000	2.8	-346	-342	
$MgCO_3$	84.3	d350	3.1	-1096	-1012	
Mg_3N_2	101.0	d800	2.7	-461	-401	

THE PROBLEM WITH OXIDATION

It is a well-known fact that molten magnesium will oxidize very rapidly when left exposed to air. Even with infinitesimal amounts of oxygen in the atmosphere, molten magnesium will oxidize. The calculations performed with FactSage in Appendix 1 show that at 700°C, a partial pressure of oxygen of $5 \cdot 10^{-54}$ or higher will give oxidation of magnesium. Thus, thermodynamically, it should not be possible to prevent oxidation of the magnesium.

Below 450°C, when magnesium is still solid, oxidation of the metal is not a problem. The oxide layer formed on the metal is protective, and the oxidation rate is nearly parabolic. However, at higher temperatures, that is from 475°C, the film becomes porous and is no longer protective. The oxidation rate is then linear with time. The metal will be oxidized until it is all consumed [Kubaschewski and Hopkins, 1953, Gregg and Jepson, 1958-1959, Gulbransen, 1945]. Above magnesium's ignition temperature, which is 623°C [Kubaschewski and Hopkins, 1953], the magnesium will burn uncontrollably in air. Obviously, this be prevented. The most common solution today is to cover the magnesium-melt with a protective gas; both SF_6 and SO_2 are used in magnesium melting-plants and foundries. There are, however, problems connected to the use of these gases. SF_6

has a very strong greenhouse-potential, which means that it contributes to the global warming of the earth. SO_2 is toxic, and it is also corrosive to the surroundings inside the plant.

The Pilling-Bedworth ratio, which is the volume ratio between a metal's oxide and the metal itself, may be employed to determine whether an oxide film will be protective or not. The idea behind is as follows:
If the oxide/metal volume ratio is less than one, the oxide will not be able to cover the entire metal surface, and the oxide film is therefore non protective. If, on the other hand, the volume ratio is higher than one, the film will cover the surface and be protective. The ratio is of limited validity. Partly the reason should be that in the, the bulk densities for the compound in the layer and for the metal are employed. However, the surface properties are different from the bulk. Also, it is not taken into account that there may be some re-alignement of the atoms at the surface. Therefore, the Pilling Bedworth ratio seems to be valid for metals with a simple atomic structure such as the alkali and alkali earth metals, but not for metals with a complex structure such as Ti, Nb and Ta.

It has been assumed that it is relevant to employ an average Pilling Bedworth ratio when two separate phases form, for instance MgO and MgS. This procedure breaks down if mixtures form, e.g. Mg-Ca-O, Mg-Be-O and Mg-Zr-O.

Table 1.2 presents Pilling-Bedworth ratios for compounds that are of interest regarding protection of molten magnesium. All the gases that are known to be protective, that is SF_6, SO_2 and CO_2, have favorable Pilling-Bedworth ratios assuming they form MgF_2, MgS or $MgSO_4$, or $MgCO_3$ respectively, in contact with magnesium.

Table 1.2: Pilling-Bedworth ratios for compounds [Kubaschewski and Hopkins, 1953, or calculated with numbers from Aylward and Findlay, 1974].

Compound	Pilling-Bedworth ratio
MgO	0.81
MgF_2	1.45
$MgSO_4$	3.2
MgS	1.4
$MgCO_3$	1.6
Mg_3N_2	0.89
CaO	0.64
BeO	1.68
ZrO_2	1.56
Al_2O_3	1.28

Magnesium's high vapor pressure is a problem as the metal will evaporate unless a protective film is formed on top of the melt. It is therefore not possible to prevent oxidation of magnesium by using an inert atmosphere. Gulbransen [1945] found that films that protect the melt from evaporation also inhibit oxidation of the metal.

It has been proposed that when the oxide film is thin, forces only act in two directions along the surface, and the film is strong enough to withstand these tensile forces [Czerwinski, 2003]. The problems start when forces start acting in three directions.

PROTECTIVE GAS MIXTURES

It is important to determine if a metal, solid or liquid, will react with its surroundings in such a way that a protective layer is created. Protective here means that the layer is thin and ceases to grow further. An example is aluminum oxide on aluminum. A protective layer on molten magnesium should also prevent evaporation. It seems to be reasonable to assume that the reaction products are protective if they -on reacting with a metal atom on the surface- give a product with the same volume, or slightly higher than the metal atom. For instance, the volume ratio for $AlO_{1.5}$/Al is 1.28. As mentioned, if the Pilling Bedworth ratio is less than one, the surface is not covered and the reaction does not stop. If the ratio is much greater than one, stress build up in the film, and the film may crack.

To study the effect of protective gas mixtures, the FactSage consortium thermochemical database has been used [FactSage 5.0]. The following solution species have been taken into account [Tang, 2004]:
1) Liquid light metal (Mg-F-C-O)
2) Liquid salt (Mg/F, O, S)
3) Liquid slag (MgO-MgF_2-MgS-$MgSO_4$)
4) Ideal gas mixture (47 gaseous species)

Magnesium nitrides are not included in the calculations. The reason is that nitrogen is known to react slowly with Mg. Thus, one can not expect magnesium nitrides to be at equilibrium. Liquid salts and slags are not stable under the conditions given here. The stable solid products after the different reactions are magnesium sulphide, magnesium oxide, carbon and magnesium fluoride.

In Figure 1.2, an Ellingham diagram is presented. The diagram gives the Gibb's free energy for formation of the various species in Table 1.1 as a function of temperature. The data used in this diagram are calculated using the "Reaction" sub-program in FactSage. The values refer to the formation from the elements, but for magnesium carbonate and sulphate, formation from CO_2 and SO_2 is assumed.

As can be seen from the Ellingham diagram, magnesium fluoride is the most stable compound and magnesium sulphide is more stable than magnesium sulphate.

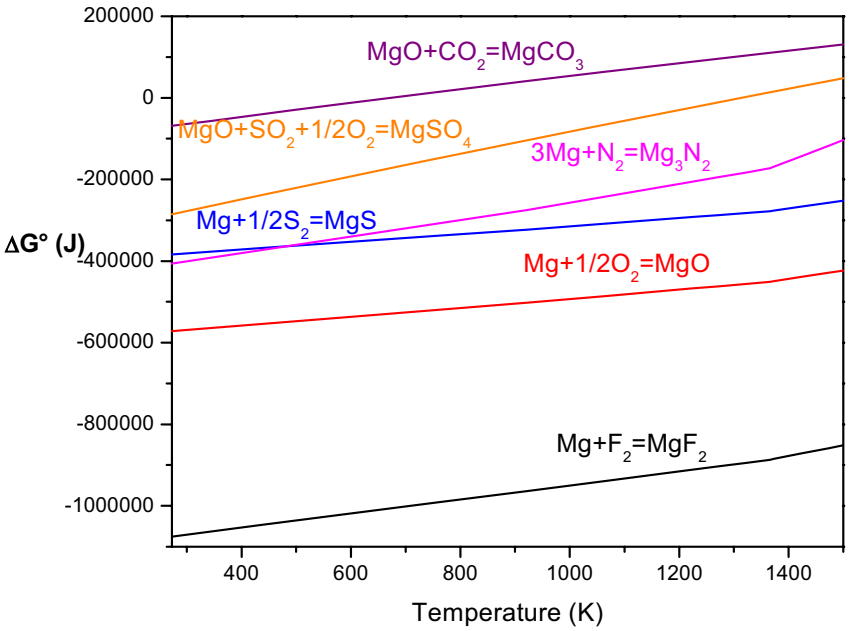

Figure 1.2 Ellingham diagram of magnesium compounds.

SF_6

SF_6 has been used as a protective gas for molten magnesium since the early 1970's [Cashion, 1998, Erickson, King and Mellerud, 1998]. At that time, the greenhouse effect was not an issue. Maiss and Brenninkmeijer [1998] state that SF_6 has a greenhouse potential 23 900 times that of CO_2 on a 100 years time horizon. The atmospheric lifetime of this gas is 3200 years, and its concentration in the atmosphere has increased by a factor 100 since the commercial production of SF_6 started in 1953. Due to the global warming potential of SF_6, taxation is introduced to restrict the consumption. It is expected that the European Union will ban HKFK gases in 2010 [Net site: Air pollution network for early warning and on-line information exchange in Europe 2003], and this will most likely also happen to SF_6 sooner or later.

Fruehling [1970] was not aware of the greenhouse problem when he wrote his thesis. He stated that SF_6 is a non-toxic gas to humans, which is agreed upon also by Maiss and Brenninkmeijer [1998].

Gaseous by-products

Fruehling [1970] considered the possibility that SF_6 can break down into SF_4 and S_2F_{10} that are highly toxic gases, but he did not register any toxic decomposition products during his measurements at 810°C. Hanawalt [1972] also mentions that SF_6 is non-toxic, while the decomposition product SF_4 is toxic and S_2F_{10} extremely toxic. However, S_2F_{10} is not stable in the high temperature area where magnesium is molten. SF_4 is very reactive, and will therefore react the moment that it is formed.

Couling, Bennett and Leontis [1977] analysed the gas above a melt protected with SF_6. The gas samples were taken from the pot-room. They were not able to detect any toxic breakdown products above the melt. During the experiments, special measurements were performed to check if there was any toxic HF in the atmosphere inside the furnace, but no HF was detected. The conclusion of these studies is that there were no toxic gases in the breathing zones of the operators. In a different study, Couling and Leontis [1980] again checked the atmosphere above the melt for HF. This time they detected HF at the ppm-level (parts per million). At 705°C, the concentration of HF was 30-40 ppm. The concentration of HF depended on the temperature and the presence of flux. The fact that they detected HF inside the furnace did not mean that the operators were exposed to HF. Measurements carried out in the operators breathing zone indicated that the HF-concentration outside the furnace was below 1 ppm.

Hanawalt [1972] found that SO_2 was formed when magnesium was protected with SF_6, and that the formation depended on the concentration of SF_6 in the gas mixture. At concentrations of SF_6 lower than 0.1%, no detectable SO_2 was formed. However, at a concentration of 3% SF_6, 0.3% SO_2 was detected above the melt under stirring. These experiments were performed at 665°C. Additional weak peaks were also found in the mass spectra, but it was not determined which gases they belonged to.

A more recent study [Bartos et al. 2003] concentrates on the decomposition of SF_6. The decomposition was found to be 10% on an average, increasing during casting and feeding, and decreasing in quiet periods. SO_2 and HF were the only gaseous by-products detected at temperatures from 653 to 658°C. The concentrations of these species remained in the order of 20 ppm as a total. It was therefore concluded that most of the decomposition occurs at the melt surface with hardly any gaseous by-products.

Table 1.3 presents the decomposition products of SF_6 at 700°C. The calculations are performed in FactSage, starting with one mole SF_6. The pressure of SF_6 is set to 0.01 bar since 1% SF_6 in air is a common gas mixture. Only a small fraction of

the gas decomposes. It is however possible that these decomposition products will react further, either with magnesium to form magnesium fluoride, or with other gaseous compounds, like for example humidity in the air to form HF.

Table 1.3: Decomposition products when 1 mole SF_6 decomposes at 700°C, pressure of 0.01 bar

Decomposition products
$1.5 \cdot 10^{-4}$ mole F
$7.7 \cdot 10^{-5}$ mole SF_4
$1.0 \cdot 10^{-6}$ mole SF_5
$4.3 \cdot 10^{-8}$ mole F_2

The reaction product between SF_6 and molten magnesium

To study the film formed between molten magnesium and SF_6, different methods can be applied to produce samples.

By first melting magnesium, and then scraping off the initial film, Cashion [1998] exposed fresh magnesium to the desired atmosphere. The furnace where the melting took place had to contain the correct atmosphere when the experiment started. The sample was lowered into a quenching zone when the experiment was finished. X-ray photoelectron spectroscopy (XPS) was used to analyze the samples, and it indicated that MgO and MgF_2 were present in the films formed. He was not able to detect any sulphur.

Walzak et al. [2001] have used a different method to study the initial reaction product between molten magnesium and SF_6. 1% SF_6 in dry air is bubbled through molten magnesium, followed by rapid quenching of the crucible containing the metal. They assume that the interface formed between the metal and the gas bubbles is the same film which is formed when molten magnesium is protected with SF_6 during handling and casting. The sample must be cut to expose the gas bubbles so that they can be studied in SEM/EDX and with laser Raman spectroscopy. On the surfaces inside the voids formed, magnesium, oxygen and fluorine was found. Walzak et al. [2001] found an association between carbon and oxygen, and between magnesium and fluorine. The surfaces

appeared to consist of a layer of magnesium oxide containing fluorine overlaid with small magnesium oxide particles. Sulphur was found not to be connected to the fluorine.

Pettersen et al. [2002] have studied films formed under SF_6 atmospheres using X-ray diffraction (XRD), electron probe microanalysis (EPMA) and transmission electron microscopy (TEM). The film formed after 5 minutes exposure was about 100 nm thick and it appears to be dense. MgO is the only phase found according to the diffraction pattern produced in TEM, but microprobe analysis also shows that the film contains a considerable amount of fluorine in addition to magnesium and oxygen. Figure 1.3 shows a TEM micrograph of the film. Sulphur was not found in this film.

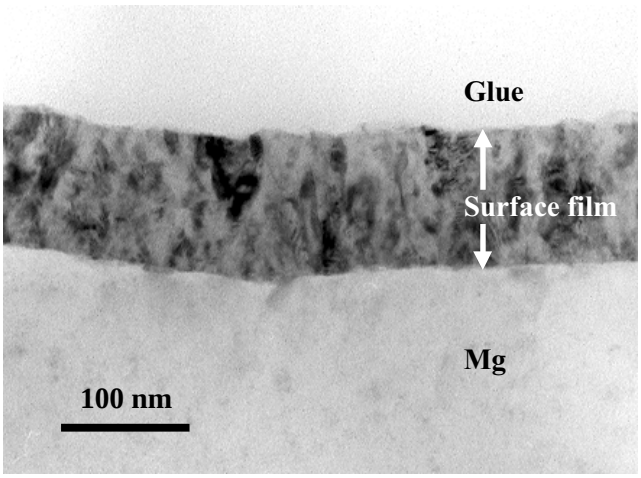

Figure 1.3 The micrograph shows the film formed on magnesium after 5 minutes exposure to 1% SF_6 in air at 700°C. Pettersen et al. [2002]

Using the computer software FactSage, it is possible to calculate which reaction products are the most thermodynamically favorable when molten magnesium is exposed to SF_6 with air as carrier gas. This is done in Figure 1.3 where the major reaction products are given. Since the ratio between the amount of gas mixture and the amount of magnesium available to react is unknown, the amount of gas introduced, given as protective gas mixture at the x-axis, is varied. The amount of magnesium is fixed. The calculations are performed for 700°C. Nitrides are not taken into account as already reasoned. It is assumed that the gas mixture enters the furnace, reacts with the liquid magnesium and then leaves the reactor.

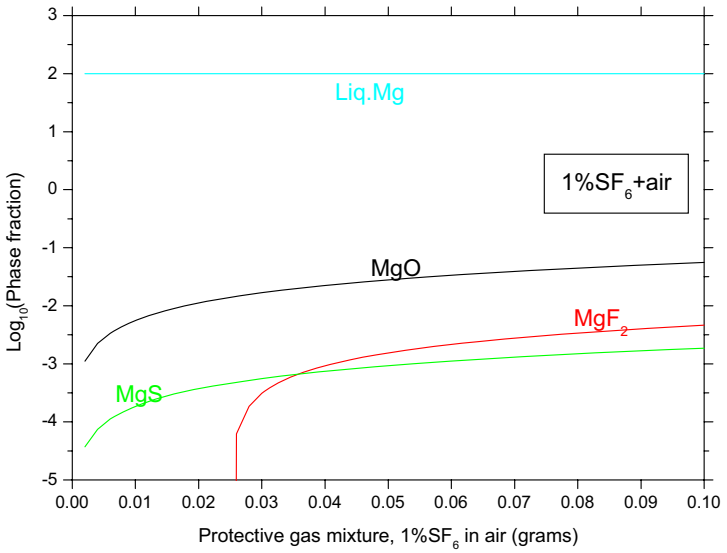

Figure 1.4 The reaction between molten magnesium and 1% SF_6 in air. The amount of gas is varied on the x-axis from 0 to 0.1 gram, while the amount of magnesium is fixed at 100 grams. Temperature is 700°C.

As can be seen from Figure 1.4, with a very small amount of gas present, compared to the amount of magnesium, only magnesium oxide and sulphide will form. No magnesium fluoride forms due to a finite solubility of fluorine in molten magnesium. However, with an increasing volume of gas available, more magnesium oxide and sulphide will form, and also magnesium fluoride after the melt is saturated with fluorine.

The amount of SF_6 needed to protect molten magnesium

SF_6 is always mixed with another gas, usually air, or air and CO_2, when used for melt protection. It is important that the gas-mixture contains enough SF_6 to give satisfactorily protection of the melt, but the level should be kept at a minimum, both to protect the environment and to reduce the costs of gas. Fruehling [1970] found that at 690°C, 0.05% SF_6 mixed with the air was enough to protect the melt. At 660°C the corresponding value was found to be 0.02%. Busk and Jackson [1980] also did some work on the lower limit of SF_6 in air. According to their paper, a volume percent of 0.02% SF_6 is sufficient to protect the molten

metal at 650°C, while at temperatures between 705°C and 815°C, the content of SF_6 should lie between 0.04 and 0.06%. In a paper by Erickson et al. [1998], the recommended amount of SF_6 is 0.04% between 650 and 705°C. Gjestland, Westengen and Plathe [1996] give exactly the same limits. They refer to the recommendations given by the International Magnesium Association.

It should be kept in mind when looking at these data, that the minimum amount of SF_6 needed given in different studies, are derived in laboratory experiments. The real amounts needed in practice are probably higher. A melting plant or a foundry will not have as ideal and controlled situations as in the laboratory.

The total consumption of SF_6 in year 2001 in the magnesium industry is 211 metric tons, which counts for 3% of the total SF_6 consumption [Smythe, 2002]. Hydro Magnesium reduced their emissions of SF_6 with 3.5 million tonnes CO_2 equivalents from 1991 to 1996. In 2002, Norsk Hydro used 0.7 kg SF_6/metric ton magnesium ingot produced in Becancour, Canada, and slightly less, 0.55 kg/ metric ton, for their remelting unit in Porsgrunn, Norway [Albright, 2002].

Proposed mechanisms

Various mechanisms have been proposed on how the SF_6 gas protects the molten magnesium. The suggested mechanisms become more detailed and specific as the experimental methods improve. Film formed on molten magnesium in air will be thick and porous and will not prevent oxidation of the underlying metal. In his thesis, Fruehling [1970] suggested that the SF_6-gas contributed to the formation of a thin, dense and continuous film of MgO. This film will not let any oxygen through, and therefore the problem with oxidation is avoided. Cashion [1998] gave a different explanation in his work. He suggested that the SF_6-gas helps the "wetting" of the magnesium surface. This means that the SF_6 gas increases the adhesion of the MgO to the magnesium surface, and a cohesive, protective film is formed so that no oxygen can reach the liquid metal. This theory is repeated by Cashion, Ricketts and Hayes [2002].

Nitrogen as carrier gas for SF_6

Performing the same calculations as was done with SF_6 in air, Figure 1.5 gives the reaction products when molten magnesium is exposed to a gas mixture of SF_6 and nitrogen. The same assumptions are made as for the previous calculation.

Magnesium sulphide and magnesium fluoride are the main reaction products. This fraction will increase with more gas available.

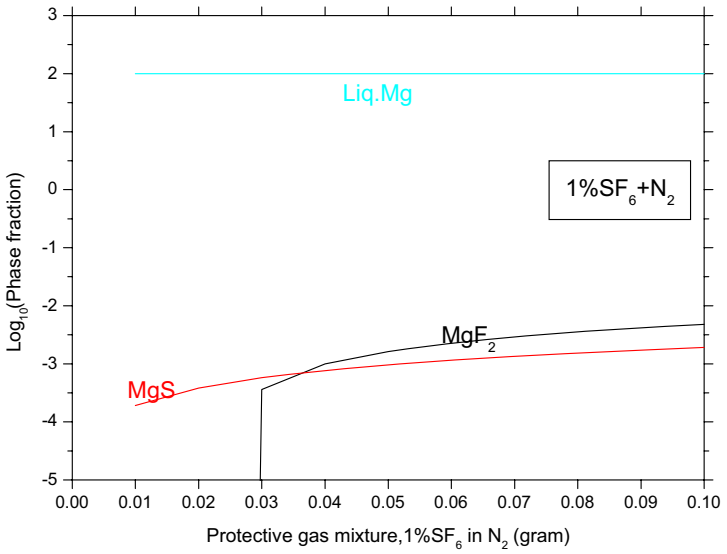

Figure 1.5 Reaction products forming when liquid magnesium reacts with 1%SF_6 in nitrogen. The amount of gas introduced is given on the x-axis. Temperature 700°C.

SO_2

As mentioned, SO_2 is poisonous to humans if inhaled [Pohanish and Green, 1996]. The long-term effects may be lung damage and mutagen. SO_2 is also a corrosive gas. This may cause problems with corrosion of equipment and material inside the building where the gas is used. In addition, SO_2 also contributes to acid rain.

The amount of SO_2 needed to protect molten magnesium

The concentrations of SO_2 in air needed to give satisfactorily protection of the melt varies considerably in the literature. Hanawalt [1972] writes in his article that the concentration of SO_2 in air has to be four or five times greater than the concentration of SF_6 to give the same protection. If a concentration of 0,04% SF_6 is used, that means that 0.2% SO_2 will protect the melt. At the other extreme, Busk and Jackson [1980] say a few percent. This is a factor ten higher than the value given by Hanawalt. Cashion [1998] refers to Loose's work [1946] on the

topic. 0.5% SO_2 will, according to his work, protect magnesium from oxidation. Aleksandrova and Roshchina [1977] have found that about 1% SO_2 in air is sufficient to form a protective film at temperatures around 700°C.

Proposed mechanisms

Aleksandrova and Roshchina [1977] state that the following reactions take place between magnesium and sulphur dioxide:

$3\ Mg + SO_2 = 2\ MgO + MgS$
$MgS + SO_2 = MgSO_4 + S_2$

In the first step, magnesium sulfide is formed. The sulfide reacts with SO_2 to give magnesium sulfate. These reactions were observed at 600°C. At 700°C the main products are magnesium oxide and sulphur. At a higher temperature, 750°C, magnesium oxide and magnesium sulfide is formed.

Kubaschewski and Hopkins [1953] have a short explanation on why SO_2 protects magnesium from oxidation. Sulfates are formed on the metal surface and the sulfates have a higher specific volume than the metal (Pilling-Bedworth ratio). This means that the sulfates can cover the metal surface completely and thereby prevent oxidation.

Performing the same calculations as was done with SF_6 in air using FactSage, gives the diagram in Figure 1.6. Only MgO and MgS are formed. Note that no magnesium sulphate is formed according to these calculations.

Looking at the decomposition of SO_2, minor amounts of SO_3, SO, S_2O and S_2 form as shown in Table 1.4. These reaction products will not likely form any other sulphur compound with magnesium than those already mentioned. The calculations are performed at 700°C with 1 mole SO_2 initially and at partial pressure of 0.01 bar.

Table 1.4: Decomposition products of 1 mole of SO_2 at 700°C, 0.01 bar partial pressure.

Decomposition product
$1.4 \cdot 10^{-6}$ mole SO_3
$1.3 \cdot 10^{-6}$ mole SO
$1.5 \cdot 10^{-8}$ mole S_2O
$7.1 \cdot 10^{-9}$ mole S_2

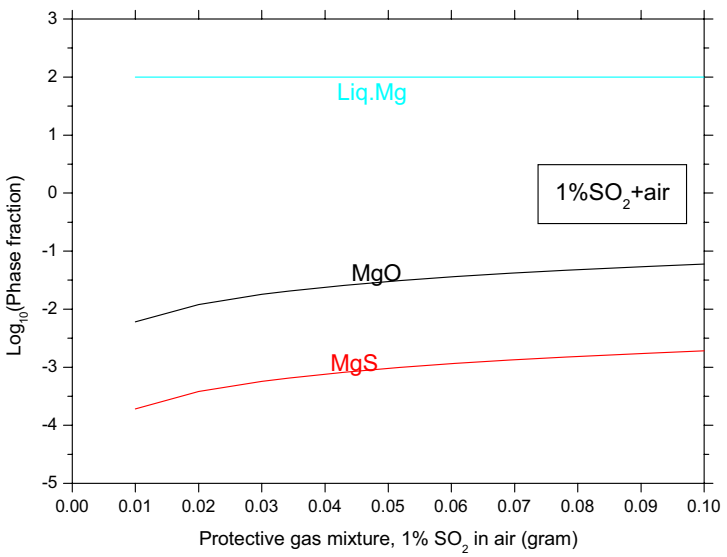

Figure 1.6 The reaction products of the reaction between molten magnesium and SO_2 in air. The amount of gas introduced is given at the x-axis, while the fraction of the reaction product is given at the y-axis. The temperature is 700°C

Nitrogen as carrier gas

Argo and Lefebvre [2003] tested nitrogen as a carrier gas instead of air in combination with SO_2. Gas mixtures with 1 and 2% SO_2 in nitrogen provided better protection than the standard air/SF_6 mixture for the particular alloy strontium tested, AJ52, which contains 5% aluminum and 2% strontium.

Figure 1.7 indicates that magnesium oxide and sulphide are the phases forming when nitrogen is used as a carrier gas for SO_2 at 700°C. No magnesium sulphate is formed. Calculations are performed with FactSage in the same way as in previous calculations.

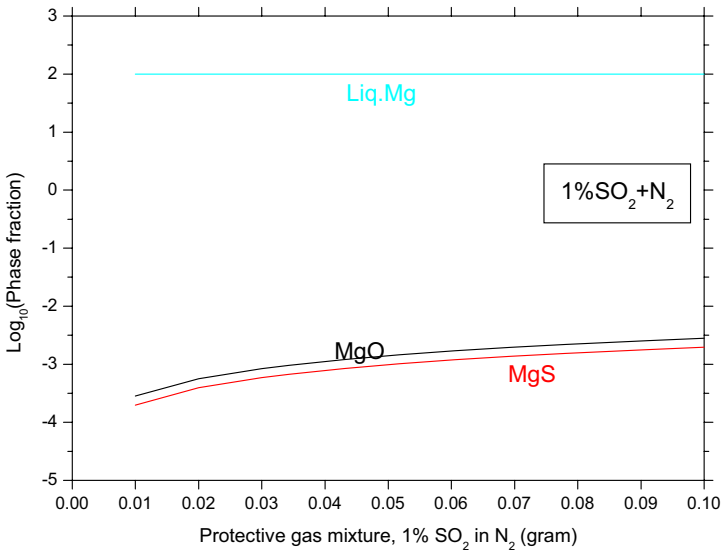

Figure 1.7 The reaction products between molten magnesium and 1%SO_2 in nitrogen at 700°C. The amount of gas introduced is given at the x-axis, while the fraction of the reaction product is given at the y-axis.

Industrial use

Norsk Hydro considers SO_2 as an acceptable alternative as long as there are no other well suited substitutes. They use a mixture of dry air and SO_2 in their remelting facilities in Bottorp, Germany and Xi'an in China, and in their research foundry in Porsgrunn, Norway [Albright, 2002]. Experiments carried out by

Norsk Hydro show that 0.5% SO_2 in air gives sufficient melt protection [Gjestland et al., 1996].

ALTERNATIVES TO SF_6 AND SO_2

So far, no real alternatives to SF_6 or SO_2 have been suggested. There are disadvantages with all the suggested solutions. Several factors have to be considered. One does not want a substance that may be toxic to the personnel working with it, or that is harmful to the environment, either inside or outside. Finally, the method used must not lead to a decline in metal quality.

CO_2

Fruehling [1970] concludes in his work that an atmosphere of pure CO_2 can protect molten magnesium perfectly well. Comparing CO_2-atmospheres to gas mixtures of air and SF_6 or SO_2, he found that pure CO_2 gave the best protection of the melt. The reaction film was smooth and metallic. After 10 minutes at 660°C the CO_2-gas was replaced with air. Breakdown of the film was registered after 6 minutes. Fruehling refers to an article by Delavault where it was observed that molten magnesium oxidizes slowly in an atmosphere of dry CO and CO_2. He also cites McIntosh and Baley's work. They did not observe ignition of magnesium when the melt was protected with flowing CO_2 at 700°C.

Aleksandrova and Roshchina [1977] have presented an equation which describes the interaction of carbon dioxide with magnesium:

$$2\ Mg + CO_2 = 2\ MgO + C$$

The equation implies that solid carbon (soot) is formed. Even if the oxidation of magnesium proceeds much more slowly in CO_2 than in air, Aleksandrova and Roshchina [1977] claim that an atmosphere of CO_2 will not protect molten magnesium against oxidation.

If one only considers CO_2 at 700°C, according to FactSage, only a minor fraction of the gas will decompose. The major decomposition products are presented in Table 1.5, assuming 1 mole CO_2 at 1 bar in the beginning.

Table 1.5: Decomposition products of 1 mole CO_2 at 700°C, 1 bar pressure.

Decomposition product
$1.0 \cdot 10^{-7}$ moles CO
$5.1 \cdot 10^{-8}$ mole O_2

In Figure 1.8, the thermodynamic calculations for the reaction between molten magnesium and CO_2 are performed. The only reaction products are MgO and carbon. No magnesium carbonate forms according to FactSage. One can see that the magnesium must be saturated with carbon before pure carbon starts forming.

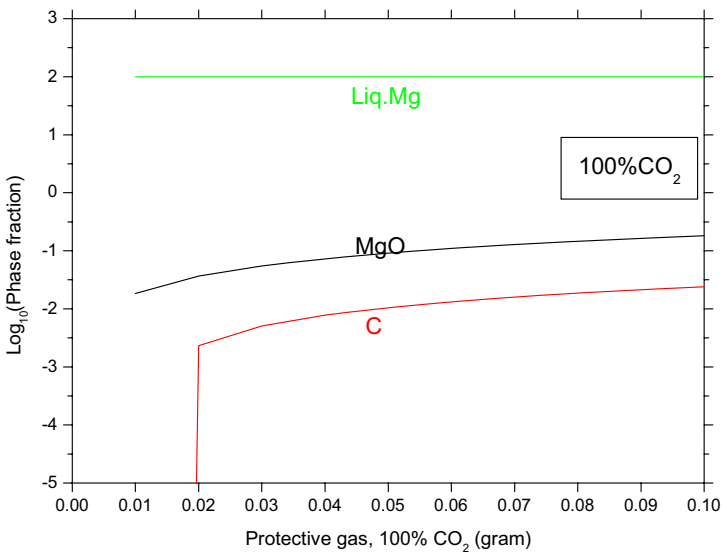

Figure 1.8 Reaction products when liquid magnesium has reacted with pure CO_2. The amount of gas introduced is given at the x-axis, while the fraction of the reaction product is given at the y-axis.

A recent paper by Bach et al. [2003] suggests the use of carbon dioxide snow instead of gaseous CO_2. It is stated that the advantage with this method is that no carbon monoxide and soot is formed.

The results regarding CO_2 are not very consistent. Not much work on CO_2 as a protective atmosphere has been carried out, and the industry needs proof that it at least works in the laboratory before they start implementing such gas in their production. If it is true that CO_2 is protective, there are some practical problems that have to be solved. As mentioned, soot may be formed at the surface. This may give a black surface on the casting, which is not desirable. There is the problem of how to close the system in order to attain an atmosphere of pure CO_2. Closing the casting system will cause problems for the operators.

Gas mixtures of air/CO_2/SF_6

Some researchers have found it advantageous to mix the SF_6-gas with both air and CO_2. Couling and Leontis [1980] claim that melt protection is improved when a mixture of air/CO_2/SF_6 is used instead of just air and SF_6. The mixture consisted of air mixed with 30 to 70% CO_2 and 0.15-0.4% SF_6. In a different paper, Couling [1979] recommends the same ratio of air and CO_2 as in the above paper. Øymo et al. [1992] chose a gas mixture of 20% CO_2, 0.2% SF_6 and dry air when they were melting magnesium scrap. Also Argo and Lefebvre [2003] declare that the addition of CO_2 to the carrier gas is advantageous, although they used a particular alloy, AJ52.

The thermodynamic calculations in Figure 1.9 show that the expected reaction products when SF_6 is used in combination with CO_2 are magnesium sulphide, oxide and fluoride.

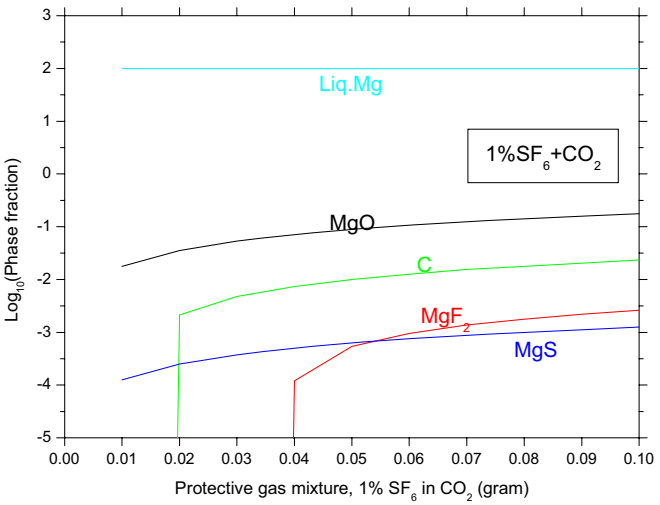

Figure 1.9 Reaction products when magnesium is exposed to 1% SF_6 in air.

It seems to be difficult to see any clear advantages of using the gas mixtures discussed above, compared to employing just a mixture of air and SF_6. It is said that addition of CO_2 improves the melt protection, but the amount of SF_6 is also increased. So if you get sufficient protection with air and 0.04% SF_6, why increase the amount SF_6 and add CO_2 to get even better protection?

Beryllium

Houska [1988] has discussed the advantages of adding beryllium to magnesium and aluminum. Beryllium prevents oxidation of the magnesium because a beryllium oxide film is formed on top of the magnesium melt. The film is formed because beryllium is more reactive to oxygen than magnesium. 0.001% Be will increase the ignition temperature for magnesium as much as 200°C. This means that you can handle molten magnesium at casting temperatures and the melt will not start burning. Spiegelberg, Ali and Dunstone [1992] have also recognized that beryllium has a positive effect on the oxidation of magnesium. It may be mentioned that the Pilling-Bedworth ratio for BeO is 1.68. In addition, beryllium will refine the melt by precipitating iron and other impurities.

Zeng et al. [2001] have performed a thorough study of the oxide film formed on a molten Mg-9Al-0.5Zn-0.3Be alloy. The oxide film is built up of two layers. One

outer layer which mainly consists of MgO, and one inner layer containing a mixture of BeO and MgO. This inner layer is said to act as a barrier to the diffusion of magnesium ions, Mg^{2+}. This alloy has a great resistance against oxidation, and it can be melted in the atmosphere without further protection.

There is obviously a disadvantage to this method. As mentioned, beryllium oxide will be formed, and the dust of the oxide is poisonous if inhaled. According to Pohanish and Greene [1996], exposure to dust of beryllium oxide may cause disease in the lymph nodes, the liver, the kidneys and the lungs. Spiegelberg et al. [1992] consider that this not to be a problem as long as the concentration of the BeO-dust in the foundry atmosphere is below the specified threshold, which is 0.002 mg/m^3 according to Pohanish and Greene [1996].

Other alloying elements

Calcium and zirconium are known to increase the ignition point of magnesium and thereby possibly prevent ignition of the molten metal [Chang et al, 1998 and Sakamoto, Akiyama and Ogi, 1997]. According to Sakamoto et al. [1997], the addition of calcium gives a CaO film on top of the melt. This layer stops oxygen from the air reaching the magnesium, and it also inhibits the strong evaporation of magnesium. The calcium oxide film is most probably formed by the reduction of MgO with calcium which is reasonable based on thermodynamical data where it can be seen that CaO is more stable than MgO. CaO has a Pilling-Bedworth ratio of 0.64 [Kubaschewski and Hopkins, 1953]. Possibly the surface layer is composed of a mixture of MgO and CaO and the Pilling Bedworth ratio calculation is difficult to apply.

Ignition can be prevented entirely with the simultaneous addition of 1.3 mass% Ca and 1.4 mass% Zr, even at temperatures higher than 810°C [Chang et al., 1998].

Flux

Before SF_6 was introduced as protection for molten magnesium, the magnesium industry used flux to inhibit oxidation. A flux is added as a powder spread out on the metal surface where it melts and gives a liquid, protective film on top of the melt. Fruehling and Hanawalt [1969] mention three disadvantages of this method. The first problem is that the flux itself oxidizes and forms a thick and hard layer. This layer may crack and expose the melt under the layer to the atmosphere. The quality of the finished casting may also be reduced because you may get flux-inclusions in the finished product. The third problem is associated to flux fumes and flux dust which can cause corrosion in a foundry.

Emley [1966] had some requirements on an ideal flux. It should have a liquidus temperature below the solidus temperature of the magnesium alloy so that at the moment the metal starts melting, the flux is liquid and able to protect the melting metal. The flux should wet the magnesium, and the fluidity of the flux has to be high enough so that it can spread out on the entire surface. Solidus temperatures for magnesium alloys can be as low as 420°C. However, a mixture of the salts $MgCl_2$, KCl and NaCl has a melting point below 400°C and may therefore protect the melt. The density of the flux has to be lower than the density of the magnesium in order not to sink to the bottom of the furnace.

Hydro fluorocarbon gases

Ricketts and Cashion [2001] suggests a hydro fluorocarbon gas as a possible replacement for SF_6. They introduce the hydro fluorocarbon gas 1,1,1,2-tetrafluoroethane, HFC-134a which has a global warming potential 18 times lower than SF_6, but still 1500 times worse than CO_2. The film formed might contain up to 50% magnesium fluoride.

In their experiments, Ricketts and Cashion used dry air, carbon dioxide and nitrogen as carrier gases, and all of them seemed to be effective. The amount of HFC-134a in the mentioned carrier gases was between 0.3 and 0.7%.

The time of protection after removal of the protective atmosphere was measured by first protecting the melt with 0.7% HFC-134a in dry air for 3 hours, then exposing the melt to 100% dry air. After two minutes, the surface was still shiny and bright with no signs of oxidation. The same experiment was also conducted with 0.7% SF_6 in dry air. In this case the protection only lasted for 15 seconds. The alloy used in both cases was AZ91D. When pure magnesium and HFC-134a was used, burning of the melt started after 5-10 seconds.

The HFC-134a was further tested at Magnesium Elektron in production scale with good results [Lyon et al., 2003]. However, this gas will most likely be banned in Europe within some years, so this is at least not a long-term alternative for producers and die casters here.

BF_3

Revankar et al. [2000] have found a method of protecting molten magnesium with BF_3 which does not have a global warming potential. It is known that BF_3 protects magnesium melts, but there has been problems with storage of compressed gas, and it is quite an expensive gas. This new method called the

Magshield system produces BF_3 in situ by thermal decomposition of KBF_4. The system is sealed to prevent leakages of BF_3.

The amount of BF_3 in dry air varied from 0.2 vol% to 1.0 vol%, but concentrations less than 0.5% gave a discoloration of the surface. The protection of the melt lasted for 45 minutes after the gas was shut of, compared to SF_6 where the protection lasted for 30 minutes.

Borontrifluoride is a highly toxic compound [Genium, 1989, The Royal Society of Chemistry, 1991]. The recommended limit for BF_3 in air is 1 ppm. However, Revankar et al. did not find concentrations exceeding 0.2 ppm in the working area.

Fluorinated ketones

The company 3M has developed a fluorinated ketone liquid that easily vaporizes to provide a protective gas. The trade name of this ketone is Novec 612. The greatest advantage of this protection fluid/gas is the Global Warming Potential which is equal to 1. The atmospheric life time is approximately 5 days, and the ozone depletion potential is 0.0. [Preliminary Product Information, 3M, 2002]

Preliminary experiments with Novec 612 shows that it is able to effectively protect molten magnesium [Milbrath and Owens, 2002, Argo and Lefebvre, 2003]. The problem is rather the thermal degradation products produced which is still an issue to be studied. Toxic gases like HF, or gases that are potential Green House Gases such as perfluorocarbon gases may be formed [Milbrath and Owens, 2002].

BIBLIOGRAPHY

Air pollution network for early warning and on-line information exchange in Europe. Netsite: http://apnee.norgit.no:8080/regional/servlet/regional/template/Pollutants.vm. Accessed December 11th 2003.

Albright D.L. (2002) Corporate perspectives: Hydro Magnesium. *Proceedings of the International Conference on SF_6 and the Environment: Emission Reduction Strategies,* San Diego, CA, November 21-22, 2002

Aleksandrova Y.P. and Roshchina I.N. (1977) Interaction of Magnesium with Gases. *Metallovedenie i Termicheskaya Obrabotka Metallov* **3:**218-221.

Argo D. and Lefebvre M. (2003) Melt Protection for the AJ52 Magnesium Strontium Alloy. *Magnesium Technology 2003* **4**:15-21.

Aylward, G.H. and Findlay, T.J.V. (1974) SI Chemical Data. Milton:John Wiley & Sons.

Bach F.W., Karger A., Pelz C., Schacht S. and Schaper M. (2003) Verwendung von CO2-Schnee zur Abdeckung von Magnesiumscmelzen. *Metall* **57**:285-288.

Bartos S., Marks J., Kantamaneni R. and Laush C. (2003) Measured SF_6 Emissions from Magnesium Die Casting Operations. *Magnesium Technology 2003* **4**:23-27.

Busk, R.S., Jackson, R.B. (1980) Use of SF_6 in the Magnesium Industry. *Proceedings of the International Magnesium Association 37th Annual World Conference on Magnesium.*

Cashion, S.P. (1998) The Use of Sulphur Hexafluoride for Protecting Molten Magnesium PhD-thesis The University of Queensland, Australia.

Cashion S.P., Ricketts N.J. and Hayes P.C. (2002) The mechanism of protection of molten magnesium by cover gas mixtures containing sulphur hexafluoride. *Journal of light metals* **2**:43-47.

Chang S.-Y., Matsushita M., Tezuka H. and Kamio A. (1998) Ignition Prevention of Magnesium by Simultaneous Addition of Calcium and Zirconium. International *Journal of Cast Metals Research* **10**: 345-351.

Couling, S.L. (1979) Use of Air/CO_2/SF_6 Mixtures for Improved Protection of Molten Magnesium. *Proceedings of the International Magnesium Association*

36th Annual World Conference on Magnesium.

Couling, S.L. and Bennett, F.C. and Leontis, T.E. (1977) Fluxless Melting of Magnesium. *Light Metals*. **1:**545-560.

Couling, S.L. and Leontis, T.E. (1980) Improved Protection of Molten Magnesium with Air/CO_2/SF_6 Gas Mixtures. *Light Metals* **4**:997-1009.

Czerwinski F. (2003) The Oxidation of Magnesium Alloys in Solid and Semisolid States. *Magnesium Technology 2003* **4**:39-42

Emley, E.F. (1966) Principles of Magnesium Technology.London: Pergamon Press

Erickson, S.C., King, J.F. and Mellerud, T. (1998) Conserving SF_6 in Magnesium Melting Operations *Foundry Management & Technology* **126**(6): 40-44.

FactSage 5.0. Computer software

Fruehling, J.W. and Hanawalt, JD. (1969) Protective Atmospheres for Melting Magnesium Alloys *Transactions of the American Foundrymen's Society* **77**:159-164.

Fruehling, J.W. (1970) Protective Atmospheres for Molten Magnesium. PhD-thesis University of Michigan.

Gjestland H., Westengen H. and Plathe S. (1996) Use of SF_6 in the Magnesium Industry - An Environmental Challenge. *Proceedings of the Third International Magnesium Conference,* Manchester, UK, 10-12 Apr 1996

Gregg S.J. and Jepson W.B. (1958-59) The High-temperature Oxidation of Magnesium in Dry and in Moist Oxygen. *Journal of the institute of metal* **87**: 187-203.

Hanawalt, J.D. (1972) Practical Protective Atmospheres for Molten Magnesium. *Metals Engineering Quarterly* **12**(4): 6-10.

Houska, C. (1988) Beryllium in Aluminium and Magnesium. *Metals and Materials* **4(**2):2.

Hydro magnesium Home Page http://www.magnesium.hydro.com/ Accessed October 27th 2003.

Kofstad, P. (1966) High-temperature Oxidation of Metals.New York: Wiley.

Kubaschewski, O. and Hopkins, B.E. (1953) Oxidation of Metals and Alloys. London: Butterworths Scientific Publications.

Leontis T.E. (1986) Magnesium: Properties. In Encyclopedia of Materials Science and Engineering. **4**:2638-2640.

Lyon P., Rogers P.D., King J.F., Cashion S.P. and Ricketts N.J. (2003) Magnesium Melt Protection at Magnesium Elektron Using HFC-134a. *Magnesium Technology 2003* **4**:11-14.

Maiss M. and Brenninkmeijer C.A.M. (1998) Atmospheric SF_6: Trends, Sources, and Prospects. *Environmental Science & Technology* **32:**3077-3086.

Metals Handbook. Ninth ed. (1979). Ohio: American Society for Metals.

Milbrath D.S. and Owens J.G. (2002) Use of Fluorinated Ketones in Cover Gases for Molten Magnesium. Presented at the 131st Annual Meeting TMS, February 17-21, 2002, Seattle, Washington.

Pettersen G., Øvrelid E., Tranell G., Fenstad J. and Gjestland H. (2002) Characterization of the Surface Films Formed on Molten Magnesium. *Materials Science and Engineering A* **332**: 285-294.

Pohanish, R.P. and Greene, S.A. (1996) Hazardous Materials Handbook. New York: Van Nostrand Reinhold.

Sakamoto M., Akiyama S. and Ogi K. (1997) Suppression of Ignition and burning of Molten Mg Alloys by Ca bearing stable oxide film. *Journal of Materials Science Letters* **16**: 1048-1050.

Smythe K.D. (2002) Update on SF_6 Global Sales Study. Proceedings of the International Conference on SF_6 and the Environment: Emission Reduction Strategies, San Diego, CA, november 21-22, 2002.

Solberg, J.K. (1996) Teknologiske Metaller og Legeringer. Metallurgisk Institutt, NTH.

Spiegelberg W., Ali S. and Dunstone S. (1992) The Effects of Beryllium Additions on Magnesium and Magnesium Containing Alloys. In DGM Informationsgesellschaft m.b.H. DGM Informationsgesellschaft m.b.H., Oberursel.:259-266.

Tang, K. (2004) Equilibrium Calculation for Mg Protection Gas Mixtures *Memo SINTEF Materials Technology*

Thonstad, J. (1997) Elektrolyseprosesser. Institutt for Teknisk Elektrokjemi, NTNU.

Zeng X., Wang Q., Lü Y., Ding W., Zhu Y., Zhai C., Lu C. and Xu X. (2001) Behavior of Surface Oxidation on Molten Mg-9Al-0.5Zn-0.3Be Alloy. *Materials science & engineering A, Structural Materials* **301**: 154-161.

Øymo D., Holta O., Hustoft O.M. and Henriksson J. (1992) Magnesium Recycling in the Die Casting Shop. *Metall: Fachzeitschrift für Handel, Wirtschaft, Technik und Wissenschaft* **46**: 898-902.

Walzak, M. J.; Davidson, R. D.; McIntyre, N. S.; Argo, D.; Davis, B. R. (2001) Interfacial Reactions Between SF_6 and Molten Magnesium. *Magnesium Technology 2001* **2**: 37-41.

Chapter 2 .
Experiments with New Surface in Vacuum Unit

INTRODUCTION

As is well known, SF_6 or SO_2 with air as a carrier gas gives a gas mixture that protects molten magnesium from uncontrolled oxidation. In these experiments, it is studied if the same protective effect is achieved with other carrier gases. The carrier gases tested are nitrogen, argon and carbon dioxide.

An experimental unit, somewhat similar to the set-up Cashion employed for his work [Cashion, 1998], was especially built for this purpose.

An atmosphere of an inert gas such as nitrogen or argon will obviously prevent oxidation since oxygen is not present, but there will be a problem with evaporation of magnesium since no dense oxide film at the surface restrains evaporation. It is investigated if the addition of SO_2 or SF_6 will help build a protective film.

The gas-mixtures tested are 1% SF_6 in air, nitrogen, argon and carbon dioxide, 1% SO_2 in air, nitrogen and carbon dioxide.

To conduct the experiments without SF_6, it was found to be necessary to take extreme measures to clean the furnace to remove remnants of SF_6 in the furnace:

Then it was tested how much air a CO_2 atmosphere can contain and still be protective. It is also studied how low the content of SO_2 in air can be.

EXPERIMENTAL

Procedure

A sketch of the furnace used is given in Figure 2.1. Note that the sketch is not drawn to scale. The furnace is a Kanthal wound furnace connected to a rotation pump and a diffusion pump. A vacuum of at least $1 \cdot 10^{-4}$ mbar can be achieved.

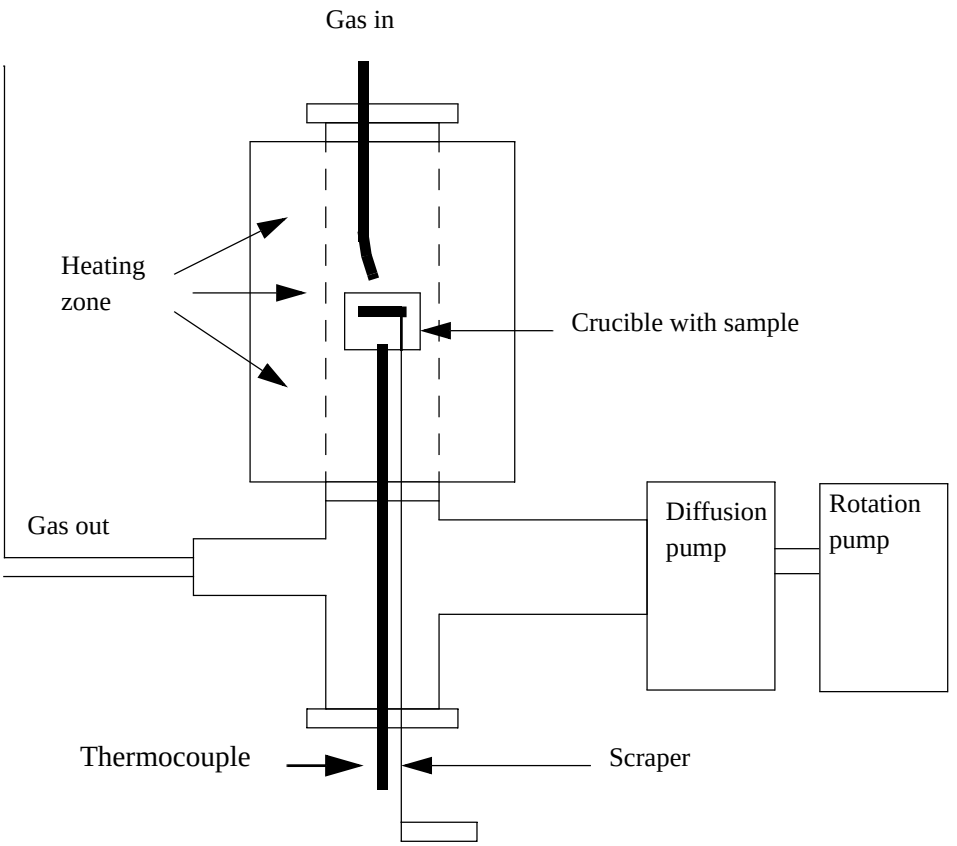

Figure 2.1. The figure shows a simplified sketch of the furnace.

About 7 g of pure magnesium from Hydro Magnesium was placed in the stainless steel crucible (quality W-1-4762) sketched in Figure 2.2, and the crucible was positioned in the heating zone of the furnace as shown in Figure 2.1. The crucible was sprayed with boron nitride before use to prevent sticking of magnesium to the crucible walls. A thermocouple is placed below the melt in a hole in the bottom of the crucible as shown in Figure 2.2. The temperature measured by this thermocouple is taken to be the temperature of the magnesium metal in the crucible.

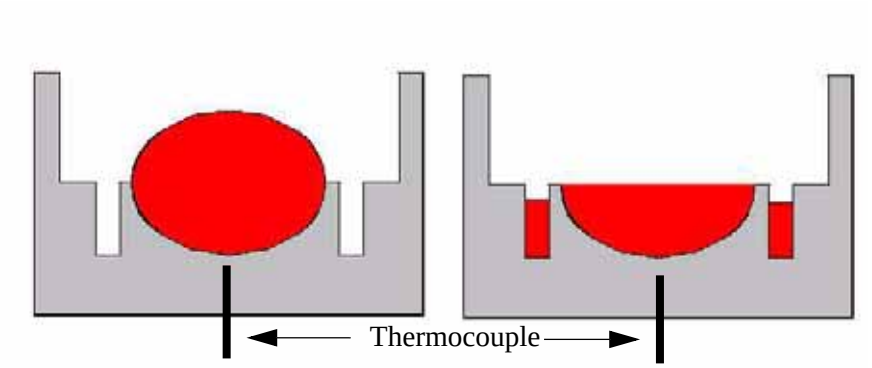

Figure 2.2 A sketch of the crucible with the molten metal (red). The sketch to the left shows the situation before the surface is scraped, the left sketch shows the situation afterwards.

Gas was introduced with a stainless steel tube through the top lid and blown down on to the melt surface. The gas flow was set to 200 ml/min. and controlled by a Bronkhorst flowmeter. Gas was let out through a valve in the lower part of the furnace.

The furnace was first evacuated down to about $1 \cdot 10^{-4}$ mbar. Then the furnace chamber was filled with either CO_2 or N_2 when these gases were used as carrier gases until the pressure reached atmospheric pressure. The evacuation procedure was repeated once more, and the chamber was filled with the specific gas-mixture. However, thermodynamically oxide can still form since there could be an oxygen pressure of the order of magnitude of 10^{-5} mbar. When the pressure inside the chamber was slightly higher than atmospheric pressure, the off-gas valve was opened, and gas was allowed to flow through the furnace. When this procedure was completed, the heating of the sample started.

At 700°C when the metal was melted, fresh metal was exposed by removing the surface of the melt with a scraper. The procedure can be understood by looking at

Figure 2.2. More metal than is necessary to fill the cavity is initially placed in the crucible. During melting, the metal will form a meniscus at the surface. The scraper will remove this meniscus and thereby expose fresh bulk magnesium to the furnace atmosphere. The excess metal will flow into the channel around the cavity.

Experiments were carried out with 5, 30 and 60 minutes exposure after the surface was scraped. After exposure, the crucible with the sample was lowered out of the heating zone down to the cooling zone where the sample was quenched with helium gas.

Experiments conducted

The experiments conducted with SF_6 and different carrier gases are given in Table 2.1. Table 2.2 presents the experiments with SO_2, and experiments in CO_2, either pure or with varying amounts of air, are given in Table 2.3.

Many of the experiments have been repeated. One reason for this is an important lesson learnt during the first series of experiments: SF_6 gas contaminated the furnace with fluorine, so that we got fluorine on samples that should not contain fluorine at all. Therefore, we carried out a second and third series where we replaced the radiation shields and the refractory materials. Parts were sandblasted and washed in acid. This time, the experiments with SF_6 were performed at the end. The experiments carried out before the replacement of the furnace equipment, are in the tables referred to as series 1. The microprobe analysis of these samples show high values of fluorine, even though there is not supposed to be fluorine there at all. For example, one should not expect that there would be fluorine on a sample exposed to SO_2 in CO_2. Still, the analysis showed that the samples contained 20%fluorine. Experiments from series 2 and 3, where the furnace is supposed to be free of fluorine, are denoted in the tables. A more thorough cleaning of the furnace was carried out before series 3 started than

before series 2.

Table 2.1 : Experiments with SF_6 in various carrier gases.

Gas mixture	5 min. exposure time	30 min. exposure time	60 min. exposure time
1|% SF_6 in air	Series 2	Series 2	Series 2
1% SF_6 in N_2	Series 1,Series 2		
1% SF_6 in Ar	Series 2		
1% SF_6 in CO_2	Series 1,Series 2	Series 1,Series 2	Series 2

As can be seen from the table, only the 5 minutes exposure experiments were performed with 1% SF_6 in N_2, 1% SF_6 in Ar. The reason is that the furnace became heavily contaminated with powder during these experiments, so we did not continue with the 30 minutes experiments.

Table 2.2 :Experiments with SO_2 in various carrier gases.

Gas mixture	5 min. exposure time	30 min. exposure time	60 min. exposure time
1% SO_2 in air	Series 2	Series 2	Series 2
0.5% SO_2 in air	Series 3		Series 3
0.2% SO_2 in air	Series 3	Series 3	Series 3
0.1% SO_2 in air	Series 3	Series 3	
1% SO_2 in N_2	Series 1		
1% SO_2 in CO_2	Series 1,Series 2	Series 1,Series 2	Series 2

Also here, only the five minute experiment was performed with 1% SO_2 in N_2 due to contamination of the furnace.

Table 2.3 :Experiments in CO_2 and CO_2 combined with air.

Gas mixture	5 min. exposure time	30 min. exposure time	60 min. exposure time
CO_2	Series 1,Series 2	Series 1,Series 2	Series 2
2% air in CO_2	Series 3		Series 3
3% air in CO_2	Series 3		
4% air in CO_2	Series 3		
5% air in CO_2	Series 3		Series 3
10% air in CO_2	Series 3		
20% air in CO_2	Series 3		

It should also be mentioned that in series 2, experiments with both SF_6 in air and SO_2 in air were carried out. This protects magnesium very well. However, these experiments were performed in order to provide a reference for what a well protected melt looks like. Also, it was attempted to determine the composition of the surface.

In addition, 2 to 20% air was added to CO_2 to see if the metal still would be protected. Also, the content of SO_2 in air was lowered to see at which percentage the protective effect ceased. Experiments were performed with 1, 0.5, 0.2 and 0.1% SO_2 in air.

Before the analysis of the samples, pictures were taken with a digital camera to document the appearance of the samples.

The samples were examined with a microprobe. Each sample was analyzed at three to five different spots at the surface. The diameter of each spot analyzed is about 50 micrometer.

Since the microprobe is intended for polished surfaces, it should be kept in mind when looking at the results that some of the surfaces were very uneven, and this will affect the results. Therefore, the numbers should not be considered as absolute values. Another factor that has to be mentioned, is the acceleration voltage. During these analysis, it was set to 15 kV since only the surface layer is interesting. This low value was chosen to avoid that the electron beam penetrates

too deep into the sample. If the electron beam penetrates down into the bulk magnesium, this bulk metal will contribute to the results and the analysis results will be too high in magnesium. It is not possible in general to tell how deep into the sample the beam goes since this depends on the density of the film. A material with high density will have a low penetration depth, while the opposite is the case for materials with low density. If the exact composition of the film is known, then it is possible by Monte Carlo simulation to tell how deep the beam goes.

The Kα peaks are used to perform the analysis, and the ZAF method is employed to correct the results. All results are given in atomic percent. Since the microprobe analyzes a volume, the compositions given here will be an average of the composition within this volume. The standard deviation of the measurements is given as the uncertainty in the measurements.

RESULTS

SF_6

SF_6 in air, series 2 (Table 2.1)

As mentioned, these experiments in Figures 2.3-2.5 were performed to provide a reference for different gas mixtures since SF_6 in air is known to provide very good protection. Also, we wished to determine the surface composition.

As is seen from Table 2.4, the surface film contains mainly magnesium fluoride and oxygen. Very small amounts of sulphur are detected.

Table 2.4 : The table shows the composition of three samples in atomic percent exposed to 1%SF_6 in air. Series 2.

	C	S	O	F	Mg
5 minutes	*0.4 ± 0.1*	*0.1 ± 0.1*	*12 ± 2*	*45 ± 15*	*43 ± 14*
30 minutes	*0.2 ± 0.1*	*0.4 ± 0.1*	*18 ± 3*	*46 ± 3*	*35 ± 1*
60 minutes	*0.4 ± 0.1*	*0.14 ±0.03*	*13 ± 2*	*49 ± 4*	*38 ± 2*

Very roughly, these results indicate that about equal amounts of MgO and MgF_2 are formed. After 60 minutes, assuming the formation of these two phases, the film consists of 13/13+25 = 34% MgO and 25/13+25 = 66% MgF_2.

These samples were, as expected, very well protected. The surface was shiny or sometimes a bit duller grey. The dullness seemed to increase with increasing exposure time.
The carbon found is probably only due to contamination of the sample during handling of the sample.

Figure 2.3 Sample exposed to 1% SF_6 in air, series 2. (See Table 2.1 and 2.4, 60 minutes.)

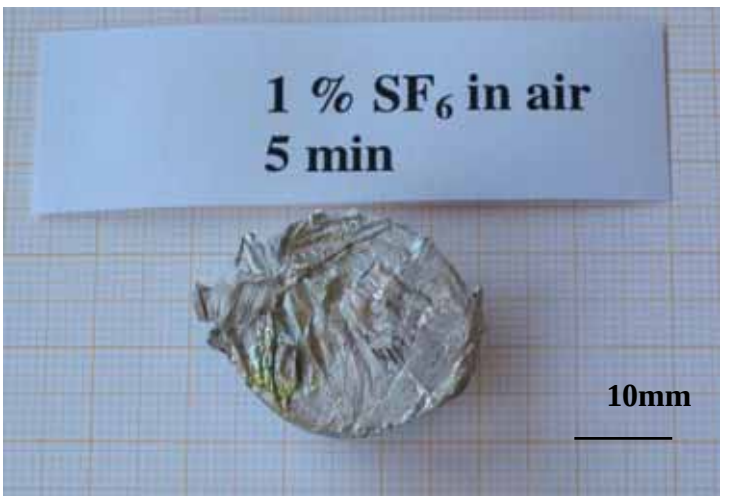

Figure 2.4 Sample exposed to 1% SF_6 in air for 5 minutes, series 2. (See Table 2.1 and 2.4, 5 minutes.)

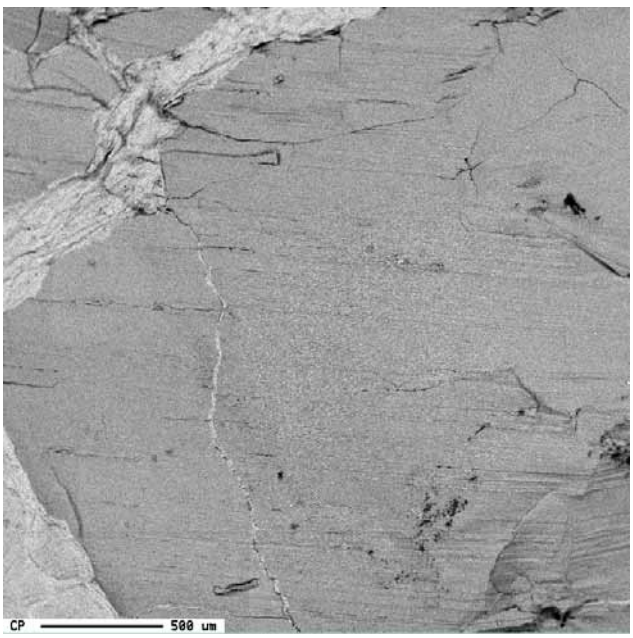

Figure 2.5 Surface of sample exposed to 1% SF_6 in air, series 2. See Table 2.1 and 2.4, 30 minutes. Picture taken with backscatter electrons in the microprobe.

1% SF_6 in N_2, series 1 and 2 (Table 2.1)

As mentioned earlier, the furnace became heavily polluted performing this experiment. A white powder covered the radiation screens, while the sample itself was covered with a very thick layer, approximately 1 mm, which detaches from the metal during handling. The top surface of the layer was black and velvet like, while the rest was white.

Table 2.5 gives the surface composition of magnesium exposed to 1% SF_6 in nitrogen. Series 2 still in italic.

Nitrogen is not detected at all, but considerable amounts of fluorine are found at the surface. The high amount of oxygen may be somewhat surprising since there should be little oxygen in the furnace atmosphere. The composition indicates somewhat more MgF_2 than MgO in series 1. It is possible that some Mg_3N_2 has formed and converted to MgO when the furnace is opened. The Mg_3N_2 may have formed in the gas phase by reaction between evaporated magnesium and nitrogen.

Table 2.5 :The composition of molten magnesium exposed to a gas mixture of 1% SF_6 in N_2 for 5 minutes.

	C	S	O	F	N	Mg
5 minutes	0.7 ± 0.1	5.9 ± 1.3	13 ± 1	46 ± 4	0.7 ± 0.7	33 ± 2
5 minutes	*0.6 ± 0.4*	*5.8 ± 3.8*	*19.6 ± 19.6*	*40 ± 21*	*0.22 ± 0.22*	*34 ± 7*

Figure 2.6 shows the surface. One can not see a distinct film here as was the case with many of the other samples.

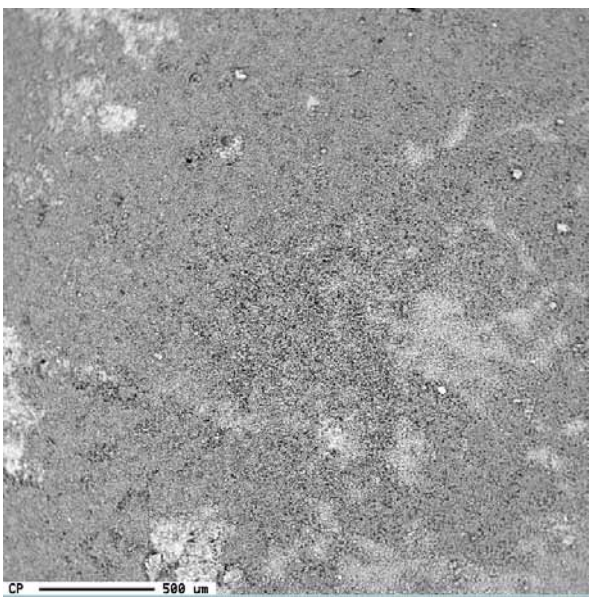

Figure 2.6 Molten magnesium exposed to 1% SF_6 in N_2 for 5 minutes, series 1. Picture taken with backscatter electrons in the microprobe. See Table 2.1 and 2.5, 5 minutes.

SF_6 in argon, series 2 (Table 2.1)

Table 2.6 gives the surface composition of one sample exposed to 1% SF_6 in argon for five minutes. This experiment was only performed once since the experiment caused a very high level of contamination in the furnace. The sample contains much oxygen, but this has probably reacted with the unprotected sample

when the furnace was opened. Also, as mentioned previously, even though the furnace is evacuated well before the experiment started, there will always be some oxygen left inside.

Table 2.6 :The surface composition of a sample exposed to 1% SF_6 in argon for 5 minutes.

	C	S	O	F	Mg
5 min	*0.4 ± 0.4*	*1.3 ± 1.0*	*29 ± 21*	*8 ± 6*	*61 ± 15*

The surface was, as expected, not very well protected. This is illustrated with a picture in Figure 2.7 and a micrograph of the surface in Figure 2.8. As can be seen in the micrograph, there are small droplets of magnesium on the surface, probably formed from magnesium vapor. There is no film protecting the metal from evaporation.

Figure 2.7 Sample exposed to 1% SF_6 in Ar. No protective film is formed. See Table 2.1 and 2.6, 5 minutes.

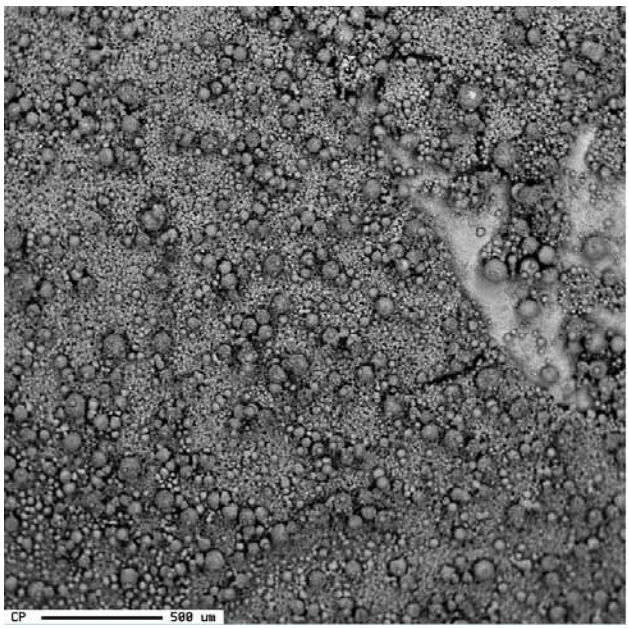

Figure 2.8 Magnesium exposed to 1% SF_6 in argon, series 2. See Table 2.1 and 2.6, 5 minutes. The Mg droplets are clearly seen. Picture taken with backscatter electrons in the microprobe.

SF_6 in CO_2, series 1 and 2 (Table 2.1)

SF_6 in CO_2 gave a black surface as can be seen from Figure 2.9, although the sample seemed to be well protected from uncontrolled oxidation.

Figure 2.9 Sample exposed to 1% SF_6 in CO_2. See Table 2.1 and 2.7, 30 minutes.

Figure 2.10 shows the surface of a sample exposed to 1% SF_6 in CO_2 for 30 minutes. The metal underneath the film seems to have contracted more than the film itself during solidification, giving the wrinkled surface. This might indicate that the film has a composition different from that obtained with SF_6 in air.

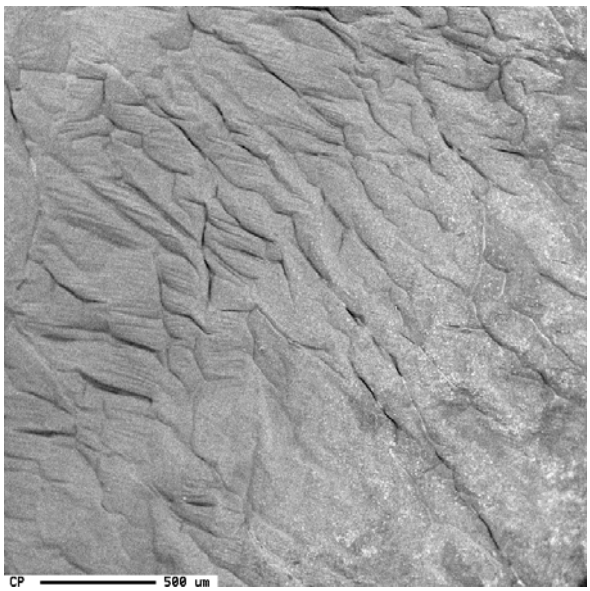

Figure 2.10 The micrograph shows a surface exposed to 1% SF_6 in CO_2 for 30 minutes, series 1. See Table 2.1 and 2.7, 30 minutes. Picture taken with backscatter electrons in the microprobe.

Table 2.7 shows the surface composition of magnesium exposed to a gas mixture of 1% SF_6 in CO_2. Series 2 in the table is given in italic typing.

Table 2.7 :The composition of magnesium exposed to 1% SF_6 in CO_2 for 5, 30 and 60 minutes.

	C	S	O	F	Mg
5 minutes	9 ± 4	2.9 ± 2.1	6 ± 6	66 ± 9	16 ± 6
30 minutes	1.2 ± 0.1	2.0 ± 1.4	0.8 ± 0.3	76 ± 9	20 ± 7
5 minutes	*6 ± 5*	*0.3 ± 0.0*	*14.3 ± 1.3*	*3.3 ± 0.4*	*76 ± 4*
30 minutes	*0.9 ± 0.8*	*0.5 ± 0.1*	*10 ± 5*	*65 ± 6*	*24 ± 4*
60 minutes	*0.3 ± 0.1*	*0.04 ± 0.05*	*1.1 ± 0.3*	*71 ± 1*	*28 ± 1*

The high value obtained for Mg after 5 minutes in series 2 may indicate that the film is thin initially. The amount of carbon has decreased with increasing

exposure time in both series. The opposite is the case with fluorine where the amount of fluorine on the surface has increased with increasing exposure time. Another significant change is the oxygen-content which decreases with increasing exposure time. Compared to magnesium, the fluorine content is high except in the five minute experiment in the last series. These analysis were performed twice since the results varied strongly in the fluorine content, but the results were the same.

SO_2

SO_2 in air, series 2 and 3 (Table 2.2)

As will be seen later, approximately 0.2% SO_2 is required to protect the metal well. Below this value, the gas does not protect the surface sufficiently.

Table 2.8 gives the surface composition of samples exposed to varying amounts of SO_2 in synthetic air for 5, 30 and 60 minutes. The small amounts of fluorine and carbon found are probably due to contamination and uncertainty in the microprobe results.

The films are most likely a mixture of magnesium oxide and magnesium sulphide or magnesium oxide with dissolved sulphur. Thermodynamically, magnesium sulphate is not expected to form. The oxygen content for many of the samples is unreasonably high, and there is still oxygen “left” even if one assumed that all the sulphur binds the oxygen as sulphate and the magnesium binds the oxygen as MgO.

Table 2.8 :The table shows the composition in atomic percent of surfaces exposed to varying amount of SO_2 in synthetic air. Series 2 in italic, series 3 in bold.

1% SO_2 in air					
	C	S	O	F	Mg
5 minutes	*0.8 ± 0.2*	*4.5 ± 1.6*	*39 ± 4*	*2.3 ± 0.4*	*53 ± 4*
30 minutes	*0.4 ± 0.3*	*7.3 ± 2.2*	*41 ± 18*	*1.2 ± 0.6*	*50 ± 18*
60 minutes	*0.7 ± 0.3*	*2.6 ± 3.4*	*26 ± 23*	*0.2 ± 0.6*	*71 ± 25*
0.5% SO_2 in air					
5 minutes	**0.6 ± 0.1**	**1.9 ± 1.9**	**33 ± 18**	**0.1 ± 0.1**	**64 ± 21**
60 minutes	**0.01±0.01**	**3.6 ± 3.6**	**77 ± 11**	**0.01±0.01**	**19 ± 8**
0.2% SO_2 in air					
5 minutes	**0.3 ± 0.3**	**6.4 ± 1.1**	**63 ± 7**	**0.01±0.01**	**30 ± 7**
30 minutes	**0.04±0.04**	**6.4 ± 3.9**	**62 ± 18**	**0.2 ± 0.1**	**31 ± 14**
60 minutes	**0**	**3.8 ± 2.4**	**63 ± 17**	**0.05±0.05**	**34 ± 14**
0.1% SO_2 in air					
5 minutes	**0.04±0.04**	**0.14 ±0.03**	**56 ± 7**	**0**	**43 ± 7**
30 minutes	**0.1 ± 0.04**	**5.1 ± 1.0**	**51 ± 6**	**0.05±0.05**	**44 ± 5**

The samples exposed to 1 and 0.5% SO_2 were well protected from oxidation. The surfaces were grey/dark grey, and in some cases and some parts, shiny. Figure 2.11 below shows a sample that was exposed for 5 minutes. Also a sample exposed to 0.5% SO_2 for 60 minutes is seen in Figure 2.13. There is a black end of the sample, but that is the film that was scraped away when the exposure started.

Figure 2.11 Sample exposed to 1% SO_2 in air, series 2. See Table 2.2 and 2.8, 5 minutes.

A closer look at the surface from Figure 2.11 is seen in Figure 2.12. The surface is not very even as is the case with SF_6, but it is still protective.The surface film seems to have expanded and wrinkled up.

.

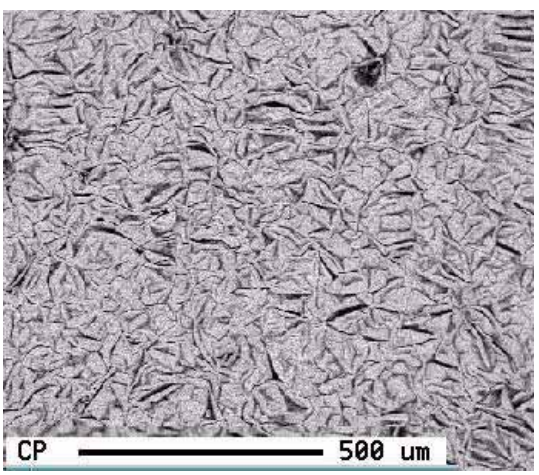

Figure 2.12 Sample exposed to 1% SO_2 in air for 5 minutes, series 2. See Table 2.2 and 2.8, 5 minutes. Picture taken with backscatter electrons in the microprobe.

Figure 2.13 Sample exposed to 0.5% SO_2 in air for 60 minutes. See Table 2.2 and 2.8.

When only 0.1-0.2% SO_2 was added to the air, the metal was not as well protected, although parts of the surfaces are shiny, Figure 2.14 and 2.15. The shiny part is just below where the gas enters the furnace through the gas tube. However, the appearance of the surface is not the major problem, but the fact that the inside of the furnace was covered with a white powder, most likely MgO, and magnesium had started condensing on the scraper.

Figure 2.14 Sample held in 0.2% SO_2 in air for 60 minutes. See Table 2.2 and 2.8.

Figure 2.15 Sample exposed to 0.1% SO_2 in air for 30 minutes. See Table 2.2 and 2.8.

A closer look at the surface that was exposed to 0.1% SO_2 in air for 5 minutes is seen in Figure 2.16. There seems to be a film on the surface, and there are also cracks in the film.

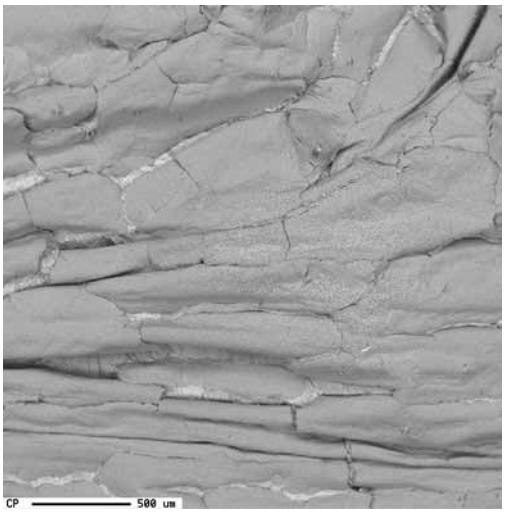

Figure 2.16 Microprobe picture of surface of sample exposed to 0.1% SO_2 in air. See Table 2.2 and 2.8, 5 minutes. Picture taken with backscatter electrons in the microprobe.

1% SO_2 in N_2, series 1 (Table 2.2)

Also in this case, white powder was formed and deposited everywhere inside the furnace, including the sample. For this to happen, there had to be a strong evaporation of the magnesium, and with a strong evaporation, the metal is obviously not protected.

Table 2.9 presents microprobe measurements of the surface composition of molten magnesium exposed to a gas mixture of 1% SO_2 in N_2. Two different areas were analyzed. Also some powder from the radiation screens was analyzed.

Table 2.9 : Surface concentration of molten magnesium exposed to 1% SO_2 in N_2, series 1.

	C	S	O	B	N	F	Mg
5 min., 1st area	0.7 ±0.1	1.2 ±0.2	51 ±11	0.08 ±0.04	4.1 ±1.0	0.6 ±0.3	43 ±11
5 min., 2nd area	0.5 ±0.4	3.3 ±3.8	52 ±14	0.09 ±0.04	1.5 ±1.5	1.1 ±0.6	42 ±11
Powder from radiation screen	1.0 ±0.6	3.6 ±3.1	50 ± 8		0	18 ± 7	28 ± 6

It is seen from the table that there is little variation between the two different areas. The surface mainly consists of magnesium and oxygen and some nitrogen, the 1st area more rich on nitrogen than the 2nd. Roughly speaking mainly MgO seems to have formed. The content of sulphur is low. Boron is included in these analysis only because the analysis set-up included boron this time. The crucible is sprayed with boron nitride in the beginning of the experiment and this is probably the reason why small amounts of boron are found on the surface.

The powder on the radiation screen contains large amounts of fluorine and oxygen, but no nitrogen. Again there is fluorine inside the furnace, but only in significant amounts on the radiation screens. This fluorine must be, as previously mentioned, “left over” fluorine from earlier experiments.

The surface of the sample is shown in Figure 2.17. As can be seen, the surface is very irregular and rough. There are small droplets of magnesium on the surface in the lower left hand corner, probably formed from magnesium vapor.

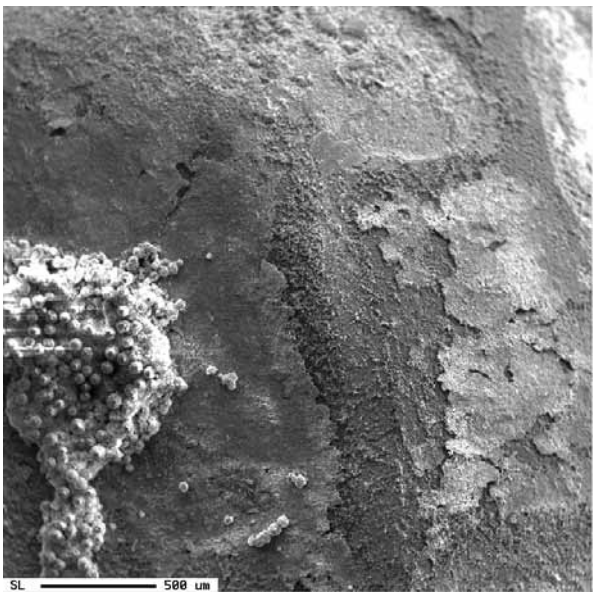

Figure 2.17 The surface of molten magnesium exposed to a mixture of 1% SO_2 in N_2 for 5 minutes, series 1. See Table 2.2 and 2.9, 5 minutes. Notice the Mg droplets. Picture taken with backscatter electrons in the microprobe.

1% SO_2 in CO_2, series 1 and 2 (Table 2.2)

The two samples protected with 1% SO_2 in CO_2 in series 1 seemed to be well protected with a golden surface film formed and with black edges. In the second series a more colorful, but still protective film formed, see Figure 2.18.

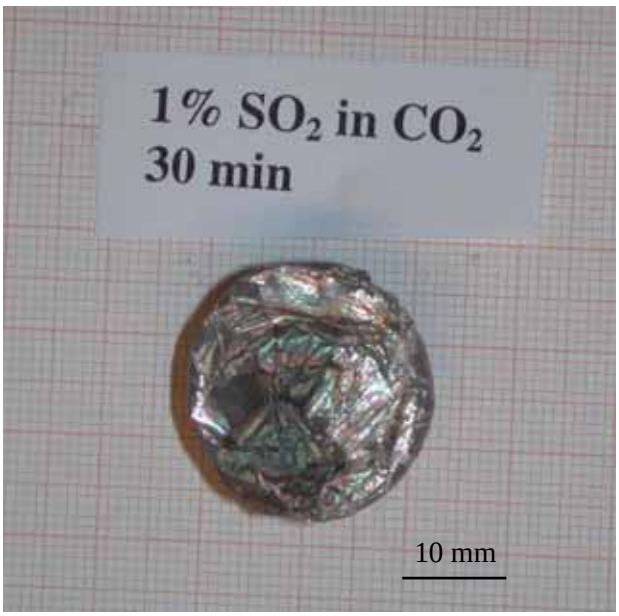

Figure 2.18 Sample exposed to 1% SO_2 in CO_2, series 2. See Table 2.2 and 2.10, 30 minutes.

Table 2.10 gives the surface composition of molten magnesium exposed to 1% SO_2 in CO_2. Two different areas were analyzed on the 30 minute sample in series 1, but the composition is very similar in both areas.

Table 2.10 :The surface concentration of molten magnesium exposed to 1% SO_2 in CO_2, Series 1 and series 2 (in italic).

	C	S	O	B	F	Mg
5 min.	0.5±0.1	0.03 ±0.03	45±5		27±1	28±6
30 min., dark area	0.4±0.1	0.03 ±0.03	47±7	1.8±0.4	21±5	29±2
30 min., light area	0.25 ±0.03	0.00	45±1	0.8±0.2	20±1	34±1
5 min.	*0.8 ± 0.04*	*0.05 ± 0.01*	*12 ± 1*	-	*0.4 ± 0.1*	*87 ± 1*
30 min.	*0.3 ± 0.1*	*0.03 ± 0.01*	*28 ± 2*	-	*1.8 ± 0.4*	*70 ± 2*
60 min.	*1.7 ± 0.7*	*0.06 ± 0.05*	*18 ± 16*	-	*1.7 ± 3.1*	*78± 19*

The high values of Mg in the second series should be noted. Possibly the films are very thin in these cases so that the electrons in the microprobe penetrate into the metal. In the first series, as mentioned earlier, the samples contained high amounts of fluorine due to contamination of the furnace. In the second series, smaller amounts were found. It is possible that some fluorine dissolved in the metal has entered the surface during the experiment, or that this amount is within the limit of error for the microprobe.

Figure 2.19 shows a micrograph of the surface of a sample from series 1 exposed to 1% SO_2 in CO_2 for 30 minutes. The surface appears very smooth, but a small crack is seen in the lower part of the picture. A different sample, exposed to the same conditions for 60 minutes, from series 2 is seen in Figure 2.20. The film is not quite as smooth in this case. A picture of a sample exposed for 60 minutes in the second series is seen in Figure 2.21. The surface is as already mentioned, partly shiny and partly colored.

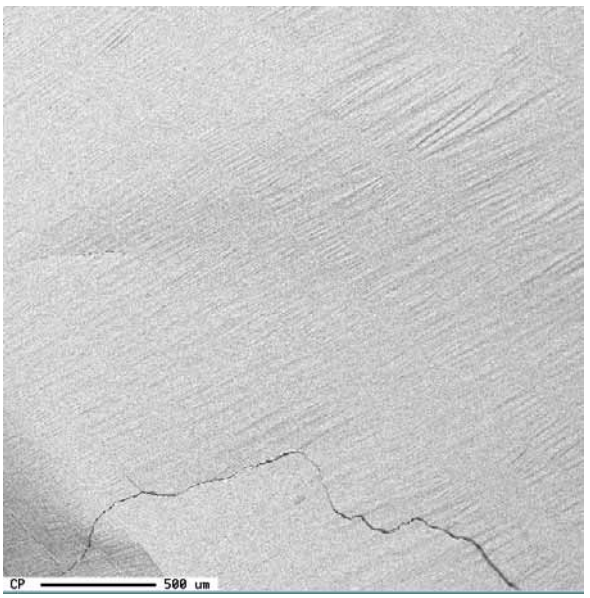

Figure 2.19 The surface of a sample exposed to 1% SO_2 in CO_2, series 1. See Table 2.2 and 2.10, 30 minutes. Picture taken with backscatter electrons in the microprobe.

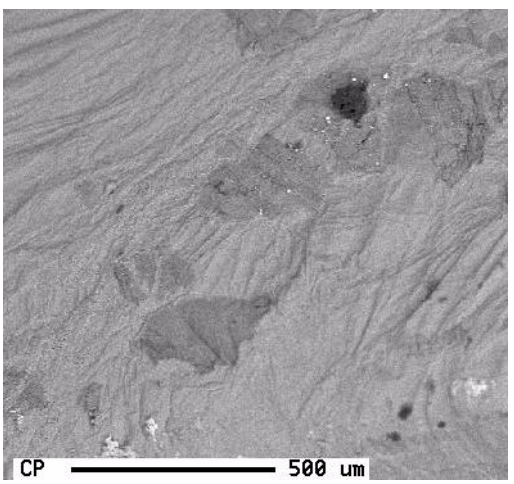

Figure 2.20 This sample is exposed to 1% SO_2 in CO_2, series 2. See Table 2.2 and 2.10, 60 minutes. Picture taken with backscatter electrons in the microprobe.

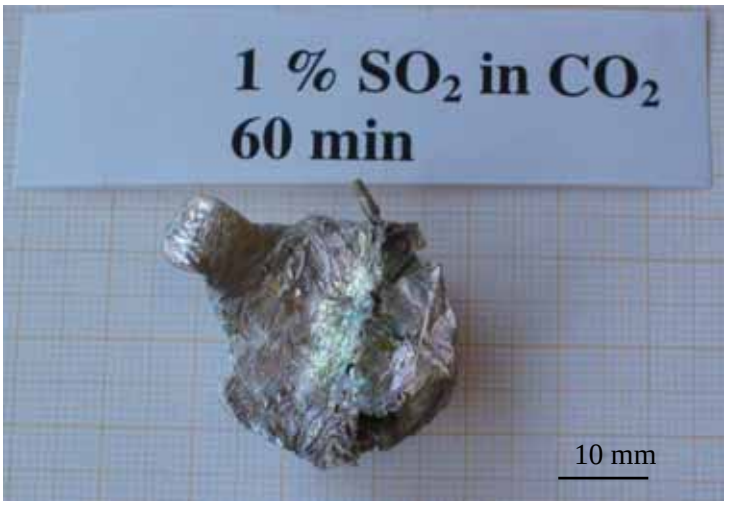

Figure 2.21 Sample exposed to 1% SO_2 in CO_2, series 2. See Table 2.2 and 2.10, 60 minutes.

CO_2/CO_2 and air

Table 2.11 shows the average composition in atomic percent of surfaces exposed to CO_2 and CO_2 in combination with air for 5, 30 and 60 minutes. Series 1 is given in regular typing, series 2 in italic and series 3 in bold.

All the surfaces are more or less discolored, whether the samples are exposed to pure CO_2 or CO_2 with added air. The surfaces seem to get more black with increasing amount of air in the gas, as will be shown.

Table 2.11 : The table shows the surface composition of magnesium exposed to atmospheres of CO_2 and CO_2 in combination with air. Series 1 in regular typing, series 2 in italic, series 3 in bold.

	C	S	O	F	Mg
100% CO_2					
5 minutes	1.7 ± 0.2	0.01 ± 0.01	46 ± 18	1.1 ± 0.1	51 ± 18
30 minutes	1.8 ± 0.3	0.01 ± 0.01	55 ± 20	1.2 ± 0.2	42 ± 21
5 minutes	*2.8 ± 1.8*	*0.006 ±0.003*	*24 ± 10*	*0.8 ± 0.5*	*73 ± 11*
30 minutes	*0.9 ± 0.6*	*0.00*	*40 ± 2*	*5.4 ± 2.1*	*54 ± 4*
60 minutes	*0.5 ± 0.2*	*0.009 ± 0.004*	*47 ± 6*	*1.0 ± 0.4*	*51 ± 6*
2% air in CO_2					
5 min	**1.8±1.3**	**0.06 ±0.06**	**15±4**	**0**	**83±4**
5 min	**0.38 ±0.17**	**0.006± 0.005**	**58±8**	**0.1±0.1**	**42±8**
60 min	**0.7 ± 0.4**	**0.001 ±0.001**	**27 ± 16**	**0.24 ± 0.07**	**72±16**
3% air in CO_2					
5 min	**1.7±0.5**	**0.007 ±0.007**	**66±2**	**0**	**33±2**
4% air in CO_2					
4% air in CO_2 5 min	**0.9±0.4**	**0.2±0.2**	**44±10**	**0**	**55±10**

Table 2.11 : (Continued)The table shows the surface composition of magnesium exposed to atmospheres of CO_2 and CO_2 in combination with air. Series 1 in regular typing, series 2 in italic, series 3 in bold.

	C	S	O	F	Mg
5% air in CO_2					
5 min	**0.7±0.3**	**0.014 ±0.007**	**26±3**	**0.24 ±0.24**	**73±3**
5 min	**1.2±0.4**	**0.005±0.005**	**53±8**	**0**	**46±8**
60 min	**0.6 ± 0.2**	**0.006 ± 0.006**	**41 ± 6**	**0.5 ± 0.1**	**58 ± 6**
10% air in CO_2					
5 min	**0.8 ± 0.1**	**0.003± 0.003**	**20 ± 1**	**0.32 ± 0.05**	**79 ± 1**
20% air in CO_2					
5 min	**0.3 ± 0.1**	**0.013 ± 0.007**	**49 ± 8**	**0.003 ± 0.003**	**51 ± 8**

The surfaces consists of small amounts of carbon, around 1%, and large amounts of oxygen and magnesium which indicates magnesium oxide. One should expect that the films at short holding times were high in magnesium since these films are thin, and vice versa, but this is not the case.

One of the samples that was exposed to 5% air in CO_2 for 5 minutes is seen in Figure 2.26. The sample to the right had one part of the surface that was black, and one which was more regular grey-brown. This sample was analyzed both at the black part and the other part. Still, one could not see a difference in composition. There does not seem to be more carbon at the surfaces that are black than the ones that are brown-grey.

Pure CO_2, series 1 and 2 (Table 2.3)

Figure 2.22 shows the sample that has been exposed to CO_2 for 30 minutes. Although this surface is shiny, many of the samples exposed to CO_2 had a grey-brown surface. Still, all the samples were well protected from oxidation. Figure 2.23 gives a closer look at the same surface through the microprobe.

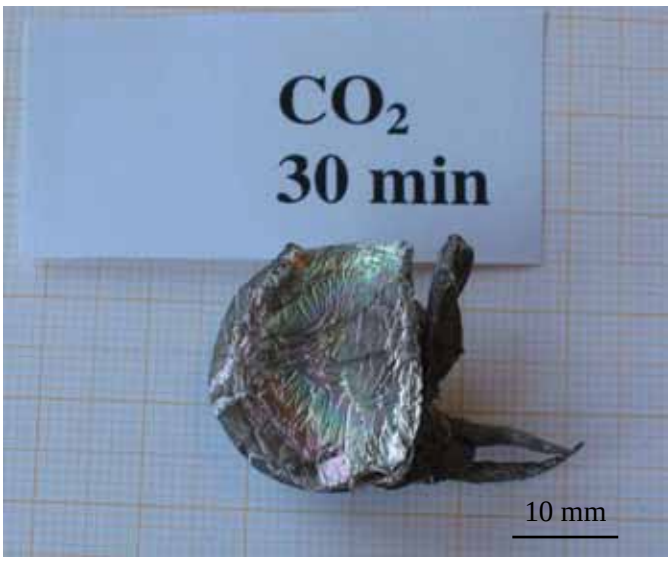

Figure 2.22 Sample exposed to pure CO_2, series 2. See Table 2.3 and 2.11, 30 minutes.

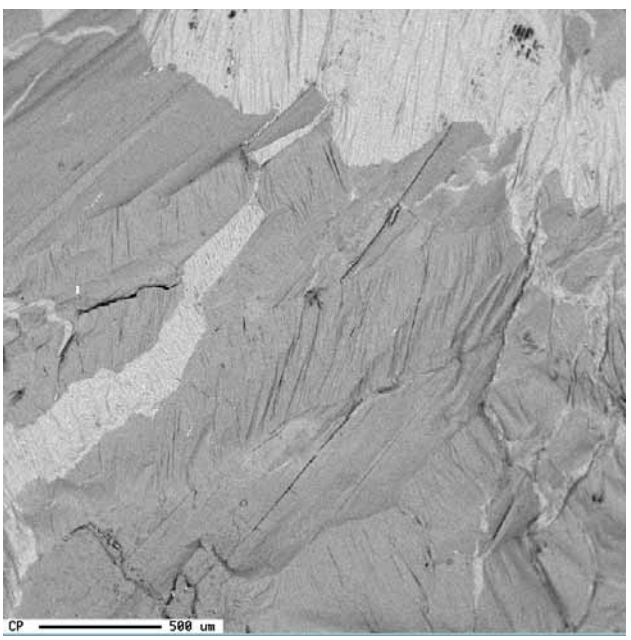

Figure 2.23 A closer look at the surface of the sample exposed to pure CO_2, series 2. See Table 2.3 and 2.11, 30 minutes. Picture taken with backscatter electrons in the microprobe.

Air in CO_2, series 3 (Table 2.3)

For air in CO_2, there seemed to be a limit at approximately 3% air in CO_2. With more air in the gas mixture, a black layer, possibly soot, forms on the sample surface. Figure 2.24 shows a sample held in 2% air in CO_2 for 5 minutes. This surface looks almost exactly like the grey-brown ones with pure CO_2. With 3% air in CO_2, the surface appears as in Figure 2.25. However, with 5% air in CO_2, the surface is covered with a black layer as seen in Figure 2.26.

Figure 2.24 Two samples exposed to 2% air in CO_2, series 3. See Table 2.3 and 2.11, 5 minutes.

Figure 2.25 Sample exposed to 3% air in CO_2, series 3. See Table 2.3 and 2.11, 30 minutes.

Figure 2.26 Two samples exposed to 5% air in CO_2, series 3. See Table 2.3 and 2.11, 5 minutes.

Figure 2.27 shows a micrograph of the surface of a sample exposed to 2% air in CO_2. This sample was grey-brown, just like samples exposed to pure CO_2. One can see that there is a film covering the surface, and that parts of the film is wrinkled.

A micrograph of a sample that had a black surface is seen in Figure 2.28. Also this film is wrinkled, although not to a large extent. The surface appeared to be covered with a layer of soot on a macroscopic scale.

However, it is not possible to distinguish between the two samples from the micrographs. The surface that was believed to be covered with soot, does not appear different from the one that was not on a microscopic scale.

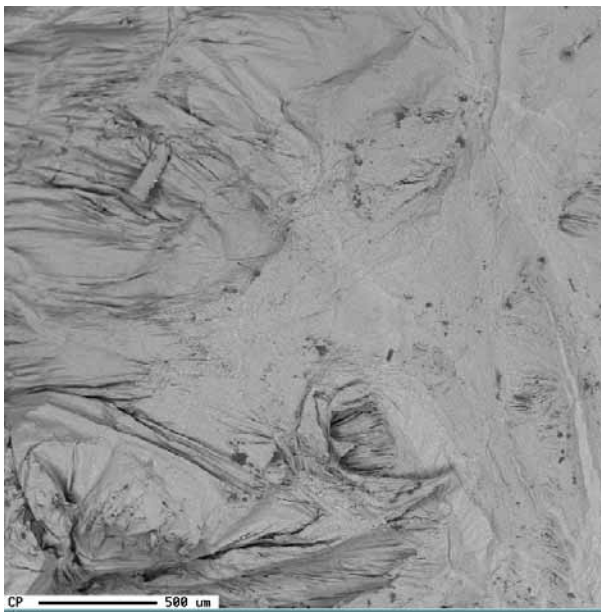

Figure 2.27 Sample exposed to 2% air in CO_2 for 5 minutes, series 3. See Table 2.3 and 2.11, 5 minutes. Picture taken with backscatter electrons in the microprobe.

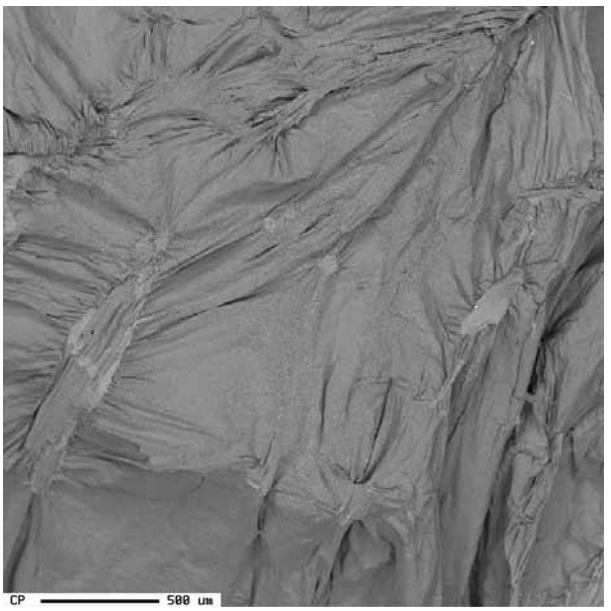

Figure 2.28 Molten magnesium exposed to 5% air in CO_2 for 5 minutes, series 3. See Table 2.3 and 2.11, 5 minutes. Picture taken with backscatter electrons in the microprobe.

DISCUSSION

Oxygen inside the furnace

The furnace can be evacuated to $1 \cdot 10^{-5}$ mbar. Since there is approximately 20% oxygen in air, the partial pressure of oxygen may be $0.2\ 10^{-5}$ mbar after evacuation. The volume of the furnace chamber is estimated to be 1.8 liters. Using these numbers and the ideal gas law makes it possible to calculate the number of moles of oxygen left inside the furnace chamber after evacuation at 25°C:

$$n = \frac{p_{O_2} \cdot V}{RT} = 1.5 \cdot 10^{-10} \text{moles } O_2$$

where R=82.05 cm^3 atm/mol K.

Assuming that all the oxygen will react with magnesium to form magnesium oxide, this gives $3 \cdot 10^{-10}$ moles MgO. This amount equals an oxide volume of $3 \cdot 10^{-9}$ cm^3. This oxide can be assumed to be distributed evenly at the sample

surface which is approximately 2 cm in diameter. This gives a thickness of the oxide film in the order of 0.01 nm.

One can therefore conclude that “left over” oxygen from the evacuation does not contribute significantly to the formation of the oxide films formed when scraping of the surface is performed. Even with an oxygen pressure decades higher, the thickness of films formed due to oxygen left in the furnace will be insignificant as the films formed are expected to be in the area of 0.1μm, see Figure 1.3.

It should also be kept in mind that the initial surface layer is scraped away when the exposure starts.

SF_6 in nitrogen/argon

SF_6 in nitrogen did not protect the molten magnesium at all. It is expected that any reaction between nitrogen and magnesium is slow [Turkdogan, 1980]. If magnesium nitride is formed, it would happen in the gas phase and not at the surface. Thus, no protective layer of magnesium nitride can form. The contamination inside the furnace indicates that there has been evaporation of the metal. The black surface is not acceptable. Pettersen et al. [2002] have suggested that a magnesium oxide film has to form to achieve protection from further oxidation of the magnesium. As seen from Table 2.5, there is too little oxygen (from leakage and left from evacuation) to give MgO.

According to the thermodynamic calculations in Figure 1.5, only magnesium fluoride and sulphide should form with nitrogen as carrier gas, and there are large amounts of fluorine at the surface. As can be seen from the figure, more fluoride than sulphide seems to form when there is sufficient gas available, so this might indicate that there is enough gas flowing though the furnace to give MgF_2. Compared to many of the other samples, there is relatively much sulphur in this sample. This sulphur may then be found as sulphide.

In the experiments reported here, there should have been little oxygen inside the furnace. Nevertheless, almost 14% oxygen is found at the surface. This oxygen could be due to a leakage in the furnace, oxygen remaining after evacuation or there could be some magnesium oxide remaining in the furnace from earlier experiments. In Appendix 1, it is calculated how little oxygen there can be in the atmosphere before magnesium oxide starts forming. At 700°C, a partial pressure of oxygen higher than $5 \cdot 10^{-54}$ bar will start the oxidation of the magnesium. In practice it is not possible to attain such low levels of oxygen.

It is also possible that there is some oxide on the steel crucible. One should expect though, that if sufficient amounts of air leaked into the furnace, the metal should be protected in the same way as with air and SF_6. As previously mentioned, it

may be that magnesium nitride, Mg_3N_2, was formed in the gas phase. When the furnace was opened, and air got into contact with the sample, the nitride was transformed to oxide. The samples were analyzed days after the experiments were performed, which could give time for the reaction.

Similar experiments with SF_6 in argon gave the same result: The gas mixture did not protect the metal surface at all, and one could tell that there had been a strong evaporation of the magnesium as seen in Figure 2.8. The conclusion for all these experiments with inert gases is that it does not seem to be possible to build a dense, protective film without oxygen. This has already been shown by Pettersen et al. [2002].

SF_6 in CO_2

Adding SF_6 to the CO_2 did not improve the surface finish of the magnesium. In fact, the surface finish was of a poorer quality than the ones with SF_6 in air. This is somewhat surprising since a mixture of SF_6, air and CO_2 is reported to give good protection, and even used for industrial purposes [Fruehling, 1970]. Couling and Leontis [1980] registered improved protection with a mixture of air, CO_2 and SF_6. The amount of CO_2 in the gas varied between 30 and 70%. Since the only difference between the two atmospheres is air, it must be oxygen that is the key to give a better surface finish. The reaction products should be the same as with SF_6 in air, with magnesium oxide as the dominant phase. However, this is not the case looking at the analysis of the sample surfaces. There is much more fluorine than oxygen, and the high values of fluorine at the surfaces of the samples suggests formation of magnesium fluoride.

SO_2 in air

As was seen in Figure 2.12, the film at the sample exposed to 1% SO_2 in air for 5 minutes had wrinkled up. It is not possible to tell whether this happened during the experiment or during quenching.

When the amount of SO_2 in air was lowered to 0.2%, magnesium oxide started depositing on the furnace walls and magnesium condensed on the scraper. A part of the surface which was situated just below the gas inlet was shiny and seemed to be well protected. Therefore, one can say that it may be possible to protect molten magnesium from oxidation with as little as 0.1 or 0.2% SO_2 in the gas, but then the gas distribution system becomes very critical. If you need a gas inlet every 5 cm, this is probably not a good solution. It should also be considered that this is a value attained in a laboratory furnace. In practice, one does not have such a closely controlled system and the amount of SO_2 needed will probably increase. This will magnify the disadvantages with SO_2 which have already been discussed in the literature review chapter.

Magnesium sulphate has a high Pilling-Bedworth ratio of 3.2, which means that a ratio of 1 is achieved with only 8% $MgSO_4$ in an MgO film. The corresponding numbers for magnesium sulphide is 1.44 and 30%. Although magnesium sulphate has the "best" Pilling Bedworth ratio, magnesium sulphide is the most thermodynamically stable phase as was seen in Figure 1.6. According to the calculations performed in FactSage, only sulphide should form.

Sulphur is found at the surfaces of these samples. It is not possible to tell whether it is bound as magnesium sulphide or as sulphur in MgO. It is also difficult to tell how much of the film that these phases add up to due to the uncertainty connected to the oxygen content.

SO_2 in nitrogen

Also SO_2 in nitrogen (Figure 2.17) did not provide satisfactory protection of the molten metal although there is oxygen in the sulphur dioxide. The calculations performed in FactSage show that these conditions should give almost equal amounts of magnesium oxide and sulphide, but relatively small amounts. The amount of oxygen corresponded to MgO, and the amount of sulphur was low.

SO_2 in CO_2

SO_2 in CO_2 seemed to protect the metal well. In the first series, the surface contained high amounts of fluorine when there was not supposed to be any fluorine there at all. This taught us an important lesson: Once you get fluorine into the furnace, it remains there for a long time. Since there was fluorine, one can not really determine whether the protective effect was due to the gas mixture of SO_2 in CO_2, or if it was due to the fluorine. However, also when the experiments were repeated after the refractory materials had been replaced, the gas mixture still gave a good protective effect. The high value of magnesium indicates that the film was very thin.

It is surprising that hardly any carbon or sulphur was found in these samples.

CO_2

The only reaction products between molten magnesium and CO_2 should be magnesium oxide and solid carbon as seen in Figure 1.8. It is not likely that magnesium carbonate will form. Magnesium carbonate will decompose at 350°C, and is therefore not stable at temperatures when magnesium is melted. There was little carbon at the sample surfaces, but much oxygen which may confirm the presence of magnesium oxide. The "secrete" of CO_2 may be that CO_2 reacts slowly with magnesium, thus giving the surface layers time to realign and prevent evaporation of magnesium.

The fact that there is less carbon than expected may imply that there was little gas available compared to the amount of metal for example in the beginning of the experiment. Then, no carbon forms due to a finite solubility of carbon in magnesium as is seen from Figure 1.8.This may lower the average carbon content of the film.

An atmosphere of pure CO_2 seemed to protect the molten magnesium well, but the surface was discolored, and that is an unwanted effect. The fact that pure CO_2 protects liquid magnesium is in accordance with Fruehling's work [1970], although the films formed in his experiments appeared metallic. One of the greatest problem with using CO_2 industrially might be to attain a sufficiently pure CO_2 atmosphere above the melt. It was therefore tested how much air the furnace atmosphere could contain while still protecting the metal from excessive oxidation.

Even with 20% air in CO_2, the magnesium did not oxidize uncontrollably. However, when the amount of air in CO_2 exceeded 3-4%, the surfaces became black with a carbon-like layer. The formation of the black surface might be a problem, but since the film/black layer seems to be very thin and partly like a powder, it might be removed mechanically. For example, the surface could be brushed with steel wool, or something similar. Of course, this is an extra step that increases the production costs. It is also a possibility to sell the metal as it is, and let the buyer do what is necessary. Perhaps magnesium producers could sell "environmentally friendly magnesium" produced with CO_2 cheaper than magnesium produced with SF_6. The costumer may have to machine away the discolored surface, but gets cheaper metal. The producer might even employ some of their CO_2 off-gases for the protection of the magnesium. The experiments demonstrate that a leakage of air is not catastrophic, and therefore the gas systems covering the melt do not have to be 100% tight.

CO_2 is already used for casting in some plants and foundries. Concern has to be taken regarding the gas delivery system. Using CO_2 as melt protection for holding furnaces may be more problematic. Since a film containing carbon may form on the surface, carbon may be drawn into the melt during operations such as alloy addition. It has been stated that carbon has a strong negative effect on the corrosion resistance in magnesium. Comparison of the carbon content from the films formed in air with SF_6 and films formed in CO_2 shows that the CO_2 films contain approximately twice as much carbon, but still only about 1% as was seen from the microprobe results.

Fluorine contamination
During these experiments, it seemed that if you let fluorine enter your system, it is almost impossible to get rid of it again. Samples exposed to pure CO_2 while the furnace was contaminated with fluorine had a very nice and shiny surface, similar to the ones exposed to SF_6 in air. Maybe this fact could be exploited in some way to protect molten magnesium. If you are able to "contaminate" your system with fluorine, it may help protect the metal as long as there is some fluorine left.

CONCLUSION

Different gas-mixtures as an alternative to SF_6 in air have been tested to determine if they protect molten magnesium from oxidation and evaporation.

Inert gases (Ar and N_2) as carrier gases for SF_6 and SO_2 do not build protective films, and can therefore not be used.

Pure CO_2 as a gas atmosphere provides good protection, although the surface finish is not excellent. A small amount of air in the CO_2, say 1-2%, does not affect the protective ability of the gas, but a black soot like layer forms at the surface as the amount of air in the gas increases to 3-4%, although there is not a significant increase in the carbon content of the surfaces with increasing amount of air in the CO_2. Even with 20% air in the CO_2 gas, the metal did not oxidize uncontrollably. CO_2 seems to react slowly with magnesium, and possibly allows the MgO to realign and prevent evaporation of magnesium.

SF_6 in CO_2 was surprisingly not a successful combination in these experiment, but experience in the industry and other people's work indicates that when air is added, it can be used with success.

0.2% SO_2 in air seemed to be a critical limit for how low it was possible to go in SO_2 content in the experimental unit employed here. The surfaces probably contain magnesium sulphide in addition to magnesium oxide, or even sulphur dissolved in MgO. SO_2 in CO_2 also provides good protection, but gives a discolored surface.

BIBLIOGRAPHY

Cashion, S.P. (1998) The Use of Sulphur Hexafluoride for Protecting Molten Magnesium PhD-thesis The University of Queensland, Australia.

Couling S.L. and Leontis T.E. (1980) Improved Protection of Molten Magnesium with Air/CO_2/SF_6 Gas Mixtures. *Light Metals*:997-1009.

Fruehling, J.W. (1970) Protective Atmospheres for Molten Magnesium. Ph.D. thesis, University of Michigan.

Kubaschewski, O. and Hopkins, B.E. (1953) Oxidation of Metals and Alloys. Butterworths Scientific Publications, London.

Pettersen, G., Øvrelid, E., Tranell, G., Fenstad, J. and Gjestland, H. (2002) Characterisation of the Surface Films Formed on Molten Magnesium in Different Protective Atmospheres. *Materials Science and Engineering A* **332**:285-294.

Turkdogan, E.T. (1980) Physical Chemistry of High Temperature Technology, Academic Press, New York, pp.253-256.

Chapter 3 .
High-temperature Microscope Studies of Films on Magnesium

Magnesium oxide/fluoride films on magnesium protected by air and SF_6 at temperatures ranging from 635°C to 705°C, are studied as they are formed. The experiments are performed with a hot stage microscope. Magnesium samples treated with SF_6 in air, are heated to various temperatures, both above and below the melting point, and held there for specified holding times. The partial pressure of SF_6 in the gas is varied between 0.5% to 5%. Under the microscope, the samples can be observed and pictures taken. Samples were taken out and examined with electron microprobe (EPMA), Transmission Electron Microscope (TEM), regular scanning electron microscope (SEM), Field Emission SEM and Focused Ion Beam Milling (FIB) to study the structure of the film, the surface and to determine the thickness of the oxide layer.

Since also CO_2 and SO_2 in air are known to protect molten magnesium, and since the hot stage provided samples with a very well-defined surface film, experiments are also performed with these gases in the hot stage. The purpose is to produce films that are suitable for further studies, for example with the microprobe to determine the composition of the surface and to see if other phases form during the experiment that can be observed through the optical microscope.

EXPERIMENTAL

Experimental unit, Linkam TS1500

The Linkam TS1500 is a high temperature heating stage for microscopy. The heating rate can vary from 1°C/min to 130°C/min and a maximum temperature of 1500°C can be reached. The desired temperature profile/run can be programmed with the controller, TMS 93. As can be seen from Figure 3.1, the heating rate can be varied during the run, and the sample can be held at a particular temperature for as long time as wanted.

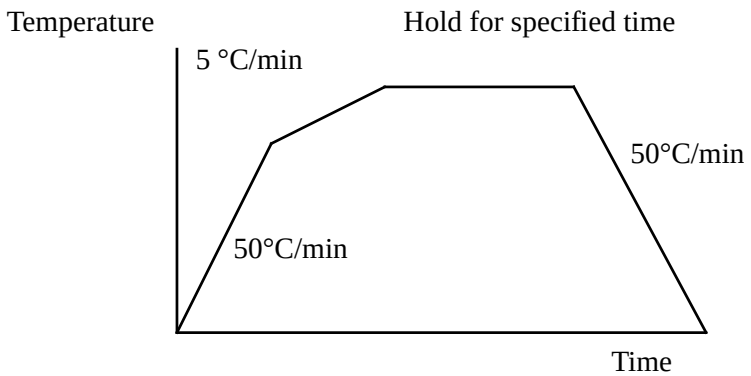

Figure 3.1 An example of a typical temperature-time profile. The sample is initially heated at a rate of 50°C/min. Then the heating is slower, 5°C/min. When the desired temperature is reached, the sample is held there for the specified time before it is cooled.

Figure 3.2 shows a picture of the heating stage. There is a window in the middle of the lid where one can look down on the sample. The chamber is water cooled, and there are inlets and outlets for water on the top lid and on the sides of the chamber. Also there is one inlet and one outlet to allow gas flow though the furnace. The gas flow can be maximum 60 ml/min without disturbing the temperature inside the chamber.

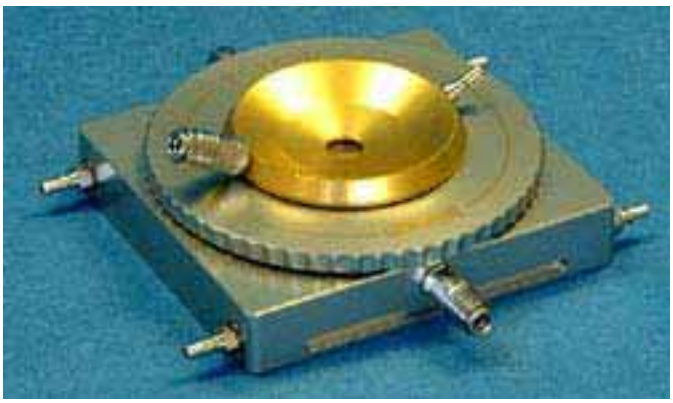

Figure 3.2 The heating stage TS1500.

Platinum heating wires are wound around a ceramic cup which forms the sample chamber shown in Figure 3.3. The reason for placing the sample on a sapphire disc is to prevent contamination of the sample chamber. Sapphire has excellent heat transfer properties and is a material well suited for high temperatures. A radiation shield is placed on top of the sample chamber. This ensures that the sample attains an even temperature, and also protects the lens of the microscope from high temperatures. The controlling thermocouple is cemented into the bottom of the sample chamber. The thermocouple, type S Pl-10% Rh/Pl is connected to the controller and the temperature registered is displayed in the window. There is, however, a difference between the temperature registered by this thermocouple and the true temperature of the sample. Therefore, a calibration has to be performed.

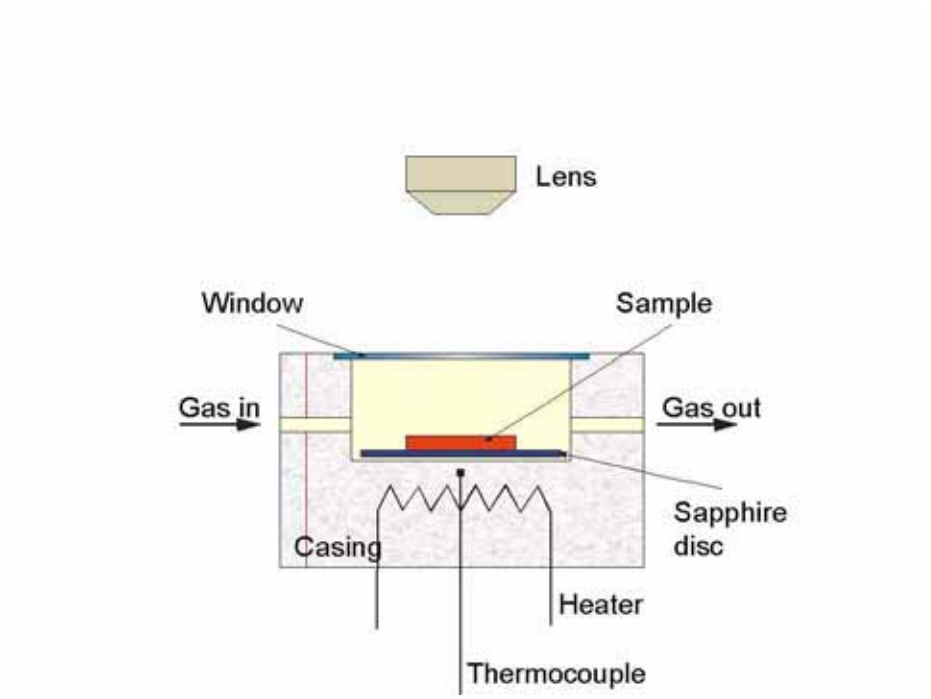

Figure 3.3 The illustration shows the sample placed inside the furnace chamber.

Calibration

The calibration was performed by melting elements or compounds with a known melting point. Several criteria have to be satisfied for a good calibration standard [Roedder, 1984]. We found that metals that form a ball during melting, are advantageous to use. Criteria for a good calibration standard are presented in Appendix 3.

In the calibration the following standards with their respective melting point were employed, Table 3.1:

Table 3.1: The standards used for calibration and their melting points.

Standard	Melting point (°C)
Te	450
NaCl	801
Ag	961
Au	1063

Attempts were made to use antimony, but this did not succeed.

A few, very small pieces of the standard were placed on the sapphire disc in the bottom of the crucible. Silver and gold shavings were used, which upon melting will form a ball. The melting point will therefore be easily observed. The standards used should of course be as pure as possible.

A stream of argon of approximately 20-30 ml/min flows through the hot stage during calibration. Hopefully, this can partly prevent oxidation of the samples during heating.

The samples were heated at a rate of 50°C/min up to 5-10°C below the known melting point. From there, the standards were heated at a low rate, usually 1°C/min until melting was observed. The temperature measured with the thermocouple shown on the controller, T_C, was registered and the deviation between T_c and the true melting point of the standard was found. The results are plotted in Figure 3.4 where the deviation is given as a function of the melting point.

As is seen from the figure, the thermocouple measures a higher temperature than the true temperature of the sample.

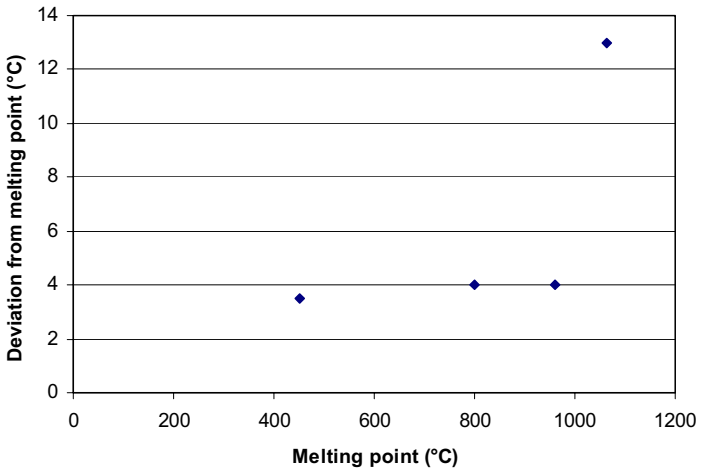

Figure 3.4 The graph shows the deviation between the true temperature of the sample and what is shown on the controller at different temperatures. Gas flow is 30 ml argon/min.

There are several reasons why there is deviation between the true temperature of the sample and what is registered by the thermocouple. As mentioned, the sample is placed on a sapphire disc. This means that the sample is not in direct contact with the thermocouple that measures the temperature displayed on the controller. The sapphire disc is supposed to provide good contact between the sample and the cemented layer around the thermocouple. Still there is a difference between the thermocouple and the sample temperatures.

Temperature measured is the temperature at the bottom of the sample, the part that is in contact with the sapphire disc.

In the following, the values of T_c given by the thermocouple are reduced by 4°C.

Sample preparation

Magnesium samples were prepared by cutting discs approximately 2 mm thick from a 5 mm in diameter magnesium rod. The analysis of the magnesium metal is given in below:

Al 0.0111 %
Zn 0.0001 %
Mn 0.0164 %
Fe 0.0011 %
Cu 0.0000 %
Ni 0.0000 %
Pb 0.0000 %
Sn 0.0000 %
P 0.0001 %
Ca 0.0003 %
Na 0.0002 %
Cd 0.00000 %
Mg 99.9363 %

The samples are mounted into plastic and ground and polished. Afterwards, the plastic with the polished samples is cooled in liquid nitrogen so that the plastic easily cracks and the samples can be taken out. The samples are kept in ethanol to prevent unnecessary oxidation before the experiments start. Still, one can expect that there is an oxide layer on the surface. Nordlien et al. [1997] studied naturally formed oxide films on pure magnesium. Samples exposed to the atmosphere with 35-55% humidity at 25-30°C for 15-60 minutes were found to have a dense film of approximately equal amounts of magnesium oxide and magnesium hydroxide. The thickness of the film was between 20 and 50 nm.

Procedure

The sample was placed on the sapphire disc inside the heating chamber. The gas mixture, either SF_6 in synthetic air, pure CO_2 or 1% SO_2 in synthetic air, approximately 30 ml/min, was allowed to flow through the furnace. The partial pressure of SF_6 in air was varied, as mentioned, between 0.5 and 5%. Five different heating programmes were used. The sample was always heated at a heating rate of 50°C/min up to 30°C below the maximum temperature. Then the heating rate was lowered to 5°C/min until the holding temperature is reached, see Figure 3.1. The five holding temperatures are 635, 665, 685, 700 and 705°C. Holding time varied between no holding time at all to 53 hours. All the experiments performed, with the maximum temperatures, holding times, partial pressure of SF_6 and analysis methods are given in Tables 3.5-3.8. Pictures were taken before the experiments is started and during the run.

Image analysis

As will be shown later in Figure 3.6, “spots” start appearing on the surface on many of the samples. The size and the number of these spots was studied, and the

fraction of the surface that they cover as a function of time. The number of spots in one particular area (≈ 50700 μm^2) of the surface was counted manually from pictures taken at various times throughout the experiment.

An average size of the spots was determined in the following way: Five different spots within the area already mentioned, were monitored on each picture taken over a period from 1 hour to 53 hours. The area of each spot was found by enlarging the pictures 160 times on the computer screen. This made it possible to count the number of pixels that one spot is made up of. The average size and the number of spots within the particular area chosen is given in Appendix 2. The greatest problem with counting manually like this, is to decide which pixels to include into the particle and which ones to exclude. To minimize this error, the counting of all spots in one experiment was done on the same day and under the same light conditions.

Given these data, it was possible to calculate the fraction of the surface covered with these spots.

It was also attempted to calculate the fraction of the surface covered with spots using image analysis. Here too, one has to determine which shadows of grey to include in the spots, and which shadows that should be excluded. Once you have made this decision, the computer does the rest of the work.

Microprobe analysis (EPMA)

Some of the samples where one clearly could see spots or different phases were analyzed with the microprobe. The samples were analyzed with so-called mapping which determines where in the sample a particular element is found. In this case, the elements of interest are of course magnesium, oxygen and fluorine. Aluminum was included in one sample since the sample material contained 0.01% aluminum. Sulphur was not included in the SF_6 samples as experience as well as other studies (Pettersen et al.[2002], Cashion et al. [2002]) have indicated that this is not an active element regarding melt protection. However, carbon and sulphur were included for the samples exposed to CO_2 and SO_2.

To try to estimate the thickness of the films, various methods were employed. These are discussed in the following. Initially, a relative electron microprobe method was used. The chemical composition of the surface of the sample was analyzed with increasing accelerating voltages. It was assumed that all the oxygen and fluorine is found as magnesium oxide and magnesium fluoride. If you then still have some “free” magnesium, that is magnesium not bound to either oxygen or fluorine, then it can be assumed that the electron beam has

penetrated through the film, and down into the bulk metal. At the particular accelerating voltage where the amount of free magnesium is zero, one can assume that the depth of the film equals the penetration depth of the electron beam which can be calculated with Monte Carlo simulations. For further details on Monte Carlo simulations, see Joy [1991]. However, using these simulations to determine thickness turned out to be a rather problematic method.

Transmission Electron Microscope (TEM)

Cross sections of three samples were prepared for the transmission electron microscope (TEM). The intention was to measure the film thickness. This gives a more reliable measurement of the film thickness since you actually can see the film. Only three samples were studied since sample preparation for TEM is both a very time consuming and demanding task.

Scanning Electron Microscope (SEM)

It was attempted to use a regular SEM to measure thickness on cross sections of the films formed. The pictures did not show the film clearly in most of the cases, and it was therefore hard to interpret the pictures and to estimate a thickness.

Field Emission SEM

Field Emission SEM gives improved resolution, and thereby better pictures.

Focused Ion Beam Milling (FIB)

Focused Ion Beam Milling was used to visualize the mophology of the surface. An electron beam of Ga ions cuts down through the sample. The beam cuts down through the surface layer and down to the bulk metal, giving a cavity in the sample.

X-ray Diffraction (XRD)

It was attempted to determine the lattice parameters of the surface films using x-ray diffraction. The samples were not ideal for this kind of analysis since the surfaces are not completely even and the films are thin. The results are therefore given in Appendix 6.

Experiments conducted

In the tables below is given a summary of all the experiments performed with the hot stage. Table 3.2 describes an initial experiment, Table 3.3 presents the experiments performed in 1% SF_6 in air, Table 3.4 the experiments in 5% SF_6 and Table 3.5 experiments in 0.5% SF_6 and Table 3.6 with 2% SF_6. In addition to the holding temperature and time for the samples, the various analysis techniques employed on each sample are included. Where pictures are presented in the text, this is referred to in the table. The names of the samples are chosen arbitrarily. However, the samples whose names start with an E-, are experiments performed by Eriksen [Eriksen, 2003].

The four experiments performed in pure CO_2 are given in Table 3.7, while the experiments in SO_2 in air are found in Table 3.8.

Table 3.2: Initial experiment in 1% SF_6 in air.

Sample name	Heating profile	Analysis
A	Heat with 50°C/min to 635°C, hold for 2 min, then heat with 2°C/min to 662°C, hold for 3 min., cool with 50°C	EPMA: Fig. 3.6

.

Table 3.3: Experiments performed in 1% SF_6 in air. Given in the table is the holding time at the maximum temperature, the various analytical methods used, referred to figures presented in the text. IA= Image Analysis MC= Monte Carlo simulations

Sample name	Holding temperature (°C)	Holding time (min)	Analysis	Sample name	Holding temperature (°C)	Holding time (min)	Analysis
H	665	120		T	635	300	MC
I	665	3120	IA:Fig.3.6-3.12, FIB, MC	U	665	0	
J	665	30	MC	V	665	60	MC
K	665	60		W	665	0	MC
M	665	0		X	665	10	MC
N	665	5	MC	Y	635	10	MC
O	665	10		Z	635	60	FIB
P	665	60		Æ	635	0	MC
Q	635	0		Ø	635	30	MC
R	635	10	MC	AA	635	60	TEM, MC
S	635	30		AB	685	5	MC

Table 3.3: (Continued)Experiments performed in 1% SF_6 in air. Given in the table is the holding time at the maximum temperature, the various analytical methods used, referred to figures presented in the text. IA= Image Analysis MC= Monte Carlo simulations

Sample name	Holding temperature (°C)	Holding time (min)	Analysis	Sample name	Holding temperature (°C)	Holding time (min)	Analysis
AC	665	300	MC	AN	635	200	MC
AD	685	0	MC	AO	665	200	TEM, MC
AE	685	20	MC	AP	685	200	MC
AG	685	5	MC	AQ	705	10	FIB
AH	685	80	MC	AR	705	30	
AI	685	160	MC	AS	705	60	Fig.3.18, EPMA:Fig.3.19
AJ	685	10	FIB, MC	AT	705	300	FIB
AK	685	40	TEM, Fig.3.26,MC, Fig.3.27	AU	705	100	
AL	685	320		AV	705	200	XRD:Appendix 6
AM	665	300	Fig. 3.13, FIB:Fig. 3.29, EPMA: Fig. 3.21				

Table 3.4: Experiments performed in 5% SF_6 in air. IA= Image Analysis MC= Monte Carlo simulations

Sample name	Holding temp. (°C)	Holding time (min)	Analysis	Sample name	Holding temp. (°C)	Holding time (min)	Analysis
BA	635	60		E4	635	30	EPMA
BB	635	30		E5	635	60	EPMA
BC	635	200		E6	635	1440	EPMA, SEM
BD	635	100		E7	665	5	EPMA
BE	685	100		E8	665	20	Fig. 3.17, EPMA, SEM
BF	685	60		E9	665	30	EPMA
BG	635	300		E10	665	60	EPMA, SEM
BH	635	10		E11	665	1440	EPMA, SEM
BI	685	10	Fig. 3.5, EPMA:Fig. 3.20	E12	685	5	EPMA, SEM
BJ	685	30		E13	685	10	EPMA, SEM
BK	685	200	XRD:Appendix 6	E14	685	20	EPMA, SEM
E1	635	5	EPMA	E15	685	30	EPMA
E2	635	10	EPMA: Fig. 3.15	E16	685	60	EPMA, SEM
E3	635	20	EPMA				

Table 3.5: Experiments performed in 0.5% SF_6 in air.

Sample name	Holding temperature (°C)	Holding time (min)	Analysis
E17	665	150	EPMA, FE-SEM: Fig. 3.22
E18	700	120	EPMA, FE-SEM: Fig.3.28
E19	700	150	

Table 3.6: Experiment performed in 2% SF_6 in air.

Sample name	Holding temperature (°C)	Holding time (min)	Analysis
DA	700	300	XRD: Appendix 6

Table 3.7: Experiments performed in pure CO_2.

Sample name	Holding temperature (°C)	Holding time (min)	Analysis method
GA	685	60	
GB	685	120	
GC	665	60	
GD	635	60	Fig.3.30 EPMA: Fig. 3.31

Table 3.8: Experiments performed in 1% SO_2 in air.

Sample name	Holding temperature (°C)	Holding time (min)	Analysis method
FA	635	180	Fig. 3.32, Table 3.14, EPMA: Fig. 3.33
FB	685	120	
FC	665	60	

RESULTS

The results from the experiments performed with SF_6 in air are presented first. The results from the experiments in CO_2 and SO_2 in air are given towards the end of this section.

First, two features of these experiments in SF_6 should be denoted: The surface film that forms on the sample seems to be very strong: The reason for this is that even though the sample melts, the surface film keeps the sample in its place. That is, there is hardly any difference in the shape between a sample that has melted, and a sample that has not.

The other issue worth noting, is that the surface film seems to "crack" when the metal below melts. This is easily observed under the microscope: As the temperature goes past the melting point, the surface suddenly "cracks", and the surface is not that smooth any more.

In 24 of 41 samples, the formation of spots were observed when samples were exposed to 1% SF_6 in air at elevated temperatures. The samples where spots were formed is indicated in Table 3.9. These spots turned out to be very rich in fluorine, and are therefore most likely MgF_2 particles.

For the experiments with 5% SF_6 in air, the surfaces do not have the distinct MgF_2 particles. Almost every sample has a finer structure as seen in Figure 3.5. This structure is discussed more thoroughly in Figure 3.20. The samples where this structure is formed are indicated in Table 3.9.

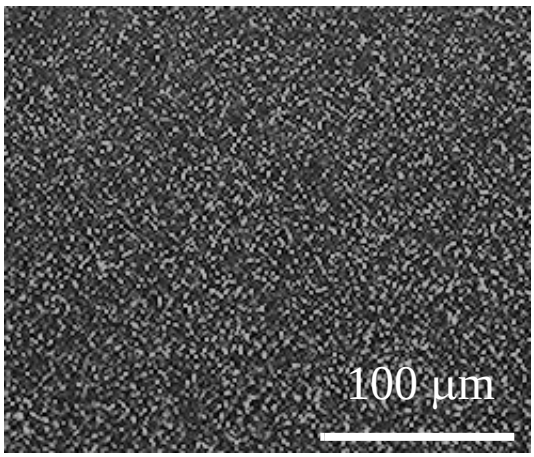

Figure 3.5 Sample exposed to 5% SF_6 in air at 685°C for 10 minutes. See sample BI Table 3.4. Picture taken in optical microscope.

For the three samples exposed to 0.5% SF_6 in air, it is not possible to say that they have a characteristic appearance. Spots were observed in one of the samples when looking at cross sections with FE-SEM, but not in the two others. See Table 3.9.

Table 3.9: Samples where MgF_2 and the finer structure is seen. + indicates the presence of the structure.

Sample name	Holding temperature (°C)	Holding time (min)	p_{SF6}(%)	MgF_2 particles	Fine structure
H	665	120	1	+	
I	665	3120	1	+	
J	665	30	1	+	
K	665	60	1		
M	665	0	1		
N	665	5	1	+	
O	665	10	1	+	
P	665	60	1		
Q	635	0	1		
R	635	10	1		
S	635	30	1	+	

Table 3.9: (Continued) Samples where MgF_2 and the finer structure is seen. + indicates the presence of the structure.

Sample name	Holding temperature (°C)	Holding time (min)	p_{SF6}(%)	MgF_2 particles	Fine structure
T	635	300	1	+	
U	665	0	1		
V	665	60	1	+	
W	665	0	1	+	
X	665	10	1	+	
Y	635	10	1		
Z	635	60	1		
Æ	635	0	1		
Ø	635	30	1	+	
AA	635	60	1		
AB	685	5	1		
AC	665	300	1		
AD	685	0	1		
AE	685	20	1		
AG	685	5	1	+	
AH	685	80	1	+	
AI	685	160	1	+	
AJ	685	10	1		
AK	685	40	1		
AL	685	320	1	+	
AM	665	300	1	+	
AN	635	200	1	+	
AO	665	200	1		
AP	685	200	1	+	
AQ	705	10	1		
AR	705	30	1	+	
AS	705	60	1	+	
AT	705	300	1	+	
AU	705	100	1	+	
AV	705	200	1	+	
BA	635	60	5		+
BB	635	30	5		+
BC	635	200	5		+
BD	635	100	5		

Table 3.9: (Continued) Samples where MgF_2 and the finer structure is seen. + indicates the presence of the structure.

Sample name	Holding temperature (°C)	Holding time (min)	p_{SF6}(%)	MgF_2 particles	Fine structure
BE	685	100	5		+
BF	685	60	5		+
BG	635	300	5		+
BH	635	10	5		+
BI	685	10	5		+
BJ	685	30	5		+
BK	685	200	5		+
E1	635	5	5		
E2	635	10	5		
E3	635	20	5		+
E4	635	30	5		
E5	635	60	5		+
E6	635	1440	5		+
E7	665	5	5		
E8	665	20	5		+
E9	665	30	5		
E10	665	60	5		+
E11	665	1440	5		+
E12	685	5	5		+
E13	685	10	5		+
E14	685	20	5		+
E15	685	30	5		
E16	685	60	5		+
E17	665	150	0.5	+	
E18	700	120	0.5		
E19	700	150	0.5		

Microscope studies, image analysis

The nine pictures below, Figure 3.6, illustrates, as the experiment proceeded, how the surface of a sample appeared looking through the optical microscope. The sample was held at 665°C for 2 days. The pictures are taken at the same position on the sample, starting at room temperature and ending when the sample had been held at 665°C for 48 hours.

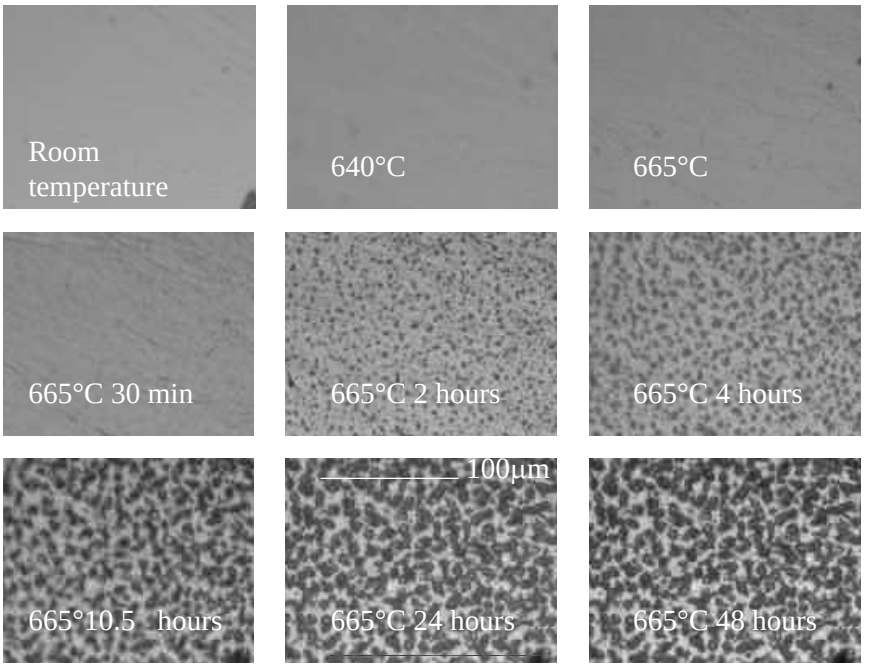

Figure 3.6 A series of micrographs taken in the optical microscope from the same surface area of a sample held at 665°C in 1% SF_6 in air. Sample I in Table 3.3.

As seen from the pictures, the surface in this case seems to be covered with spots. These spots will later be shown to be MgF_2 particles.

Expanded images of the sample surface are given in Figures 3.7-3.9 after 4, 24 and 48 hours.

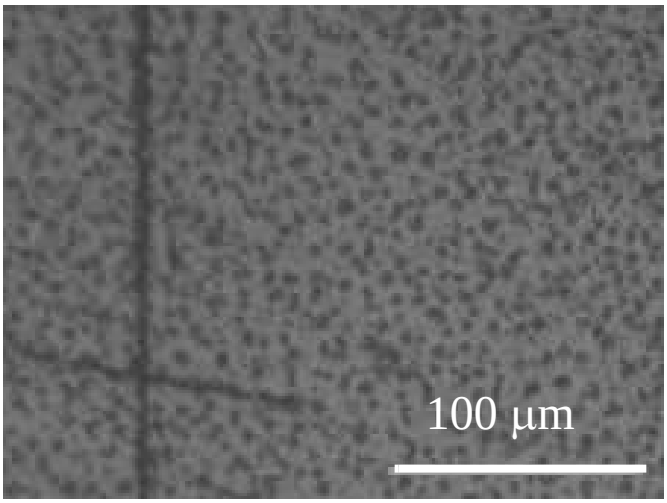

Figure 3.7 The surface of sample I in Table 3.3 after 4 hours in 1% SF_6 in air at 665°C, same sample as in Figure 3.6. Picture taken in optical microscope.

In Figure 3.7, the MgF_2 particle size can be estimated to be approximately 5 μm after 4 hours. The distance between the particles is roughly 10 μm.

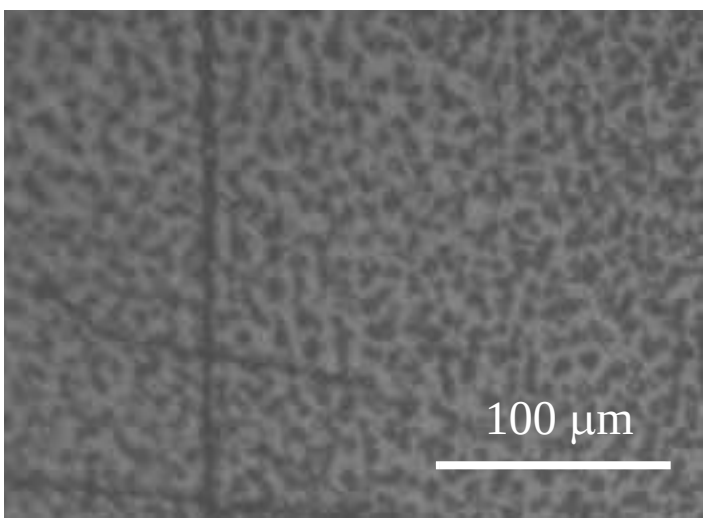

Figure 3.8 The surface of sample I in Table 3.3 after 10.5 hours in 1% SF_6 in air at 665°C, same sample as in Figures 3.6-3.7. Picture taken in optical microscope.

The particle “diameter” in Figure 3.8 is somewhere between 5 and 10 mm, and the spacing between them has decreased.

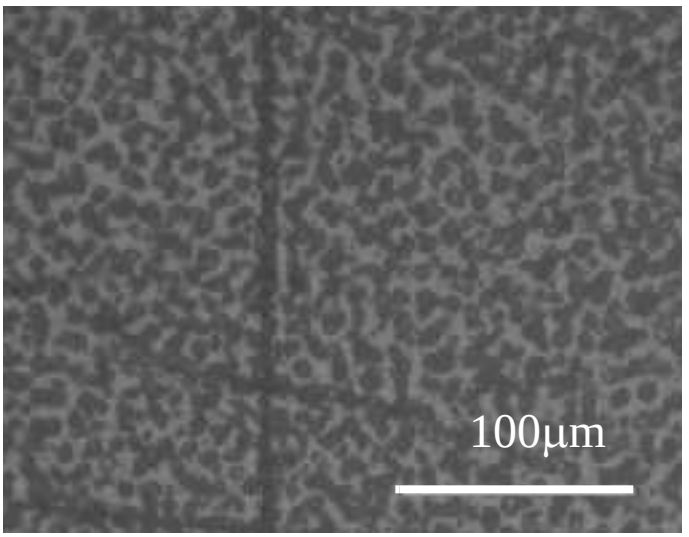

Figure 3.9 Closer look at surface of sample I in Table 3.3 after 48 hours in 1% SF_6 in air at 665°C. Picture taken in optical microscope.

In Figure 3.9, the spots have grown together, so that it is hard to separate them. However, approximately 10 μm would be a qualified guess for the size.

A comparison of the MgF_2 particle sizes and the distances between them found from various figures in the text, is presented in the discussion section, Table 3.15.

The number of spots (MgF_2 particles) within one particular area for the same sample as above is given in Figure 3.10. The actual numbers may be of limited interest, but the trend is important: The number of spots decreases as a function of time. After approximately 10 hours, the decrease seems to level out. The explanation for the decrease is most likely that since the spots grow with increasing exposure time, spots grow into each other and appear as one spot.

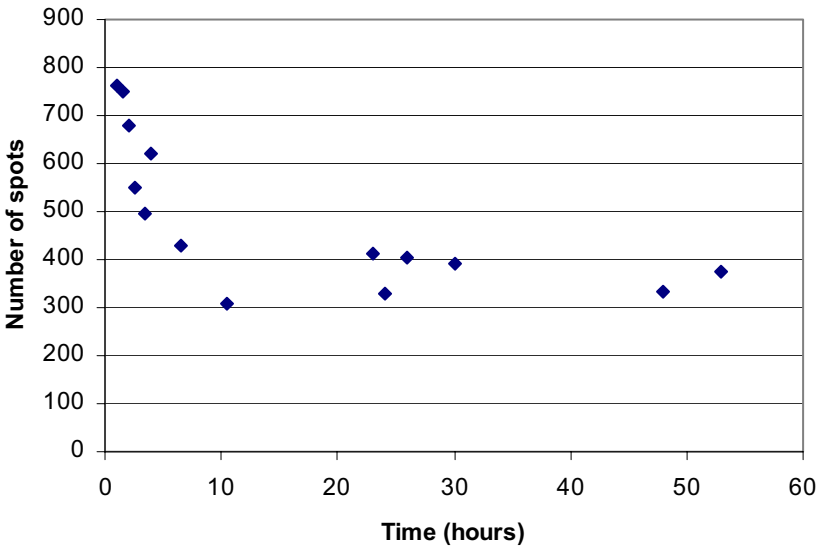

Figure 3.10 The number of spots in a particular area as a function of exposure time. Sample I in Table 3.3, same sample as in Figures 3.6-3.9.

Still considering the same sample as in Figure 3.10, Figure 3.11 gives the average size of five randomly chosen spots as a function of time. The size seems to level out after 10-20 hours. However, this does not have to mean that the spots cease growing. Possibly they can still grow in the direction perpendicular to the surface inwards into the film and bulk metal as will be discussed later.

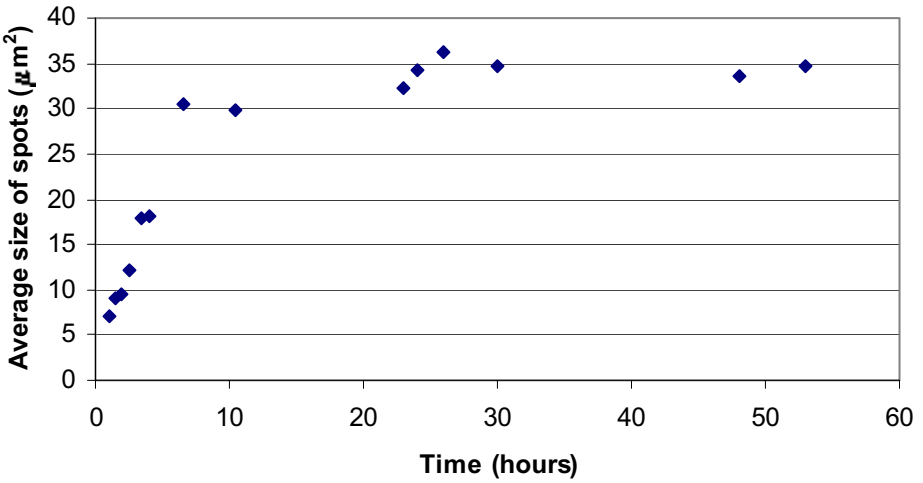

Figure 3.11 The figure gives the average size of one spot as a function of time for a sample held at 665°C in 1% SF_6 in air. Sample I in Table 3.3, same sample as in Figures 3.6 -3.10.

This analysis could have been performed by image analysis on a computer, but as mentioned there is one critical aspect, and that is the lighting used on the microscope when the pictures are taken. In the beginning of the experiment, very little light is necessary to take a good picture. As the experiment proceeds and the surface of the sample is getting duller, more light is needed to get a good picture. It is therefore a problem to compare two pictures since they are taken under different lighting conditions.

When the average size of the particles and the number of particles within one specific area is known, the fraction of the surface which is covered with spots can be calculated. This calculation is performed in Figure 3.12 from the data given in Figure 3.10 and 3.11. The triangles are the manually generated numbers and the squares are the fractions that were calculated using image analysis.

For the manually calculated fractions, the fraction covered levels out after approximately 10 hours. At that point, approximately 25% of the surface is covered with spots. For the computer generated numbers, the curve does not level out as early, but after two days, according to this estimate, 50% of the surface is covered with the spots.

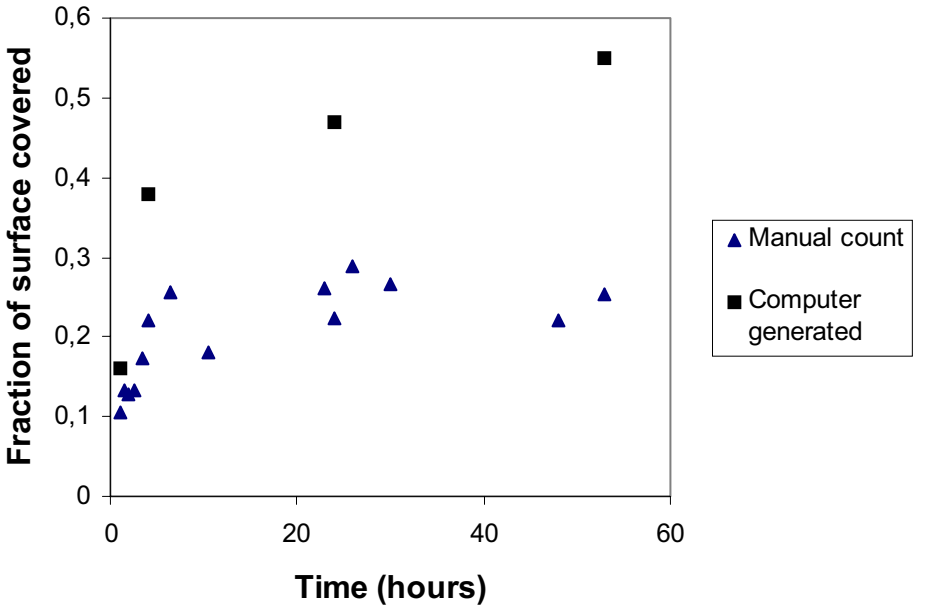

Figure 3.12 The figure shows the fraction of the surface which is covered with spots as a function of time. The data are from Figure 3.10 and 3.11. Sample I in Table 3.3, held in 1% SF_6 in air at 665°C.

Figure 3.10-3.12 are produced from the data given in Appendix 2.

Figure 3.13 shows a sample different from that in Figure 3.6 in the optical microscope. The "diameter" of the small MgF_2 spots is approximately 5 μm, while the distance between them is approximately 10 μm. Also some larger oxide flakes on top of the surface is seen in addition to the smaller MgF_2 particles. The size of the oxide flakes is approximately 10-20 μm.

It is difficult to say whether the flakes are formed during the experiment, or if they were formed after the sample were taken out of the hot stage and exposed to the atmosphere.

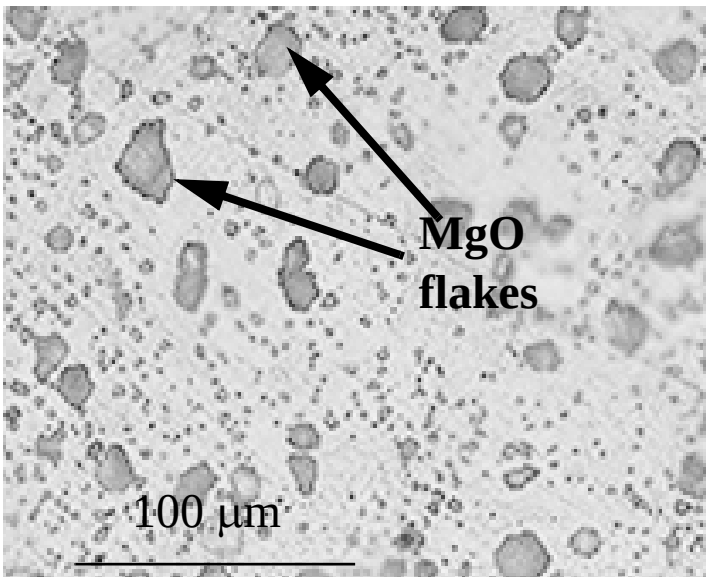

Figure 3.13 Micrograph taken with optical microscope of sample AM in Table 3.3, 665°C for 300 minutes in 1% SF_6 in air. Large magnesium oxide flakes on the surface are seen in addition to the smaller MgF_2 spots.

Microprobe "mappings"

A microprobe "mapping" from a test sample in 1% SF_6 in air, held at 640°C for 2 minutes, then 3 minutes at 667°C, is presented in Figure 3.14. An intensity scale for each element is given to the right in the figure. The analysis of the selected areas denoted in the upper left picture in Figure 3.14, is given in Table 3.10.

As can be seen from the element map, the spots that started appearing on the surface around 640°C contain large amounts of fluorine, which indicates that they are magnesium fluoride particles. This is confirmed by the point analysis, points 5 and 6 in Table 3.10: The spots contain large amounts of fluorine. The analysis showed that the areas with the spots contained 20/(20+17+6) = 47% MgF_2, 17/(20+17+6) = 40% MgO and 6/(20+17+6) = 14% Mg. The fact that there is not only magnesium fluoride, but also magnesium oxide and pure magnesium, is most likely due to the analytical method: It is not possible to focus the electron beam just exactly at the spot. The electron beam, which in this case is 10 μm in diameter, is larger than the spots, and the areas around will also contribute. The pure magnesium is a contribution probably because the electron beam penetrates through the film and down into the bulk metal.

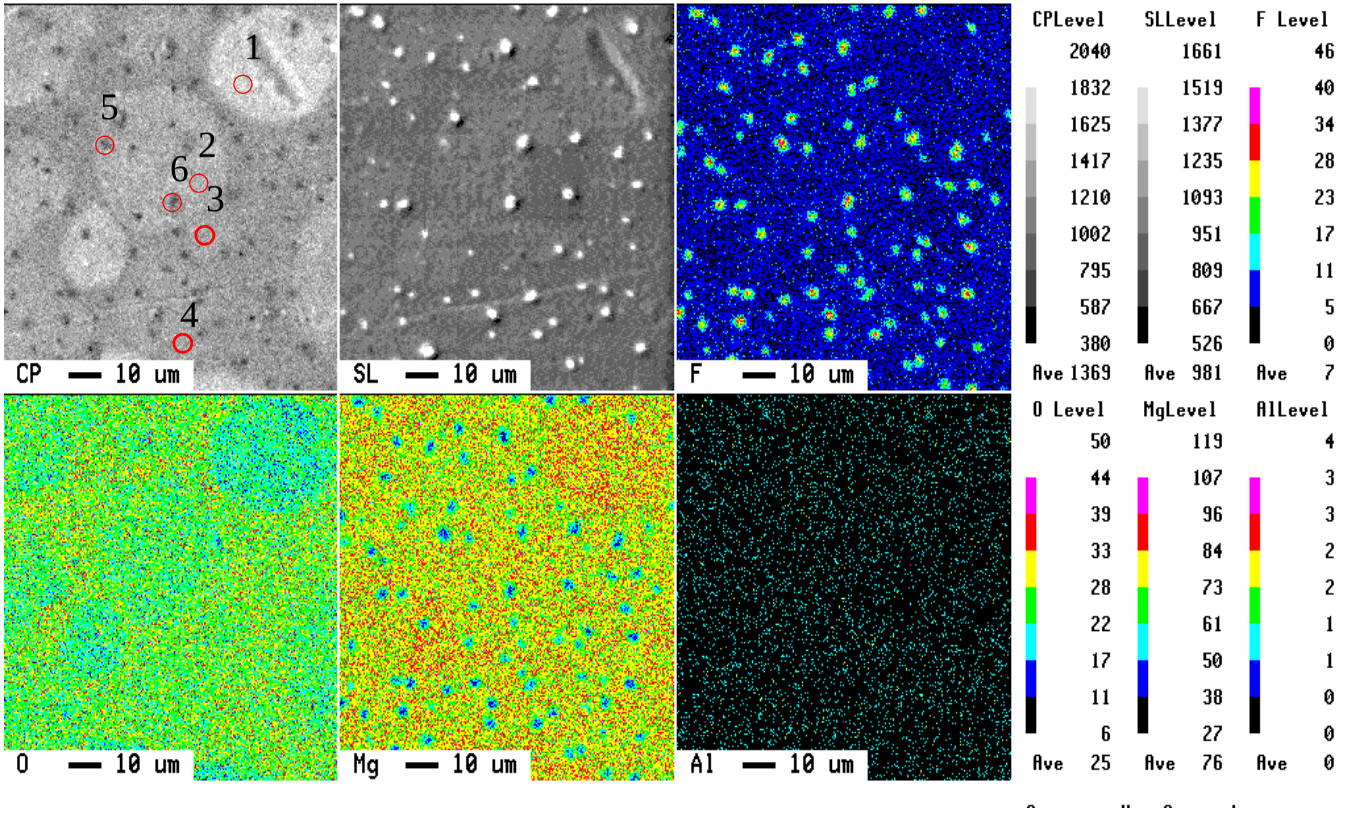

Figure 3.14 Microprobe element mapping of the magnesium surface exposed to 1% SF_6 in air. The sample is held at 640°C for 2 minutes, then 3 minutes at 667°C. Sample A in Table 3.2.

Again, we make a balance in terms of MgO, MgF_2 and Mg. The areas with no spots may be taken to contain 7/(7+22+35) = 11% MgF_2, 22/(7+22+35) = 34% MgO and 35/(7+22+35) = 55% Mg. The high amount of magnesium should mean that there is a large contribution from the bulk metal.

As will be seen later, the MgF_2 particles do no stand out from the surface as it may appear from the upper left picture in Figure 3.14. The MgF_2 particles form "droplets" at the interface between the film and the metal that go down into the metal. When one analyzes on such particles, the electron beam hits these droplets in addition to the bulk metal, and the analysis does not show that much magnesium.

In the upper left corner of Figure 3.14, some circular, lighter areas can be observed. From the mapping, it seems that they are a little poorer in oxygen. Points 1 and 2 in Table 3.10 are from such areas, and it is seen that we are only talking of areas with 1-2% less oxygen than in the areas around.

Table 3.10: Composition in atomic% of points denoted in Figure 3.14 measured with microprobe.

Point in Figure 3.14	C	S	O	F	Mg
1	0.7	0.2	20.0	12.5	66.7
2	0.7	0.1	21.3	13.4	64.5
3	0.7	0.2	23.1	13.6	62.5
4	0.7	0.2	22.5	13.7	62.9
5	0.5	0.1	16.6	39.1	43.6
6	0.6	0.1	17.3	39.8	42.1

The MgF_2 particles are approximately 5 μm in diameter. The distance between these particles is estimated to be approximately 10μm.

An other sample is studied in Figure 3.15. In this case, the sample is held at 635°C for 10 minutes. The gas mixture is 5% SF_6 in air. An intensity scale is given to the right in the picture.

The situation is a bit different in Figure 3.15 from other experiments with 5% SF_6: It appears that there are large magnesium oxide grains on the surface. The

phase in between these large grains seems to be slightly richer in fluorine than the grains themselves. Possibly it is magnesium fluoride since this phase is also low in oxygen. Between these large particles, at the grain boundaries, there are smaller particles. The ones that appear white in the picture in the upper left corner are low in fluorine, but high in magnesium. Also one can see some particles that appear darker in the same picture. It is difficult to determine the chemical composition of these particles. An illustration is sketched in Figure 3.16. The particles with unknown composition are drawn as small black spots.

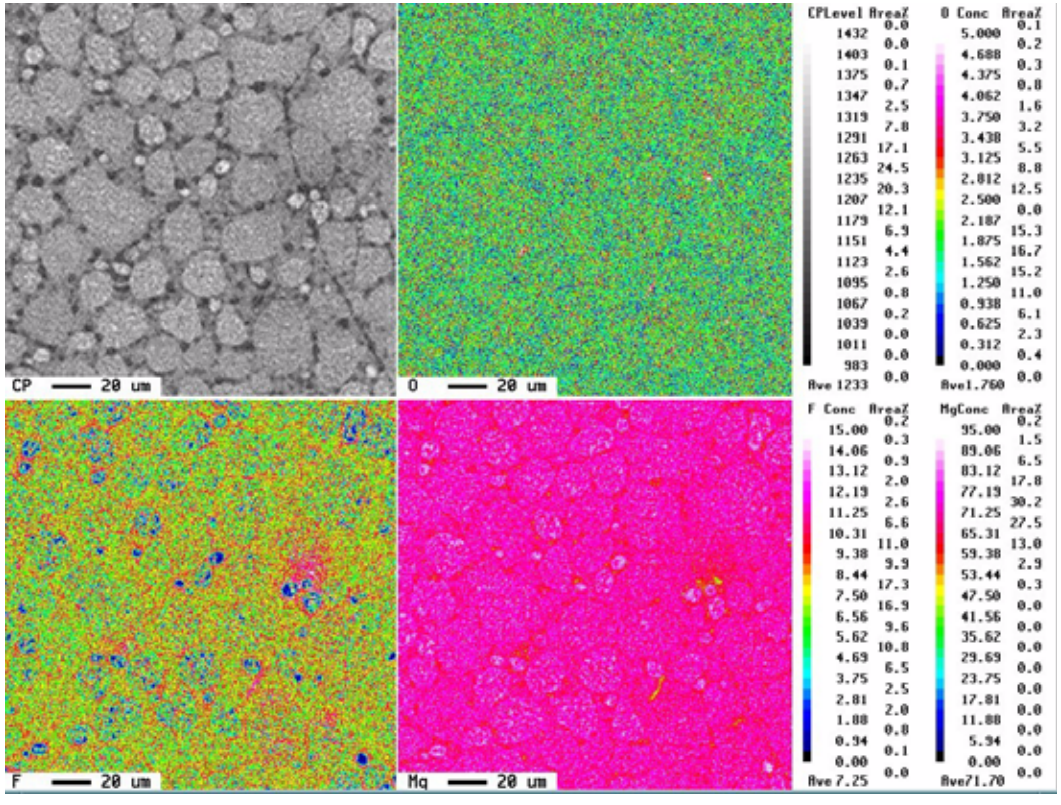

Figure 3.15 Microprobe “mapping” of sample held for 10 minutes at 635°C in a gas mixture of 5% SF_6 in air. Sample E2 in Table 3.4.

The oxide grain size in this sample is around 20-30μm, although some grains are even larger.

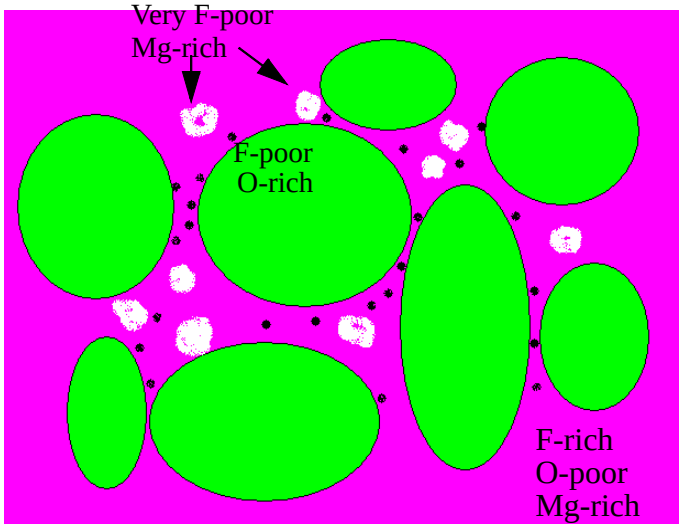

Figure 3.16 A simplification of Figure 3.15: The large oxide grains (green), matrix (red) and particles (white)

An almost similar structure is also seen on a sample held at 665°C for 20 minutes, also in 5% SF_6 in air, Figure 3.17. Ignoring the large grains, the structure looks very much alike the other structures formed in 5% SF_6, for example Figure 3.20.

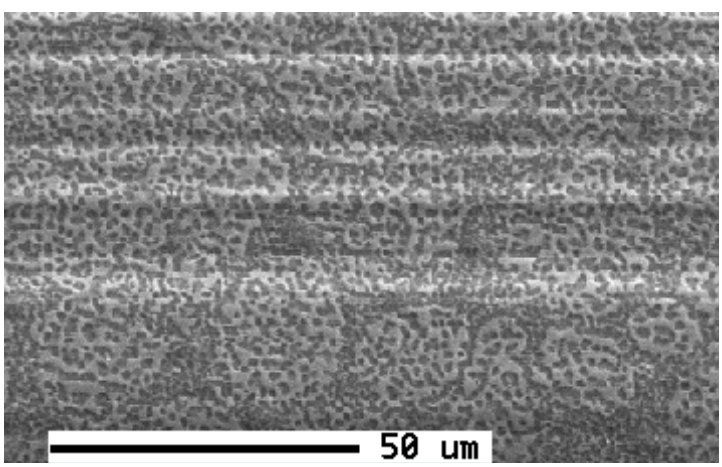

Figure 3.17 Sample held at 665°C for 20 minutes in 5% SF_6 in air. Sample E8 in Table 3.4. Picture taken with microprobe.

Unfortunately, there are some stripes disturbing the picture in Figure 3.17. Still, it is possible to see a structure somewhat similar to the one seen in Figure 3.15. The coarser magnesium oxide grains are observed, and also smaller “spots”. These “spots” seem to be evenly distributed all over the surface, not only at the grain boundaries as seen in Figure 3.15. Their composition has not been determined.

A third example of this particular structure is seen in Figure 3.18 and 3.19. This sample has been held at 705°C for 60 minutes. Also here it is seen that there are large grains that are rich in oxygen and magnesium, which probably means they are magnesium oxide. The matrix phase is richer in fluorine. Due to topography at the surface, there are some shadow effects on the edges of the oxide grains in Figure 3.19.

The micrograph from the optical microscope of this sample is presented in Figure 3.18. Here, one can see some smaller, dark particles which are most likely magnesium fluoride particles. Studying the mapping in Figure 3.19, one can see that the particles that lie inside a larger grain, are richer in fluorine than the grain itself, but not as rich as the matrix. This may be due to the experimental method, since the magnesium fluoride particles are positioned underneath the film, and the low acceleration voltage applied here has the purpose of only analyzing the surface.

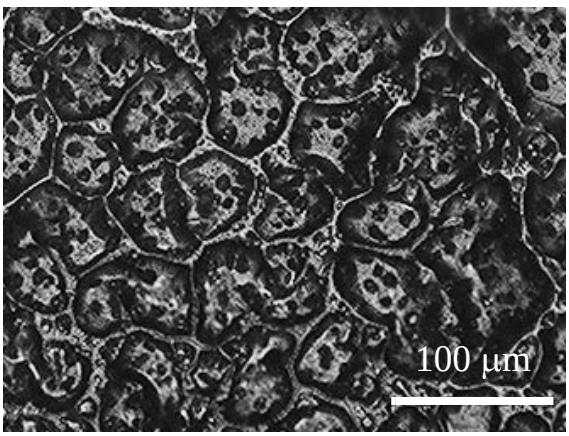

Figure 3.18 Micrograph taken in optical microscope. Sample AS in Table 3.3, 705°C for 60 minutes in 1% SF_6 in air.

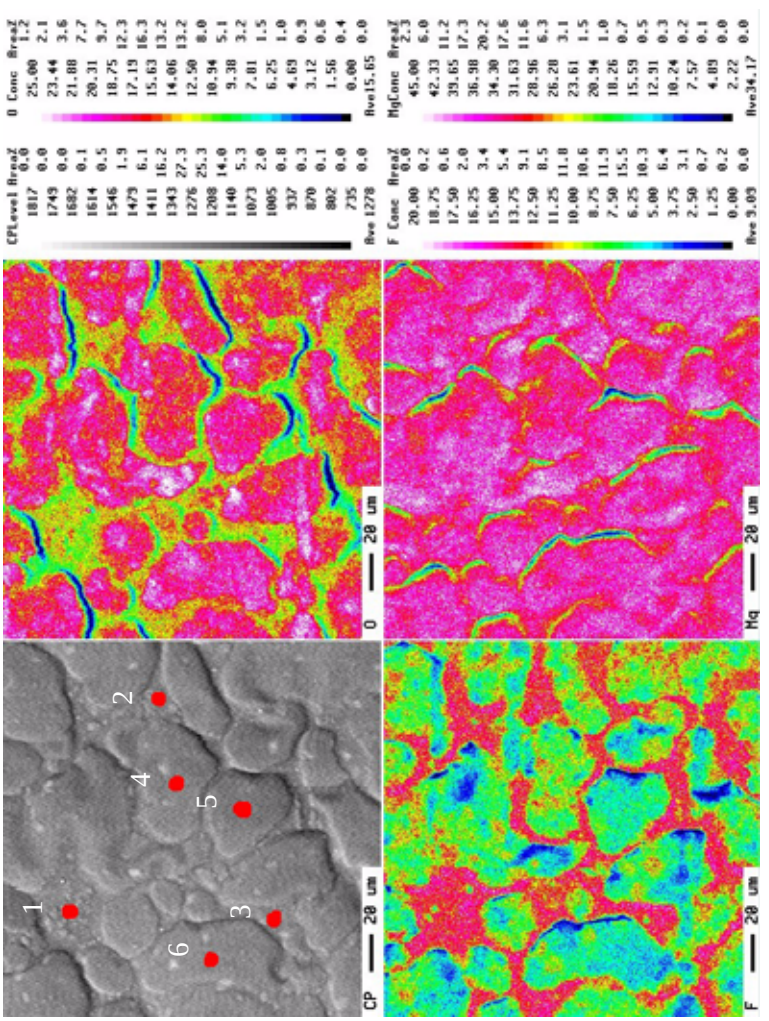

Figure 3.19 Microprobe "mapping" of sample AS in Table 3.3, 705°C for 60 minutes in 1% SF_6 in air.

The composition (atomic percent) of the six spots denoted in Figure 3.19 is given in Table 3.11. The three first points are from the matrix. This phase is very rich in fluorine, and if it assumed that all the fluorine is bound as magnesium fluoride, and all the oxygen as magnesium oxide, we get for the matrix phase approximately: 21/(18+21) = 54% MgF_2 and 18/(18+21) = 46% MgO.

The same calculation for the grains, gives 15/(15+30) = 33% MgF_2 and approximately 30/(15+30) = 67% MgO.

The diameter of the electron beam used in these analysis is 10 μm.

Table 3.11: Composition in atomic% of points indicated in Figure 3.19. Sample AS in Table 3.3, held at 705°C for 60 minutes in 1% SF_6 in air.

Point in Figure 3.19	C	S	O	F	Mg
1	0.2	0.05	19.0	42.1	38.6
2	0.3	0.03	18.6	42.7	38.3
3	0.3	0.07	17.4	44.7	37.5
Average	0.27±0.05	0.05±0.01	18.4±0.8	43.2±1.3	38.1±0.5
4	0.4	0.05	24.0	36.4	39.1
5	0.4	0.03	31.5	27.4	40.6
6	0.4	0.04	33.6	25.2	40.8
Average	0.36±0.01	0.04±0.01	29.7±5.1	29.7±6.0	40.2±0.9

A microprobe mapping was also performed on the surface of a sample that had the characteristic fine structure that was seen in may of the samples with 5% SF_6. This mapping is shown in Figure 3.20.

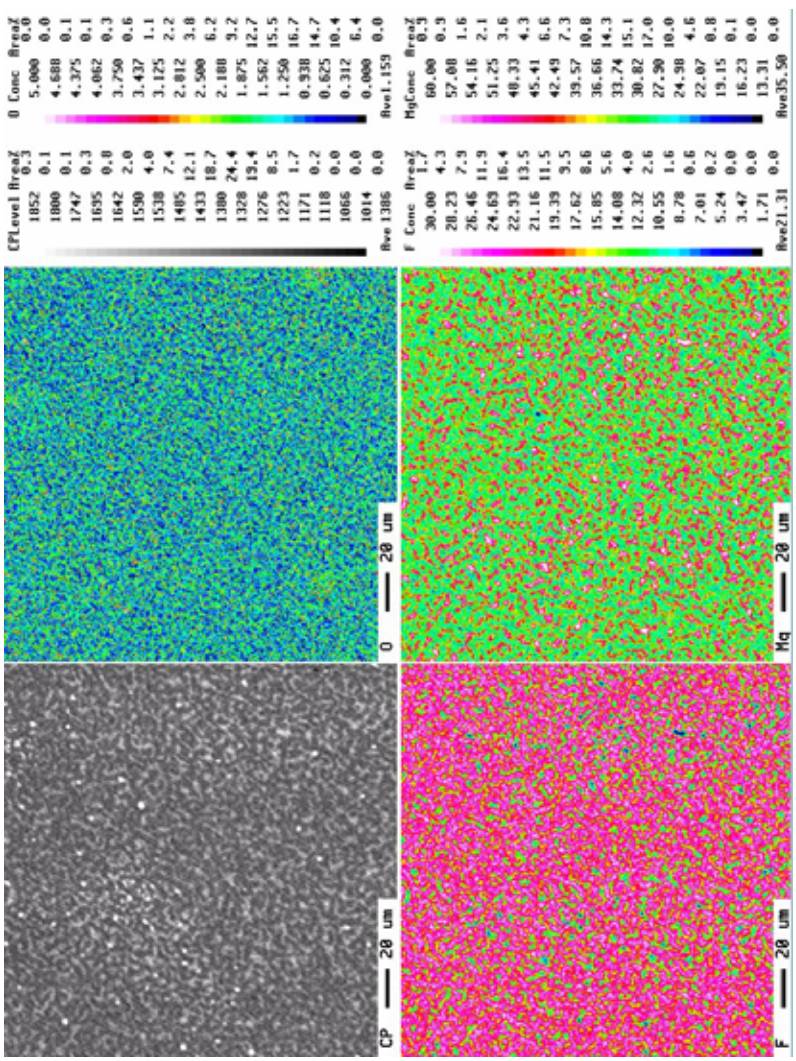

Figure 3.20 Microprobe mapping of sample BI in Table 3.4, 10 minutes at 685°C in 5% SF_6 in air.

The composition of the dark phase (matrix) and the light phase (grains) as they appear in the upper left corner in Figure 3.20 is given in Table 3.12.

From Table 3.12, it is seen that the matrix phase consists of almost pure MgF_2. The grains seem to contain 9/(9+3+66) = 12% MgF_2, 3/(9+3+66) = 4% MgO and 66/(9+3+66) = 85% Mg.

The probe diameter is 10 μm in diameter in these analysis.

Table 3.12: Composition in atomic% of matrix and grains as they appear in Figure 3.20. Sample BI in Table 3.4, 685°C for 10 minutes in 5% SF_6 in air.

Area	C	S	O	F	Mg
Matrix	0.3	0.01	1.3	67.3	31.1
Matrix	0.3	0.01	1.1	68.2	30.3
Matrix	0.3	0.01	1.5	66.5	31.7
Average	0.31±0.02	0.01±0.00	1.3±0.2	67.3±0.9	31.1±0.7
Grain	0.4	0.00	5.6	18.0	79.1
Grain	0.5	0	3.8	17.1	78.6
Grain	0.6	0.00	2.1	20.0	77.3
Average	0.49±0.07	0.00	2.8±0.9	18.4±1.5	78.3±0.9

Cross sectional examination of MgF_2 particles

A micrograph of the cross section of a sample held at 665°C for 5 hours in 1% SF_6 in air is shown in Figure 3.21. This figure illustrates very well the situation with the spots seen in for example Figure 3.6 and the surface film: The darker spots lie **underneath** the surface film, not on top as is the impression at first glance in the optical microscope. The particles are magnesium fluoride, and they are situated under the protective film, going down into the bulk metal.

The reason one could see them with the optical microscope, is that the magnesium oxide is transparent.

This is the same sample as in Figure 3.13. The "diameter" of the particles in the microprobe picture seen here in Figure 3.21 is 5-10μm. The distance between them is 10-20 μm.

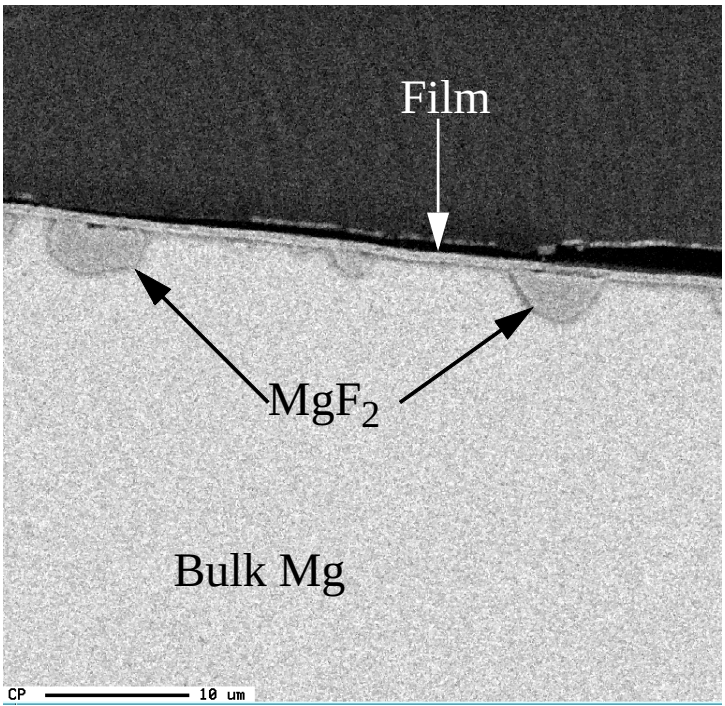

Figure 3.21 Cross section of sample held at 665°C for 300 minutes in 1% SF_6 in air taken with microprobe. Sample AM in Table 3.3.

The formation of magnesium fluoride particles on the interface between the oxide and the metal could also be seen in the Field Emission SEM. Figure 3.22 shows a sample that has been held at 665°C for 150 minutes in an atmosphere of 0.5% SF_6 in synthetic air. For this sample, the diameter of the magnesium fluoride particles is approximately 2 μm, and the distance between particles is 1-1.5 μm.

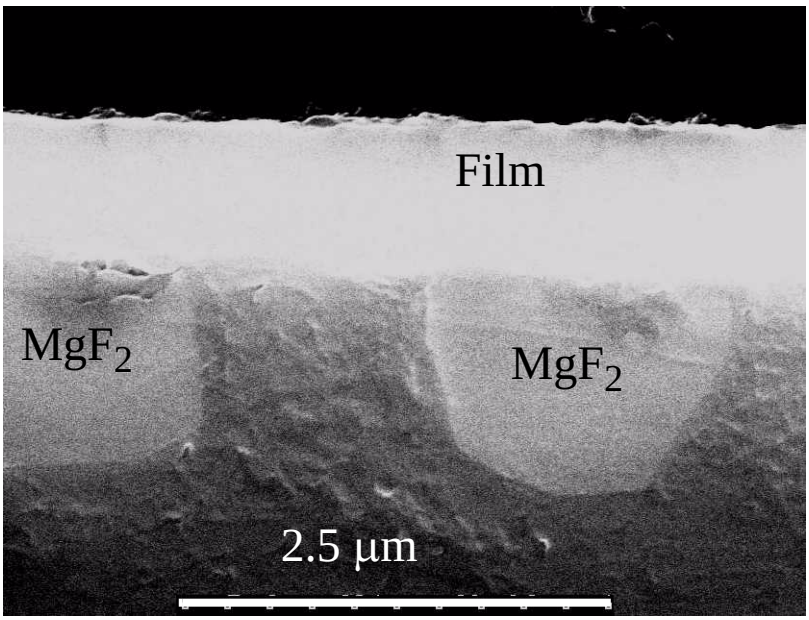

Figure 3.22 Magnesium fluoride particles formed underneath the protective film, going into the bulk metal, shown with Field Emission SEM. Sample is held at 665°C for 150 minutes in an atmosphere of 0.5% SF_6 in synthetic air. Sample E17 in Table 3.5.

Film thickness

The attempt to determine the thickness using the microprobe and Monte Carlo simulations was not very successful as will be discussed below. The results are included since they give an indication of the relative thickness as a function of temperature. The results are presented here in Figure 3.23. The composition data at various acceleration voltages, which are the data employed in these calculations are given in Appendix 7.

As can be seen, the thickness increases with exposure time. The increase in thickness seems to level out at 2-3 μm after approximately 100-150 minutes. In most cases, the samples that have been held at 685°C have a thicker film than the ones at lower temperatures.

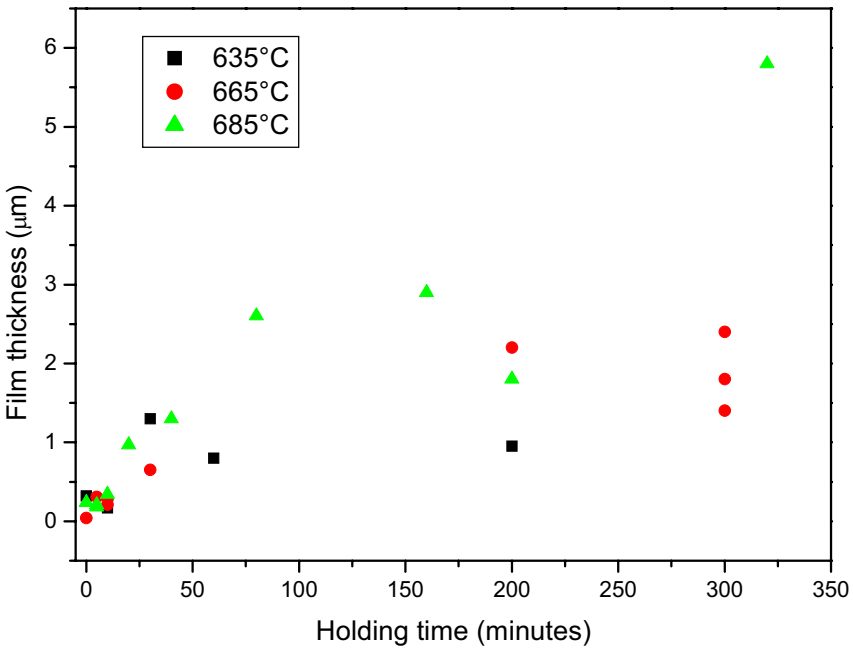

Figure 3.23 Thickness of film, estimated with Monte Carlo simulations. Films formed on magnesium at temperatures from 635 to 685°C in an atmosphere of 1% SF_6 in air. (See Table 3.3)

The thickness of the three samples studied in the Transmission Electron Microscope (TEM) is given in Table 3.13. In addition, the thicknesses calculated with the Monte Carlo simulations are found in the same table. As can be seen, the Monte Carlo simulation gives values that are approximately 2.7 times higher than the TEM measurements.

Table 3.13: Thicknesses of protective films formed in a gas atmosphere of 1% SF_6 in air, measured with TEM and estimated with Monte Carlo simulations. Samples AA, AO and AK in Table 3.3.

Sample	TEM thickness	Monte Carlo simulation
60 minutes at 635°C	0.28 µm	0.8 µm
200 minutes at 665°C	0.75 µm	2.2 µm
40 minutes at 685°C	0.50 µm	1.3 µm

The thicknesses found from the SEM and the FE-SEM pictures are presented in Figure 3.25. There is an increase of thickness with increasing time, but the results vary considerably. It is not easy to determine thickness from regular SEM pictures since the films appear rather blurry [Eriksen, 2003]. An example of such a regular SEM picture is given in Figure 3.24.

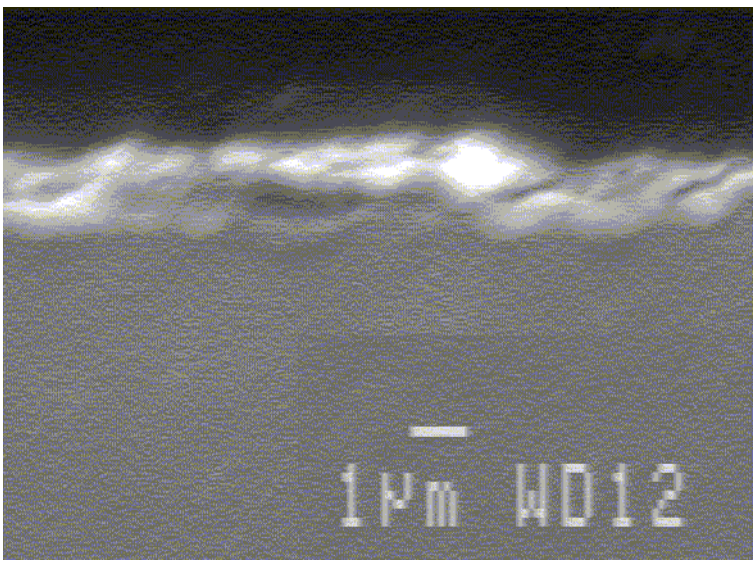

Figure 3.24 Example of SEM micrograph of cross section of film. Sample E10 in Table 3.4, 60 minutes at 665°C in 5% SF_6 in air.

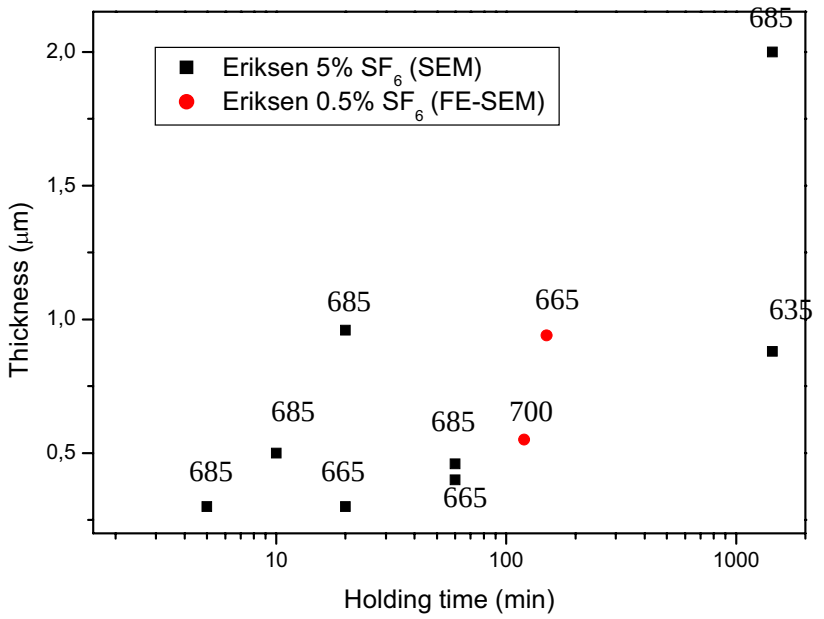

Figure 3.25 Thickness of films formed on magnesium in 5 and 0.5% SF_6 in air. Samples E6, E8, E10-E14 and E16 in Table 3.4, and samples E17 and E18 in Table 3.5.

Figure 3.26 shows one of the micrographs from the TEM examination. As can be seen, there is a continuous film. The film seems to consist of a cellular structure reaching out from the surface. The thickness of the film is 0.5 µm, see Table 3.13.

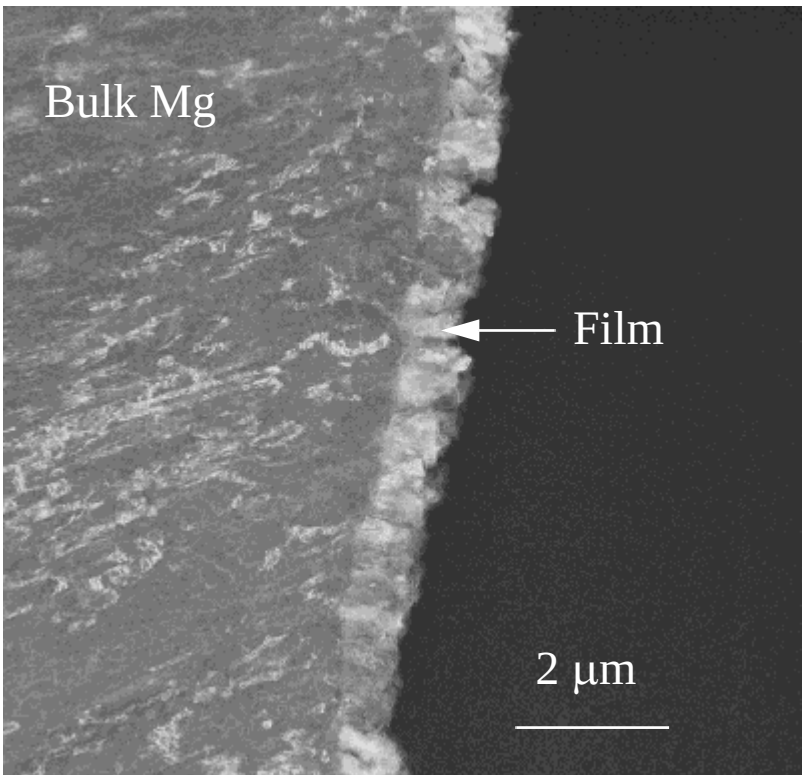

Figure 3.26 A TEM micrograph of the protective film. Sample held at 685°C for 40 minutes in 1% SF_6 in air. Sample AK in Table 3.3.

No spots were observed forming at the surface of sample AK. A part of the surface seen through the optical microscope is shown in Figure 3.27. No spots are observed at this picture as well. The “grain size” in this picture is 30-50μm.

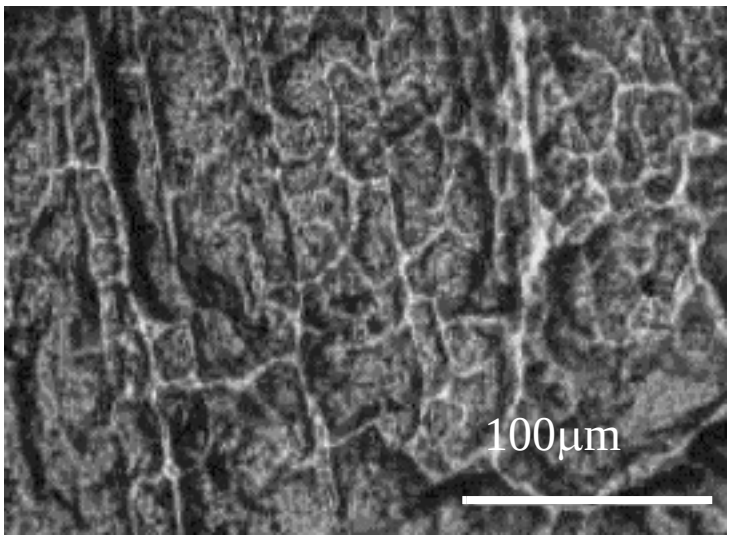

Figure 3.27 Picture from the optical microscope of sample AK in Table 3.3, 685°C for 40 minutes in 1% SF_6 in air.

The Field Emission SEM provided better pictures of the film compared to the regular SEM as seen in Figure 3.28. The thickness of the film is measured to be 0.55 μm.

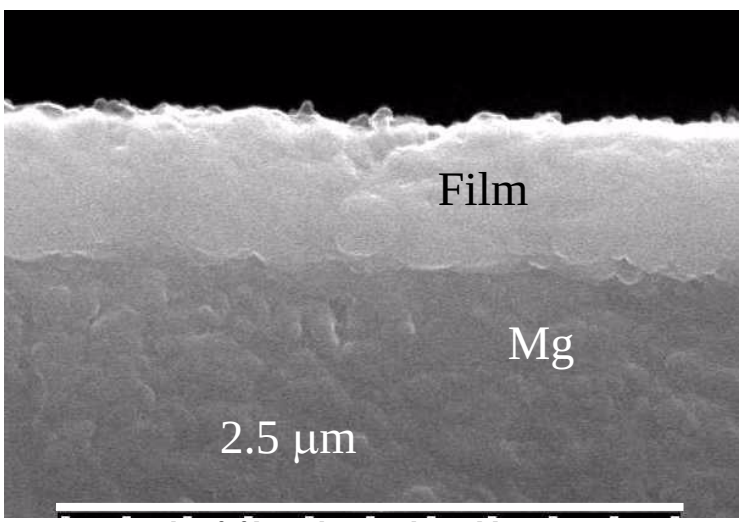

Figure 3.28 Micrograph of film taken with Field Emission SEM. Sample held at 700°C for 120 min. in 0.5% SF_6 in synthetic air. Sample E18 in Table 3.5.

Focused Ion Beam Milling (FIB)

In Figure 3.29, the situation with the oxide flakes, the film and the magnesium fluoride particles is illuminated using FIB. As can be seen, there is a large oxide flake on top of the surface, approximately 20-30 μm in "diameter". Underneath the protective film, one can see the magnesium fluoride particles, also referred to as spots. The largest MgF_2 spot to the left, partly seen in this picture, is approximately 5μm, while the distance between the two spots is about 10 μm.

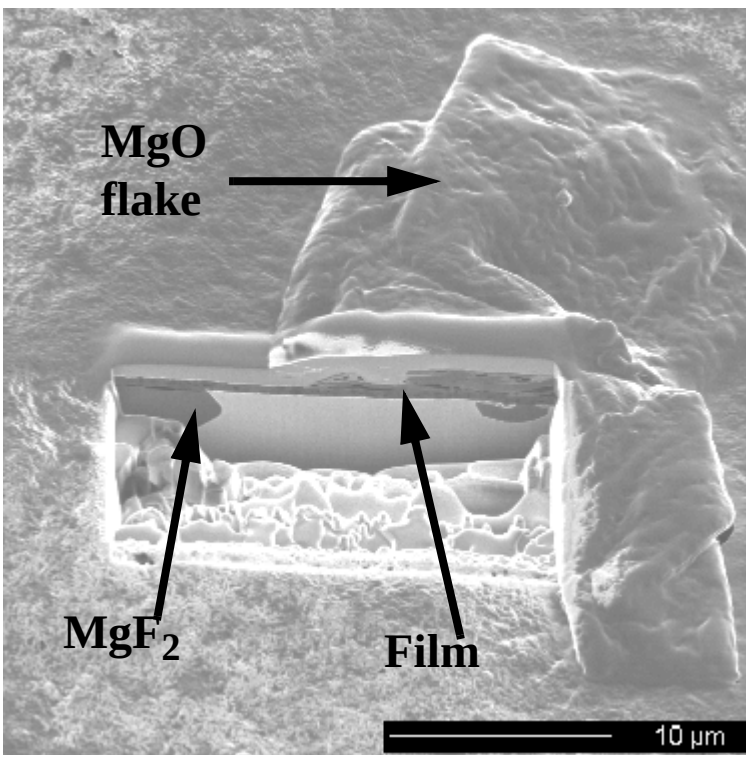

Figure 3.29 FIB-micrograph of a sample held at 665°C for 5 hours in 1% SF_6 in air. Sample AM in Table 3.3.

CO_2

All the samples that were held above the melting point, samples GA-GC, had a black surface after the experiments were finished. The surfaces were uneven, and the samples were not in the original shape. It was therefore not possible to get useful pictures with the microscope.

Sample GD on the other hand, which was held at 635°C for 60 minutes, had a smooth, shiny surface after the experiment was finished, and the sample had the

same shape as initially. An image of the surface taken with the optical microscope is seen in Figure 3.30. If one looks closely, one can see small, darker spots on the surface of the sample.

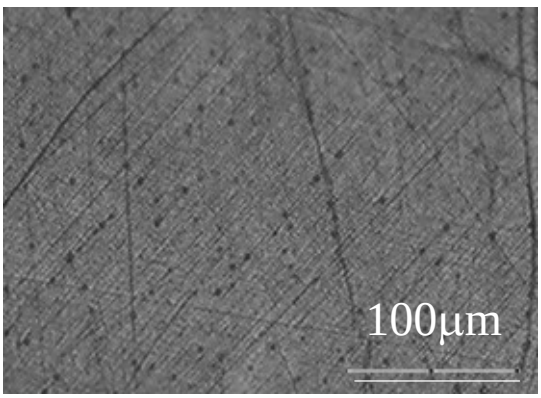

Figure 3.30 Surface of sample exposed to pure CO_2 at 635°C for 60 minutes seen in the optical microscope. Sample GD in Table 3.7.

A microprobe mapping of the same sample GD, is seen in Figure 3.31. The surface consists mainly of magnesium, which means that this is a thin film. There is also some oxygen, and insignificant amounts of carbon and fluorine. It is not possible to say something about the small darker spots that are seen in the upper left picture.

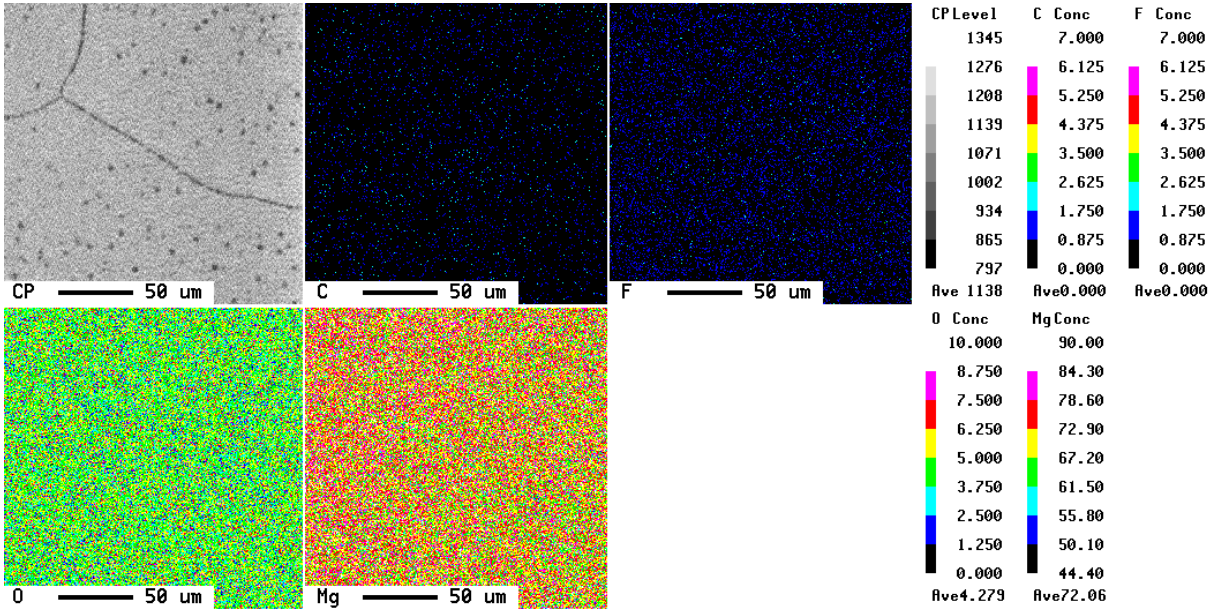

Figure 3.31 Microprobe mapping of sample GD in Table 3.7, 60 minutes at 635°C in 100% CO_2.

SO_2

A part of a surface exposed to 1% SO_2 in air is seen in Figure 3.32. It looks like there are some large grains at the surface which may be up to 1-200 μm in "diameter".

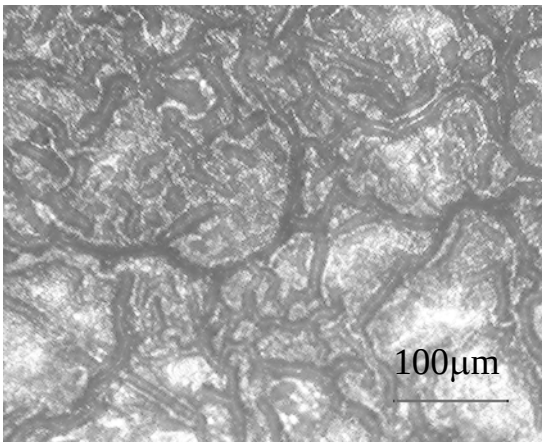

Figure 3.32 Surface exposed to 1% SO_2 in air at 635°C for 180 minutes seen in the optical microscope. Sample FA in Table 3.8.

A microprobe "mapping" of the same sample is seen in Figure 3.33. One can see that there is a slight variation in the distribution of sulphur: What appears to be larger grains seem to be a little richer in sulphur.

Point analysis of the surface gave the composition in Table 3.14. The diameter of the electron beam is 10 μm also in this case. As is seen, the surface contains approximately 7% sulphur and 42% oxygen. As expected, there is some fluorine on the surface due to previous use of SF_6 in the hot stage.

Table 3.14: Composition of surface of sample FA in atomic percent.

Measurement #	C	S	O	F	Mg
1	0	7.9	41.7	4.0	46.4
2	0	6.1	41.9	6.3	45.8
3	0	5.6	42.0	5.5	46.8
4	0	8.2	43.5	3.6	44.7
5	0	7.0	40.4	4.7	47.6
Average	0	6.9±1.1	42±1	4.9±1.1	46±1

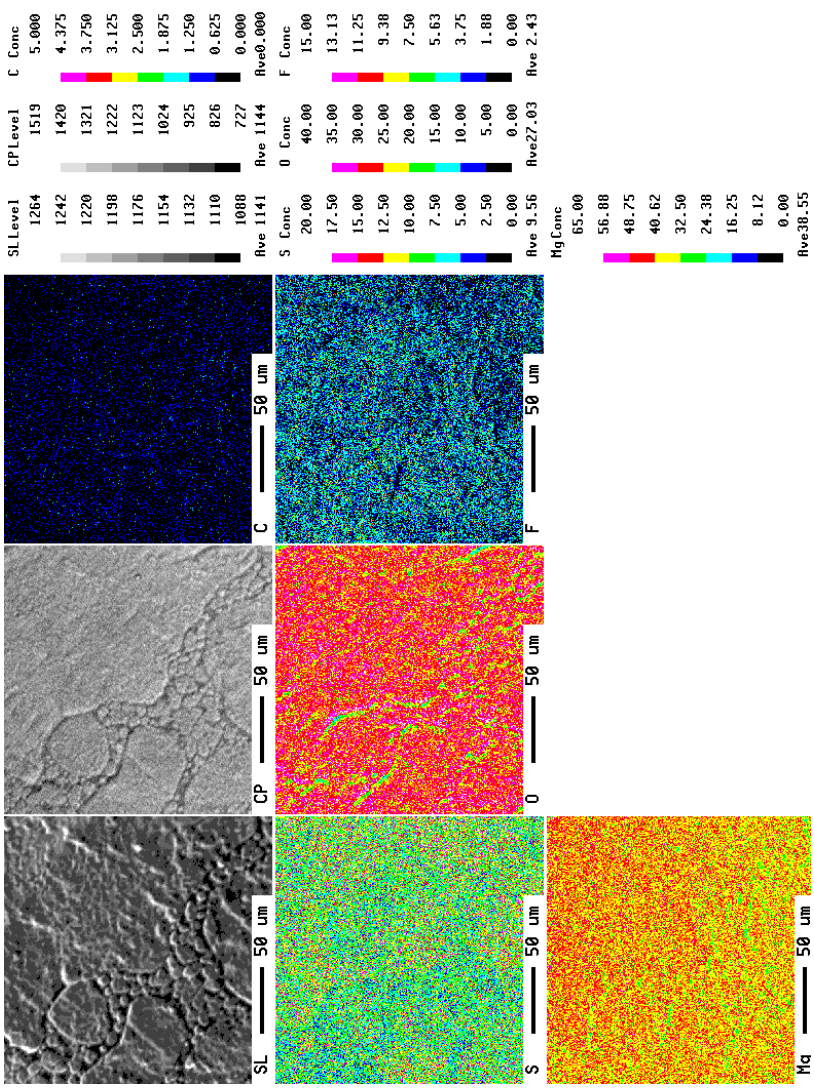

Figure 3.33 Microprobe "mapping" of sample FA in Table 3.8, 180 minutes at 635°C in 1% SO_2 in air.

DISCUSSION

First, there is an issue that should be brought up: In this work, it is often assumed that all the fluorine in the samples is bound as magnesium fluoride and all the oxygen as magnesium oxide. We do not really know that this is the case. Sharma [1988] studied the phase equilibria in the system MgF_2-MgO. This system has an eutectic point at 8.5 mol% MgO at 1228°C. Samples that were slowly cooled to room temperature showed the separation into the two primary phases. No solid solution or compound formation was detected. Putz, Schön and Jansen [1998] have published a computational thermodynamics paper where they investigated if it is possible that the phase Mg_2OF_2 forms. They varied the composition between Mg_3OF_4 and $Mg_3O_2F_2$, but the result was that the ternary system Mg/O/F is most likely to separate into the binary compounds MgO and MgF_2 and that the synthesis of magnesium oxide fluoride (Mg_2OF_2) should be a difficult task. Still, we do not know to what extent magnesium fluoride may contain oxygen or magnesium oxide can contain fluorine.

An important finding in this study is the formation of the magnesium fluoride particles underneath the protective surface film. It is, however, difficult to tell under which conditions these spots form. They form both at low temperatures (635°C) and at high temperatures and at short and with long holding times. Spots were only observed when the percentage of SF_6 in the gas was 1 or 0.5%. With 5% SF_6 in the gas, a finer structure was observed instead of the characteristic spots.

A comparison of the MgF_2 particle sizes and distance between them is summarized in Table 3.15. Although the parameters may vary, it is possible to compare some of the samples, for example Sample I after 240 minutes, and Sample AM. As is seen from the table, the particle size is approximately 5 μm, and the distance between them about 10μm. A sample held at the same temperature, but not for so long, and with less fluorine in the gas, Sample E17, has smaller particles. The MgF_2 spots in Figure 3.22 are only approximately 2 μm which is reasonable considering that this sample has not been held at the given temperature for as long as most of the other samples presented here. Surprisingly, the distance between the particles is very short. This may be a coincidence since when the pictures were taken, we were looking for an area with a high density of particles. The two spots seen in Figure 3.22, may even be so close that they appear as one spot looking at it from above in the optical microscope.

Another sample that may have unreasonable large MgF_2 spots, is Sample A in Figure 3.14. This sample has fluoride particles that are equal in size to samples

that have been held at the sample temperature for much longer time, e.g. Sample AM that was held at 665°C for 300 minutes.

Table 3.15: Comparison of MgF_2 particle sizes, distance between them, and size of oxide flakes where seen, measured on pictures presented in the text.

Figure	Sample name	Holding time(min), temp(°C),%SF_6	MgF_2 particle size (μm)	Distance (μm)	Oxide flake (μm)
3.7	I	240 min at 665°C, 1%SF_6	~5	~10	
3.8	I	630 min at 665°C, 1%SF_6	5-10	<10	
3.9	I	2280 min at 665°C, 1%SF_6	~10	~5	
3.13	AM	300 min at 665°C, 1%SF_6	~5	~10	10-20
3.21	AM	300 min at 665°C, 1%SF_6	~7	10-20	
3.29	AM	300 min at 665°C, 1%SF_6	~5	~10	20-30
3.14	A	2 min at 640°C, 3 min at 667°C, 1%SF_6	~5	~10	
3.22	E17	150min at 665°C, 0.5%SF_6	~2	1-1.5	

The same sample as is given in the three first rows in the table here, Sample I, is the basis for Figure 3.11. One should therefore expect that the results in the Table 3.15 and Figure 3.11 should correspond well. After 240 minutes (4 hours), the average particle size from Figure 3.11 is approximately 4 μm, and there is good correspondence. After 2280 minutes (48 hours) on the other hand, Figure 3.11 gives a size of approximately 6 μm, while the size given in Table 3.15 is 10 μm. The reason for this is probably that Figure 3.11 is produced in a more accurate way: The pictures were enlarged 160 times which made it possible to count pixels to determine the size. The numbers given in the table here are only measured with a ruler at the magnification on the pictures, which may give a larger source of error.

The spots that were observed under the protective surface film, are probably formed when the oxide film is saturated with fluorine, and magnesium fluoride starts forming from the excess fluorine. This indicates that the fluorine diffuses downwards through the surface film and down to the bulk metal.

In a few cases, the formation of grains in a matrix was very clear. In Figure 3.15 and 3.19 we also see that a fluorine rich phase forms in between the larger grains. The matrix composition in Figure 3.19 corresponds to 54% MgF_2 and 46% MgO when measured with the microprobe. The composition analysis showed that the grains contained more oxygen and less fluorine than the matrix phase, that is 33% MgF_2 and 67% MgO. For the sample that was exposed to 5% SF_6 in Figure 3.20, the matrix phase contained solely magnesium fluoride. The grains, which are very small in this case, seem to contain large amounts of pure magnesium, 85%. A reason for this, may be that the film thickness is very thin in this area, and that the bulk magnesium underneath contributes. Since the grains are so small, it is possible that the area around the grain will also contribute in the analysis. If one neglects the contribution from the bulk magnesium to get the composition of the film only in the grains, the ratio between the MgF_2 and the MgO in the film is 4:1. Since these spots contain more oxygen than matrix, this may be sites where oxidation began, but after a while was stopped by the formation of fluoride.

A simplistic explanation of the protective effect of SF_6 may be that the magnesium fluoride fills “cracks” in the oxide film and forms a continuous film. Considering Pilling Bedworth’s ratio, it is possible to calculate how much of the surface that has to be magnesium fluoride to achieve an average Pilling Bedworth ratio of at least one. Using the Pilling Bedworth ratio for both magnesium oxide and magnesium fluoride, 0.81 and 1.45 respectively, it can be calculated that at least 30% of the surface layer should be magnesium fluoride. It is seen in several cases that large parts of the surface are covered with magnesium fluoride, e.g. in Figure 3.19. There are however many cases where one can not clearly see two phases. Maybe the surface films in these cases were a mixture of magnesium oxide and fluoride, and that the phases did not separate.

Some of the fluorine probably remains in the lattice of the oxide film. Hodge and Gordon [1978] estimated that fluorine in magnesium oxide lattice may vary between 0.002 and 0.07 anion%. This probably expands the lattice somewhat. This is seen for the samples in this work in Appendix 6. Especially for the sample exposed to 5% SF_6, sample BK in Table 3.4, one can see that the lattice is slightly expanded. An explanation for the formation of the protective oxide layer could be that the lattice of the magnesium oxide that forms, expands due to the fluorine present while it is built. This modified oxide may have a higher volume than pure magnesium oxide, and is able to cover the molten metal surface. To cover the magnesium melt, the oxide would have to expand almost 20% by volume. However, if the oxide lattice were to expand that much, the unit cell might be expected to collapse.

The presence of fluorine at the grain boundaries may give enhanced grain growth and creep due to increasing diffusion rates of magnesium both in the lattice and at the grain boundaries. Magnesium lattice diffusion in MgO containing fluorine is three time higher than in pure MgO [Hodge and Gordon, 1978]. They suggest that the mechanism for enhanced lattice diffusion is due to the formation of magnesium vacancies due to the substitution of fluorine on oxygen sites.

A possible explanation for the effect of fluorine may be a combination of these mechanisms; the fluorine gives increased grain growth and creep. In addition, magnesium fluoride forms and fills grain boundaries in the oxide film. However, it should be kept in mind that the particular structure in Figure 3.15 is seen only in a few samples, for example sample AS in Table 3.3, E2 and E8 in Table 3.4. Notice that sample E2 in Figure 3.15 is held below the melting point, while sample E8 in Figure 3.17 is held at a temperature above the melting point. The SF_6 content in the gas was 5% for samples E2 and E8, and 1% for sample AS. Since the structure seen in Figure 3.15 is formed both below and above the melting point, this indicates that what happens within the oxide layer is independent of the metal below.

This is also the case for the magnesium fluoride spots which formed mainly for 1% SF_6: Spots are formed both above and below the melting point, and also at short and long holding times. There seems to be no pattern when they form. It has not been observed that the magnesium fluoride particles form for example at the oxide grain boundaries. Even where oxide grains clearly were seen, e.g. in Figure 3.18, the spots seemed to form everywhere at the surface.

The four different situations that are observed are summarized in Figure 3.34: Situation 1 is when there is magnesium fluoride particles underneath a continuous oxide film, e.g. sample I in Figures 3.6-3.9. Situation 2 is the case when both magnesium fluoride particles form and there are larger oxide grains instead of a continuous surface film as was seen in sample AS in Figures 3.18-3.19. Situation 3 is when either magnesium fluoride particles or oxide grains are observed, but there is still fluorine present. This was the case with sample AK as shown in Figure 3.26 with a TEM micrograph. Finally, situation 4 illustrates the case when a fluorine richer matrix forms in between the oxide grains which was the case in Figure 3.15.

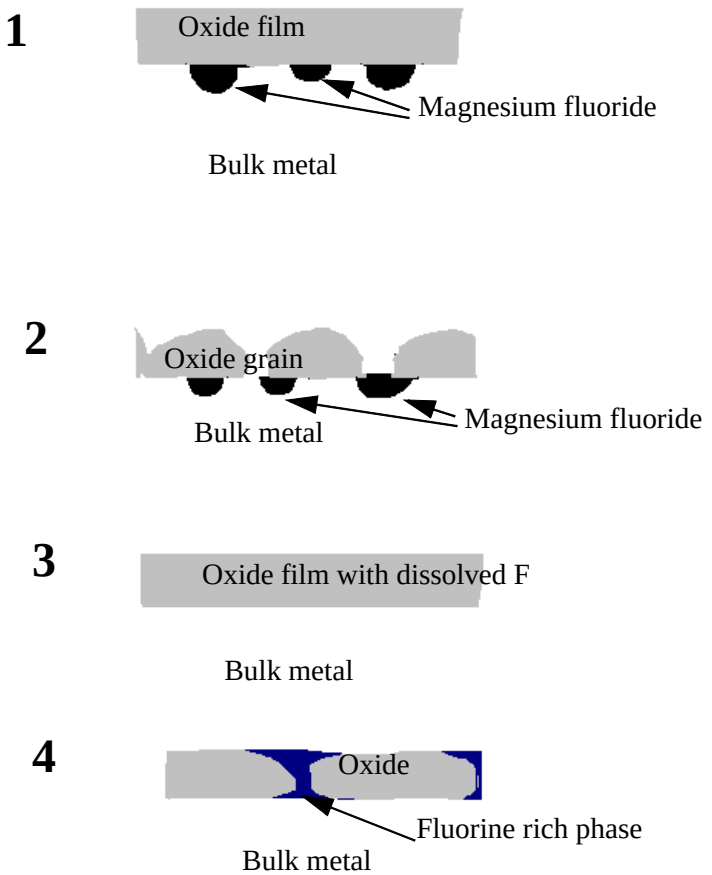

Figure 3.34 Illustration of the four different situations seen in these experiments when magnesium is exposed to SF_6.

The formation of the magnesium fluoride spots has not been reported before. This is probably a merit of the experimental method used here. The hot stage gives a very calm and smooth surface and a melt with no agitation compared to some equipment employed in previous studies.

Thickness of films

Cashion et al. [2002] have also studied the thickness of films produced in an atmosphere of 0.3% SF_6 in air. The method they used to determine the thicknesses was Auger Electron Spectroscopy. The film thickness was proportional with the square root of time, and varied between 0.08 μm for a sample held at 700°C for 1 minute to 0.50 μm for a 60 minute exposure sample.

Figure 3.35 compares the measurements of thickness using TEM, FE-SEM and Auger Electron Spectroscopy. The content of SF_6 in the gas and temperature is given in the figure. The TEM samples are denoted AA, AO and AK in Table 3.3. In these samples, MgF_2 particles are not seen. The experiments by Eriksen (FE-SEM) are included because the micrographs of the film seem to give a well defined thickness. However the temperature dependence is not in accordance with the TEM measurements. One would expect the thickness to increase with temperature. Magnesium fluoride particles are seen in the sample at 665°C. Possibly, a greater thickness is measured when magnesium fluoride particles are formed. Therefore, the two points obtained from Eriksen are not used in the following calculations. All the various methods that have been used to try to determine thickness are compared in Appendix 4. The data from the Monte Carlo simulations are not included here since they seem to give unreasonably high values. The thicknesses determined from SEM micrographs are also rather uncertain, and are therefore also excluded in Figure 3.35.

The measurements performed by Cashion using Auger Electron Spectroscopy follow a straight line when the thickness squared is plotted against exposure time. It would seem that the Auger Electron Spectroscopy is a superior way to measure thickness although it is desirable to have pictures of the films.

Transmission Electron Microscopy gave pictures of the film which made it easy to determine the film thickness. There is one great disadvantage with this method, that the sample preparation is very time consuming and requires considerable experience. The other methods that were used also demand careful sample preparation, but not to the same extent.

As can be seen from Figure 3.35, the TEM measurements lie both below and above Cashion's results. A closer look shows that the TEM sample at 635°C lies below Cashion's results. This is reasonable since the formation of the film should be slower at low temperatures. The sample at 665°C also lies below Cashion's results but not as much, while the one at 685°C is above. There is one obvious explanation to this, and that is the content of SF_6 in the gas. The samples examined with TEM were exposed to 1% SF_6 in air, whereas the samples examined with AES were exposed to only 0.3% SF_6 in air.

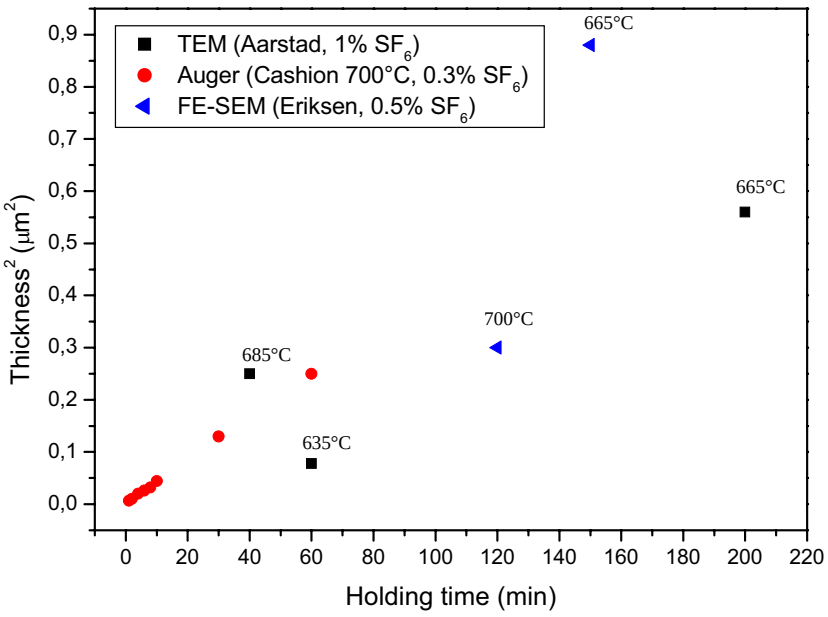

Figure 3.35 Thickness of film squared as a function of holding time using TEM and AES to determine the thickness.

To quantify the results, the following calculations were done:

The growth of the film thickness (L) is assumed to follow the equation:

$$L^2 = k \cdot \text{time} \qquad (3.1)$$

The basis for equation 3.1 is that transport of a component such as F or Mg through a film of thickness L is given by Fick's law: $\dot{n}_F = -D_F \cdot \frac{dc_F}{dx}$

where $\dot{n}_F$ is the flux given in moles/(m^2 s). D_F is a diffusion coefficient given in m^2/s. $\frac{dc_F}{dx}$ is the concentration gradient of F down through the film in units of moles/m.

If accumulation of F inside the film is neglected, $\frac{dc_F}{dx} \sim -\frac{\text{constant driving force term}}{L}$

The growth rate of the film, $\frac{dL}{dt} \sim \dot{n}_F$

Thus, $\frac{dL}{dt} = \frac{\text{constant}}{L}$

Integration of this equation gives equation 3.1.

It is assumed that D_F is constant, also the simultaneous transport of Mg and F must be taken into account. The problem is taken to be planar (one dimensional). The driving force for transfer of fluorine is determined by SF_6 in the gas and MgF_2 under the film.

To determine k in Equation 3.1, a line was drawn from origin and out towards the three TEM measurements. Also a line was plotted through origin, and fitted to Cashion's measurements to determine the slope of this line as well. This is illustrated in Figure 3.36.

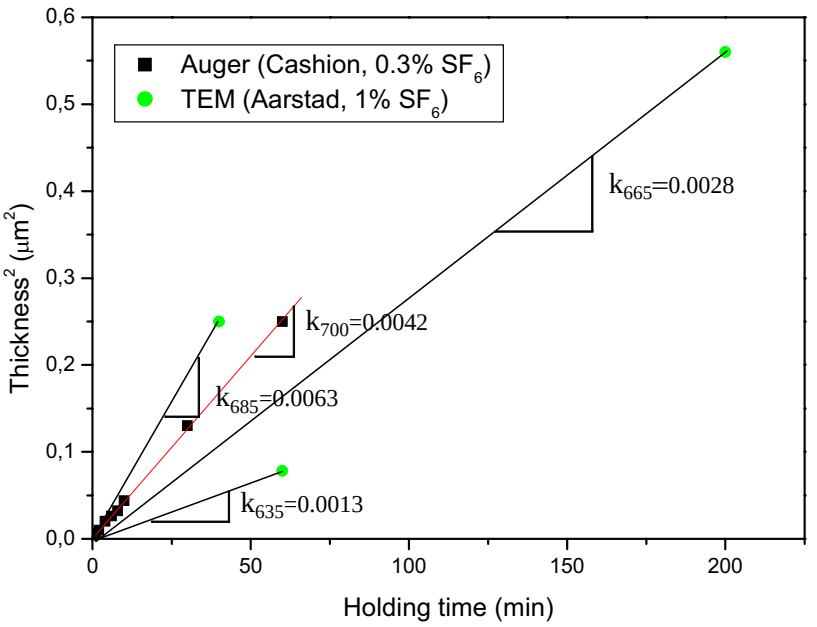

Figure 3.36 Determination of k-values for the various measurements.

The three values of k determined from the TEM measurements were plotted against temperature. These values were fitted using a non-linear curve fitting method in Origin 6.1, shown in Figure 3.37.

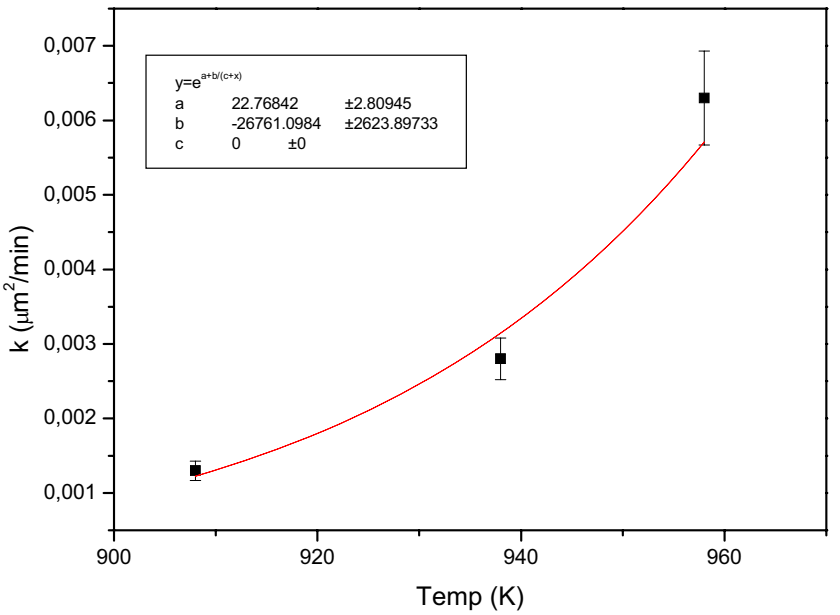

Figure 3.37 Curve fitting to determine k as a function of temperature for the TEM measurements.

k is expressed as a function of the activation energy E and temperature, T:

$$k(\mathrm{E,\ T}) = k_0 \cdot e^{-\frac{E}{RT}} \qquad (3.2)$$

From this it is seen that k_0 equals e^a from the fitting, and E=b·R in Figure 3.37.

To determine k^*_0 which is the slope if the partial pressure of SF_6 is 1%, and the temperature 700°C, equation 3.2 can be rewritten:

$$k(T) = e^{a - \frac{E}{R \cdot 973} - \left(\frac{E}{RT} - \frac{E}{E \cdot 973}\right)} \qquad (3.3)$$

$$k(T) = k(973)e^{-\frac{E}{R}\left(\frac{1}{T}-\frac{1}{973}\right)} \quad (3.4)$$

where

$$k(973) = k^*_0 = e^{a-\frac{E}{R\cdot 973}} \quad (3.5)$$

Inserting the numbers from the fitting in Figure 3.37, we get the following values:

E = 22 000 J/mol
k^*_0 = 0.009 $(\mu m)^2$/min

The dependence of the partial pressure of SF_6 in the gas is assumed to follow a relation

$$k_{700} = \left(\frac{p_{SF_6}}{1\%}\right)^n \cdot k_o^*$$

Knowing k^*_0, it is possible to calculate n employing the line obtained from Cashion's results for p_{SF6} = 0.3:
This gives

n=0.6

Finally, we obtain:

$$k(T, p_{SF_6}) = k^*_0 \cdot e^{-\frac{E}{RT}+\frac{E}{R\cdot 973}} \cdot \left(\frac{p_{SF_6}}{1\%}\right)^{0.6} \quad (3.6)$$

inserting numbers for k^*_0, E and R gives:

$$k(T, p_{SF_6}) = 0.009 \cdot \left(\frac{p_{SF_6}}{1\%}\right)^{0.6} \cdot e^{-2600\left(\frac{1}{T} - \frac{1}{973}\right)} \quad (3.7)$$

The above equation may not be valid when MgF_2 particles form.

An alternative way to do this calculation is presented in Appendix 5. This method gives E = 24 000 J/mol, $k^*_0 = 0.010$ $(\mu m)^2$/min and n = 0.7.

CO_2

The samples above the melting point were black after being exposed to a flow of pure CO_2, while the sample that was held below the melting point was shiny. No magnesium carbonate was detected in sample GD which was held at 635°C for 60 minutes. This is also what was predicted with thermodynamic calculations: The only reaction products should be C and MgO (see Figure 1.8).

The surface oxide films that formed in CO_2, can not be that strong since the samples above the melting point did not maintain their original shapes, as was the case with the samples that were exposed to SF_6. Since the surface was quite uneven on these samples, it was not possible to get good pictures from the optical microscope. Also, these samples were not suitable for microprobe examinations because of the topography.

The sample below the melting point appeared to be almost exactly the same as before the experiment started. It is therefore probably best to produce samples at low temperatures if the aim is to study the film that forms. It is seen in the experiments with SF_6 that it does not matter whether the film forms below or above the melting point. The only thing that differs, is the thickness of the film, and that the film “cracks” when the metal underneath melts.

SO_2

It was seen that there is sulphur in the samples that were exposed to SO_2. It is, considering the analysis methods employed here, not possible to tell whether this sulphur is found as magnesium sulphide or if sulphur is dissolved in the MgO matrix. The sulphide is most favorable thermodynamically as was shown in Figure 1.6, while the sulphate has the highest Pilling-Bedworth ratio. The Pilling-Bedworth ratio for MgS is 1.44. To achieve an average Pilling-Bedworth ratio of 1, it is necessary that 30% of the surface film is MgS.

First, using the analysis in Table 3.14, and assuming that the film consists of a mixture of MgO and MgS: There is 7% S, which means that there is 7 “parts” MgS, 42% O equals 42 “parts” MgO. The fluorine is not taken into account. The composition of the surface film is then 7/(7+42) = 14% MgS and 42/(7+42) = 86% MgO. If it is the case that MgS forms, this is not enough to give a Pilling-Bedworth ratio of 1.

In Figure 3.32, the structure that was seen through the optical microscope may resemble structures that were seen with SF_6 with grains in a matrix. It was also seen in Figure 3.33 that there is a variation in the sulphur content between the grains and the matrix. The grains seem to be slightly richer in sulphur than the matrix. This difference in composition is almost not detectable, and not as dominant as was the case with fluorine and SF_6.

CONCLUSION

Protective films formed both on liquid and solid magnesium in gas atmospheres with varying partial pressure of SF_6 in air, pure CO_2 and SO_2 in air have been studied in a hot stage. The method used made it possible to actually observe the surface of the film as it was formed. It also provided a smooth surface film that was very well suited for further studies with different types of analysis and microscopic equipment.

When the content of SF_6 in the gas was 1%, in more than half of the samples, magnesium fluoride particles formed underneath the protective film, down into the bulk metal. See Figures 3.21 and 3.22. These spots started appearing just below the melting point, and they grew in size as the samples were held at temperatures ranging from 635 to 685°C. After a given time, the film growth seemed to level out. At this point, the spots covered 25-50% of the total surface. The positions where the particles formed, seemed to be randomly distributed.

With 5% SF_6 in the gas, a very fine structure was seen with very small grains in a matrix. The grains contained less fluorine than the matrix phase which was almost pure MgF_2.

In some cases, a fluorine rich matrix is formed in between grains which are lower in fluorine and richer in oxygen, see Figure 3.19. As an explanation to the protective effect of SF_6, it is suggested that magnesium fluoride fills the openings between the magnesium oxide grains. Also, in the lattice, fluorine diffuses down through the MgO while Mg^{2+} diffuses up through the film. The presence of fluorine may slightly expand the MgO structure.

The thickness, L, (μm) of the films are found to follow the equation

$L^2 = k \cdot \text{time}$

where k is given by the expression below. The equation may possibly only be valid when magnesium fluoride particles do not form.

$$k(T, p_{SF_6}) = 0.009 \cdot \left(\frac{p_{SF_6}}{1\%}\right)^{0.6} \cdot e^{-2600\left(\frac{1}{T} - \frac{1}{973}\right)}$$

In future work it would be interesting to determine the crystal structure of the Mg-O-F film.

CO_2

The preliminary experiments with CO_2 in the hot stage, showed that it might be difficult to produce smooth surfaces above the melting point. The sample held below the melting point had a shiny and smooth surface while the samples that were held above the melting point, had a black, uneven surface after the experiments were finished. Below the melting point, the sample keeps the initial shape, and the surface can be studied with various techniques.

The surface films formed with CO_2 do not seem to be as strong as the films that are formed with SF_6.

SO_2

Considerable amounts of sulphur were found in the films of the samples that were exposed to SO_2. It is not possible to tell if the sulphur is bound as MgS or as sulphur dissolved in MgO. There seems to be a very small, but detectable, variation in the sulphur content between grains and matrix.

BIBLIOGRAPHY

Cashion, S.P., Ricketts, N.J., Hayes, P.C.(2002) Characterisation of Protective Surface Films Formed on Molten Magnesium Protected by Air/SF_6 Atmospheres *Journal of Light Metals* **2**: 37-42.

Chiang Y.M., Birnie D.P. and Kingery W.D. (1997) Physical Ceramics - Principles for Ceramic Science and Engineering. Wiley, New York.

Goldstein J.I, Newbury D.E., Echlin P, Joy D.C., Romig A.D., Lyman C.E., Fiori C, Lifshin E.(1992) Scanning Electron Microscopy and X-ray Microanalysis 2nd ed. New York:81-83.

Hodge, J.D., Gordon, R.S. (1978) Grain Growth and Creep in Polycrystalline Magnesium Oxide Fabricated with and without a LiF Additive *Ceramurgia International* **4** (1): 17-20.

Joy, D.C (1991) An Introduction to Monte-Carlo Simulations *Scanning Microscopy* **5**(2): 329-337.

Nordlien J.H., Ono S., Masuko N. and Nisancioglu K. (1997) A TEM Investigation of Naturally Formed Oxide Films on Pure Magnesium. *Corrosion Science* **39**: 1397-1414.

Pettersen, G., Øvrelid, E., Tranell, G., Fenstad, J., Gjestland, H. (2002) Characterisation of the Surface Films Formed on Molten Magnesium in Different Protective Atmospheres *Materials Science and Engineering A* **332** (1-2): 285-292.

Putz H., Schön J.C. and Jansen M. (1998) Investigation of the Energy Landscape of Mg_2OF_2. *Computational Materials Science* **11**: 309-322.

Roedder E. (1984) Reviews in Mineralogy: Fluid Inclusions. Mineralogical Society of America, Washington.

Sharma R.A. (1988) Phase Equilibria and Structural Species in MgF_2-MgO, MgF_2-CaO, and MgF_2-Al2O_3 Systems. *Journal of the American Ceramic Society* **71** (4): 272-276.

Semploinski D.R., Kingery W.D. and Tuller H.L. (1980) Electronic Conductivity of Single Crystalline Magnesium Oxide. *Journal of the American Ceramic Society* **63**: 669-675.

Chapter 4.
Solubility of Fluorine in Magnesium

INTRODUCTION

The solubility of fluorine in magnesium at different temperatures is studied by melting pure magnesium in a magnesium fluoride crucible. The reason for doing this is that fluorine is the active component of SF_6 which protects the magnesium melt from oxidation. Therefore, it might be a solution to introduce fluorine directly into the melt. If fluorine could be introduced directly into the melt, one should expect that the maximum possible concentration of fluorine is determined by the formation of an MgF_2 phase.

In addition to measuring the solubility of fluorine in pure magnesium, we would also like to measure the solubility of fluorine in molten magnesium saturated with iron. The reason for doing this is that magnesium is melted in steel crucibles, and the melt will therefore be saturated with iron. However, the iron solubility is low.

It is also interesting from a fundamental point of view to find the solubility of fluorine in magnesium.

Nayeb-Hashemi and Clark did an extensive literature search before publishing their book on phase diagrams of magnesium in 1988. They were not able to find any data on the solubility of fluorine in magnesium, which is the same experience as in this work.

THEORY

In these experiments, it is assumed that we have equilibrium between the solid magnesium fluoride crucible and the liquid magnesium.

The following data for $\Delta G°_1$ and $\Delta G°_2$ are used [Engh, 1992]. The values are checked against the FACT database for 1000K:

$MgF_2 = Mg + F_2$	$\Delta G°_1 = 1\ 120\ 000 - 171.2T$
$Mg = Mg\ (l)$	$\Delta G°_2 = 8\ 960 - 9.71T$
$F_2 = 2\underline{F}$	$\Delta G°_3$
$MgF_2 = Mg\ (l) + 2\underline{F}$	$\Delta G°$

The experiments should give us $\Delta G°$ and thereby $\Delta G°_3$.

The equilibrium for the total reaction above can be written as:

$$\frac{(a_F)^2 \cdot a_{Mg}(l)}{a_{MgF_2}} = e^{-\Delta G°/RT} \qquad (4.1)$$

Setting

$a_{Mg(l)} = 1$

$a_{MgF_2} = 1$

and taking f_F equal to 1 so that:

$a_F = [\%\ F]$

Equation 4.1 reduces to:

$$[\%F] = e^{-\Delta G°/2RT} \qquad (4.2)$$

EXPERIMENTAL

The crucible

MgF_2 from Merck, quality 5836, was mixed with polyvinyl alcohol. The polyvinyl alcohol acts as an adhesive, and 2% by weight was dissolved in 250 ml water and heated to 80°C. The solution was poured into a bottle together with 250g magnesium fluoride. The bottle was left on a ball grinder for two hours to make sure that the solution was mixed completely. The solution was then left in a vacuum furnace at 80°C over night to evaporate the water. What was left was crushed and pressed in a rubber mould at 2000 bar.

It is necessary to sinter the crucible afterwards to give strength. This was carried out by holding the crucible at 1050-1100°C for about an hour. The size of the crucible after sintering was then about 50 mm in outer diameter with a height of 80 mm.

The furnace

Figure 4.1 shows a sketch of the inside of the furnace. The magnesium fluoride crucible is placed in the middle of the furnace. There are radiation shields both above and below the crucible to make sure that a uniform temperature of the melt is achieved.

Before the experiments were started, the furnace was evacuated to 1 mbar. The chamber was filled with argon (purity 99.99%), evacuated once more, filled with argon so that the pressure was a little higher than atmospheric pressure and the outgas valve was opened and Ar was allowed to flow through the furnace. The gas flow was controlled by a Bronkhorst flowmeter and was set to approximately 70 ml/min.

The temperature in the melt was measured with a thermocouple placed inside an alumina tube. There is also a hole in the top lid that can be opened and a sampling tube can be lowered into the melt. The sampling tubes are alumina tubes that are open in both ends.

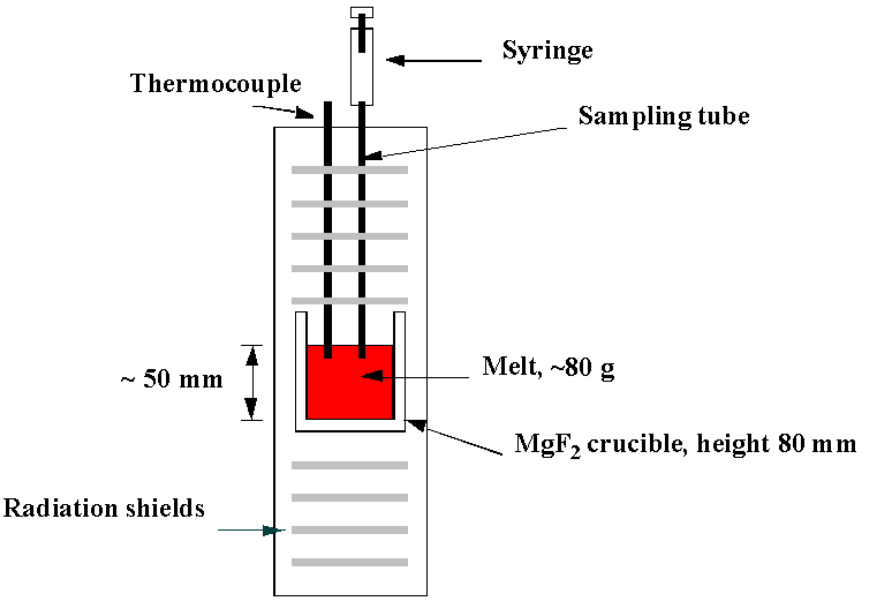

Figure 4.1. A sketch of the inside of the furnace where the samples are taken.

Sampling

The flow of argon was increased before the lid of the sampling hole was removed and the sampling tube was lowered into the furnace. This was done to create an excess pressure inside the furnace so that air is not drawn into the furnace.

Samples are taken by placing a syringe at the end of an alumina tube. The tube was carefully lowered into the melt, and liquid metal drawn into the tube. The tube was then quickly taken out of the melt and cooled with helium at the top of the furnace in the cooling zone. The sample was allowed to cool for a few minutes before the alumina around the sample was removed with a hammer.

Samples were taken after holding the melt at the given temperature for a specified time. With long experimental holding times at high temperatures in some series, the evaporation of magnesium was so significant that at the end of the

experiments, samples had to be drawn from points close to the bottom of the crucible in order to reach the magnesium. In these cases, there was practically no magnesium left in the crucible when the experiment ended.

ANALYSIS OF FLUORINE IN MAGNESIUM

It is not an easy task to analyze small amounts of fluorine in magnesium. Three different methods have been employed with varying degree of success. The first method employed is called the Sintalyzer method. This method gave a straight line in a 1/T - log [F] plot, as may be expected, for the first three series performed. The next ten series gave very scattered results. Since the first three series gave very reasonable results, we believed that there was something wrong with the experiments rather than the analytical method. However, when the samples were split and one part analyzed with the Sintalyzer and one with a second method, Glow Discharge-Mass Spectrometry, the results from GD-MS gave a straight line in a 1/T -log[F] plot, whereas the results from the Sintalyzer did not give corresponding results. See Appendix 8.

In a search for alternative methods to analyze fluorine, we ended up with Glow Discharge Mass Spectrometry. These analysis are performed by Shiva Technologies, USA. In addition, analysis using Secondary Ion Mass Spectrometry (SIMS) were also carried out. These analysis are performed by Ulf Sødervall at the SIMS laboratory at Chalmers Tekniska Högskola.

In addition to the methods mentioned here, an attempt was made initially to dissolve the samples in acid and use an ion selective electrode. This did not succeed due to contamination of the samples from the glass where the samples were dissolved. A different method, Inductively Coupled Plasma (ICP-MS), was also considered, but it was argued that this is not a suitable method for analyzing fluorine.

Sintalyzer

The “SINTALYZER” is an analysis method developed by Sintef for use in the aluminum industry. The method is based on ion selective electrodes.

The samples are dissolved in a buffer and the EMF of this solution is determined, illustrated as the blue square placed on the y-axis in Figure 4.2. This particular buffer provides ligands for complexes with a higher stability than for those of magnesium and fluorine. Hence, the fluorine ions remain free in the solution and can be detected by the LaF selective electrode.

Controlled amounts of fluoride in the form of NaF are added to the solution three times, seen as the green square indicators in the figure. After each addition, the EMF of the solution is measured. The amount of fluorine added is given on the x-axis. Then it is possible to calculate a regression line through the four points, and extrapolate this line to the x-axis intercept. This interception relates the EMF of the initial sample to the fluorine concentration of the sample. The total amount of fluorine in the sample is given on the lower x-axis.

$$E_i = E^0 + (RT/nF) \ln K$$

$$\Rightarrow f \cdot [\%F] = \exp [nF/RT(E_i - E^0)]$$

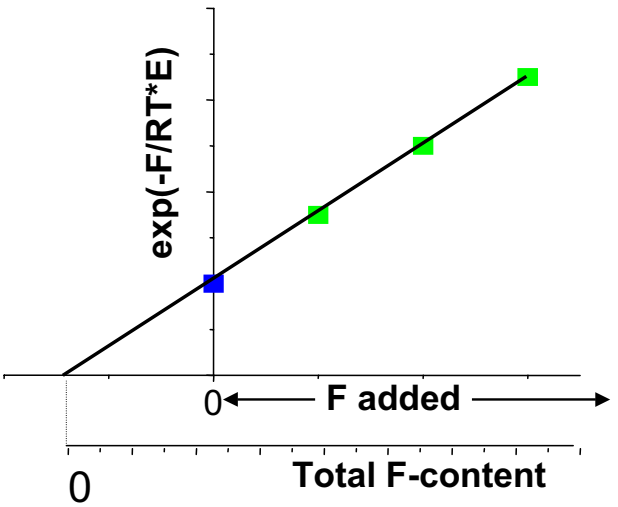

Figure 4.2 An illustration of the principle that the Sintalyzer is based on.

It should be mentioned that also this method measures the total amount of fluorine in the sample, so if there are particles, these will also contribute to the measured fluorine.

The uncertainty in the measurements is given by the laboratory to be 10% for values higher than 5 mg F/kg and 20% for values less than 5 mg F/kg.

Glow Discharge Mass Spectrometry (GDMS)

Glow Discharge Mass Spectrometry is a method for analyzing trace elements in solid, inorganic materials. The analysis principle is that the solid sample is atomized by sputtering in a low-pressure DC plasma. The atoms are then ionized in the plasma and can be extracted out of the plasma by a gas flow and electrical potential. The ions are accelerated through a series of electronic optics, and separated by their mass to charge ratio in the high-resolution mass analyzer. The instrument used in this case can detect any element in the periodic table with atomic masses from one to 260 down to concentrations as low as in the ppt wt level. [http://www.shivatec.com/new/gdmsdesc.php4, 2003]

Figure 4.3 illustrates what happens in the first step of the GDMS analysis when the magnesium sample first is atomized and then ionized. The plasma, or discharge gas if you like, is usually ultra high purity argon. In some cases different gases like helium, neon or krypton may be used. This support gas will be partly ionized because of the current applied (electrical breakdown). These positively charged discharge gas ions start accelerating towards the negatively biased cathode (the sample) and the sputtering process and the atomization of the sample starts. Secondary ions formed are returned to the sample surface again. The ionization process of the magnesium atoms takes place in the negative glow region of the plasma. There, the atoms collide with electrons and metastable argon atoms and the ionization process is complete. [http://www.shivatec.com/new/gdmsdesc.php4, 2003, King, Teng and Steiner, 1995, Becker and Dietze, 2000]

From the glow discharge, the ions are transported through the optical system to achieve a focused beam into the mass analyzer. Here, the ions are separated by their mass to charge ratio. Two different detectors are used: A Faraday cup to measure major species and elements down to 1000 ppm, and a Daly detector for trace elements. The detection limit for the Daly detector is below the ppb level. [http://www.shivatec.com/new/gdmsdesc.php4, 2003, King, Teng and Steiner, 1995]

In many mass spectrometric methods, such as Thermal Ionization Mass Spectrometry (TIMS), Laser Ion-desorption Mass Spectrometry (LIMS) and Secondary Ion Mass Spectrometry (SIMS), the ionization takes place concurrently with the atomization. This may give matrix effects which you do not get when you do the atomization and the ionization in two separate steps as you do with GDMS. [King, Teng and Steiner, 1995]

To quantify the results from the GD-MS, the ion intensities have to be multiplied by a relative sensitivity factor (RSF) to obtain real concentrations [Bogaerts and Gijbels, 1999]. The laboratory conducting the analysis remarked that they did not

have a well characterized Mg base reference material, that would be good for accurate RSF(F) evaluations. Therefore, a calculated value, based on analogies with Cl and O, was used for fluorine. This factor was set to 2.

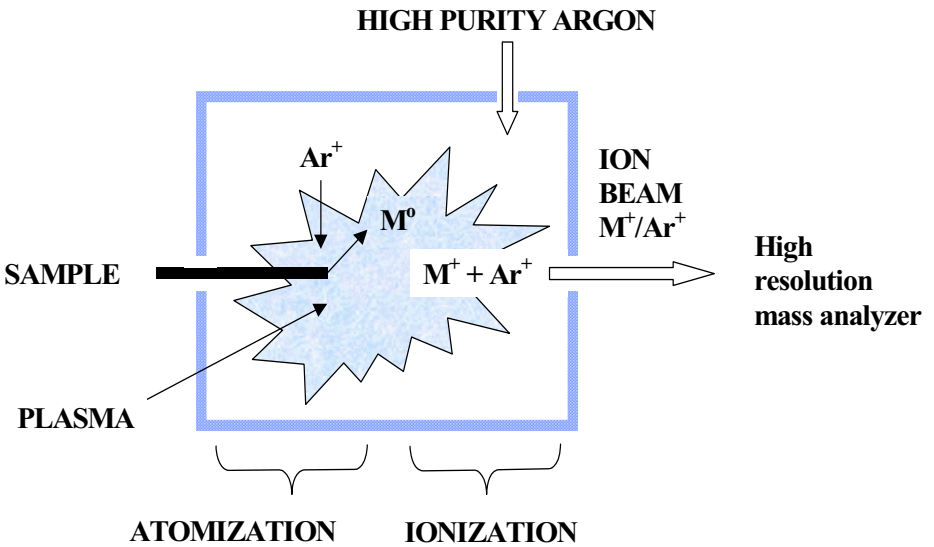

Figure 4.3 The figure illustrates how the sample is atomized and ionized before the ion beam is analyzed in the mass spectrometer. (Reproduced from Shiva Technologies internet pages, http://www.shivatec.com/new/gdmsdesc.php4)

The samples analyzed are 2 mm in diameter and 20 mm in length. Half of the length of the sample is sputtered.

Secondary Ion Mass Spectrometry (SIMS)

Secondary Ion Mass Spectrometry is a surface sensitive technique with excellent depth resolution. The method is illustrated in Figure 4.4. A focused ion beam, consisting of Ar^+, Cs^+, Ga^+, O^- or O_2^+ ions, sputters the surface, producing ionized secondary particles to be analyzed. In the case of fluorine in magnesium, both O_2^+ ions and Cs^+ ions were used in two separate analysis to sputter the sample. The oxygen ions give positively charged secondary ions while cesium ions give negative ions, e.g. F^- which are analyzed with a mass spectrometer. Cs ions are assumed to give the best sensitivity for fluorine.

Most of the secondary particles produced are neutral, and only the secondary ions are extracted by electric fields. The detectors used are electron multiplier, Faraday cup or ion sensitive image amplifier for imaging [Wilson, Stevie and Magee, 1989 Katz, 1993, Becker and Dietze, 2000].

As also can be seen from Figure 4.4, three types of results may be produced with SIMS. The mass spectrum gives the intensity of the secondary ions of the given element as a function of mass. The second alternative is ion images. Secondary ions from the sample which are detected with the mass spectrometer are used to form an image. The image can be a map which shows where specific elements can be found. The results can also be given as a depth profile which gives signals from further and further down into the sample.

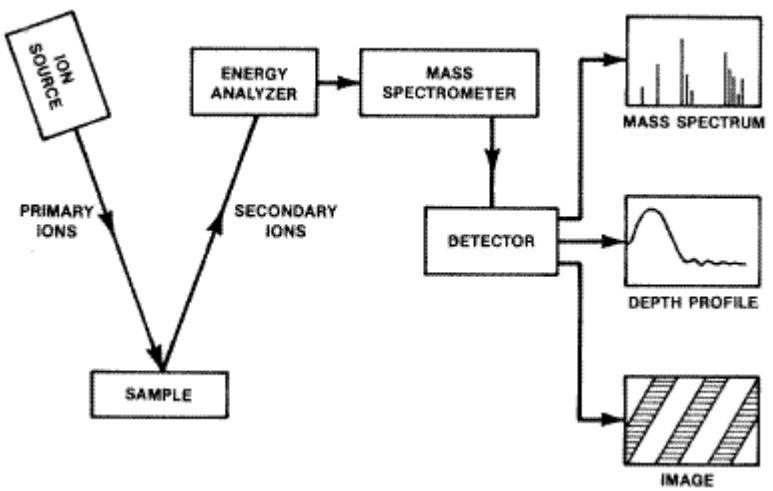

Figure 4.4 An illustration of the SIMS technique.[Wilson, Stevie and Magee, 1989]

To be able to quantify the concentration of fluorine, it is necessary to have a reference with a known amount of fluorine. This was provided by ion implantation of 19F ions into one of the samples sent them. Measurements are carried out on the original sample and also after implantation of fluorine. Then it is possible to determine the initial amount of fluorine in the sample.

The area sputtered is approximately 200 by 200 micrometers, but only ions from the center 50 microns in diameter are analyzed.

RESULTS

Solubility of fluorine in pure magnesium

The results for the solubility of fluorine using the various analytical methods are presented below. The solubilities are given in ppm (wt) as a function of 1/T.

Sintalyzer

As mentioned, the three first experimental series that were analyzed with the Sintalyzer, gave a straight line when plotted in a log[F]-1/T diagram. This is seen in Figure 4.5. The next six series, performed exactly the same way, are presented in Figure 4.6. However, these measurements seem to be distributed in a random manner, and there is no trend in the data. Note that the scale on the y-axis is different in the figures.

Samples were taken both after a short time (approximately 5 hours) and a long time (approximately 24 hours). This is indicated in the figures, but there seems to be no significant difference between the samples taken after 5 hours and the ones after 24 hours.

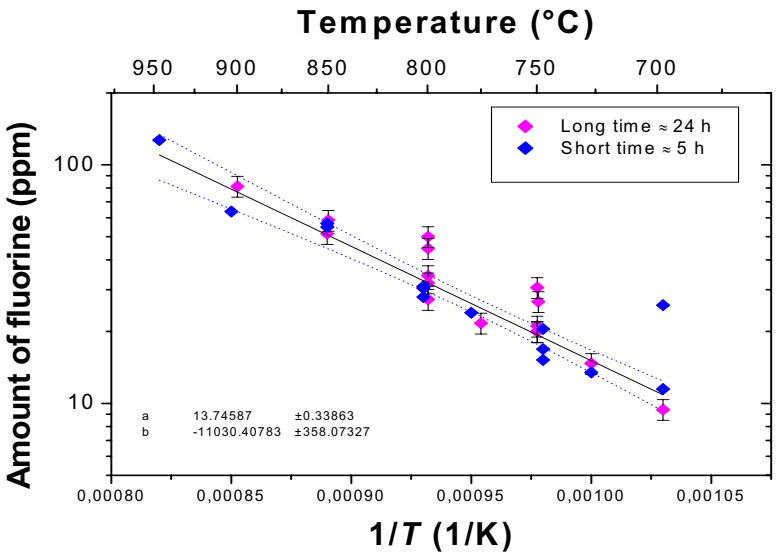

Figure 4.5 Results for fluorine in molten Mg in equilibrium with MgF_2 from the three first series of experiments that were analyzed with the Sintalyzer method.

The data in Figure 4.5 are fitted to the following equation using a non-linear curve fitting method [Press, 1992]:

$$[\%\,\mathrm{F}] = 10^{-4} \cdot [\mathrm{ppm\ F}] = e^{a+bx} \cdot 10^{-4} = e^{\left(a+\frac{b}{T}\right)-4\ln 10} \qquad (4.3)$$

This is compared to Equation 4.2:

$$e^{\left(a+\frac{b}{T}\right)-4\ln 10} = e^{-\Delta G^\circ / 2RT}$$

From this, the expression for ΔG° is derived:

$$\Delta G^\circ = -2RT\left(a+\frac{b}{T}-4\ln 10\right) \qquad (4.4)$$

The uncertainty is used as weight during the fitting, and the result is given as a black line in the figure. In addition, a 95% confidence interval is also presented as dotted lines.

The values for ΔG° and ΔG°_3 are already published [Aarstad, Syvertsen and Engh, 2002]:

$\Delta G^\circ_3/2 = (-473\,000 \pm 3250) + (53 \pm 3)T$

$\Delta G^\circ = (183\,400 \pm 6000) - (75 \pm 6)T$

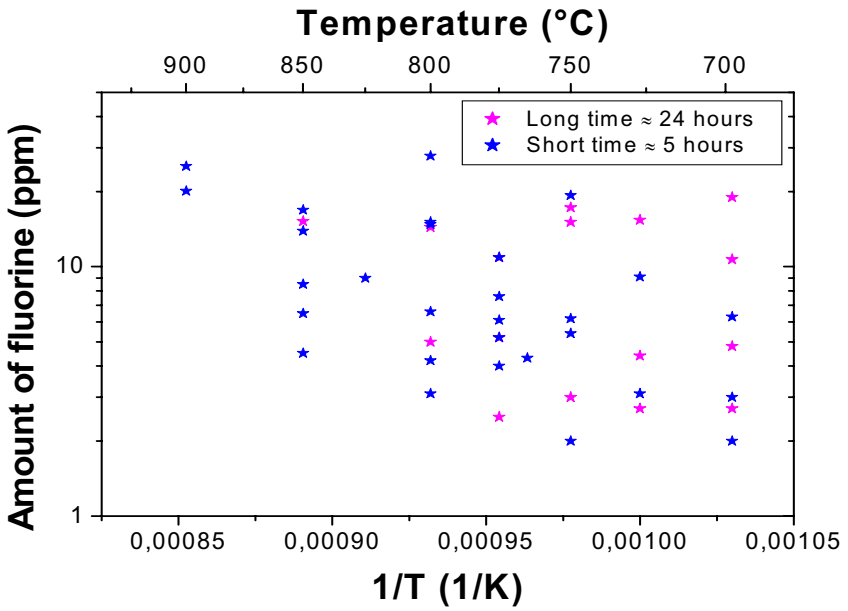

Figure 4.6 Solubility of fluorine in molten Mg in equilibrium with MgF_2 from six more series that were analyzed with the Sintalyzer method.

Glow Discharge Mass Spectrometry

The results from three experimental series analyzed with GD-MS are presented in Figure 4.7. The solubility of fluorine in magnesium is given as a function of inverse temperature. As can be seen, the solubility increases with increasing temperature. The standard deviations for the fluorine measurements are given as error bars. The measurements are fitted to equation 4.3 by a non-linear curve fitting method [Press, 1992], using the uncertainty as weight. The fitting is shown as the black line in the diagram. A 95% confidence interval is also calculated, given as dotted lines.

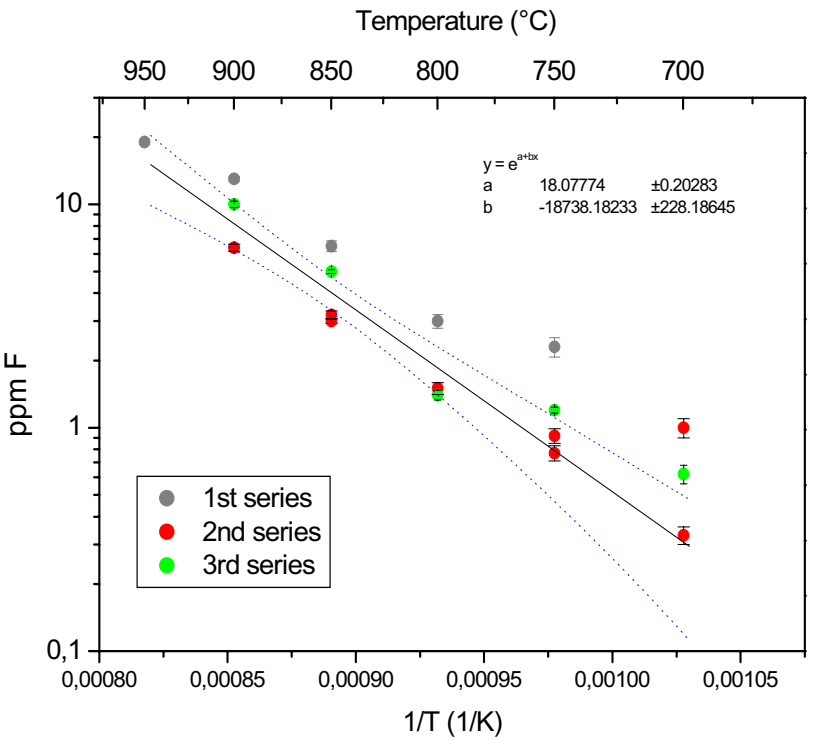

Figure 4.7 Solubility of fluorine in molten magnesium in equilibrium with MgF_2 as a function of temperature. Method of analysis is GD-MS.

There were no indications that increased holding time increased the solubility. The samples were reported to be very homogenous. The first series seems to lie a bit higher than the following two.

ΔG^o for these series of experiments are found to be:

$$\Delta G^o = 311\ 566 \pm 228 - (147 \pm 4)\ T \qquad (4.5)$$

This gives for the reaction $F_2\ (g) = 2\underline{F}$ (in mass%):

$$\Delta G^\circ_3 = (-\ 818\ 000 \pm 3800) + (34 \pm 4)T \qquad (4.6)$$

when GD-MS is used as the method of analysis.

Secondary Ion Mass Spectrometry

The analysis with SIMS was performed with two different types of ions used to sputter the sample: Cs^+ and O^{2+}. As mentioned, the Cs^+ ions usually give the best accuracy. The results from the Cs^+ and the O^{2+} analysis are given in Figure 4.8 and 4.9, respectively. As one can see, using O^{+2} ions instead of Cs^+ ions gives higher fluorine values.

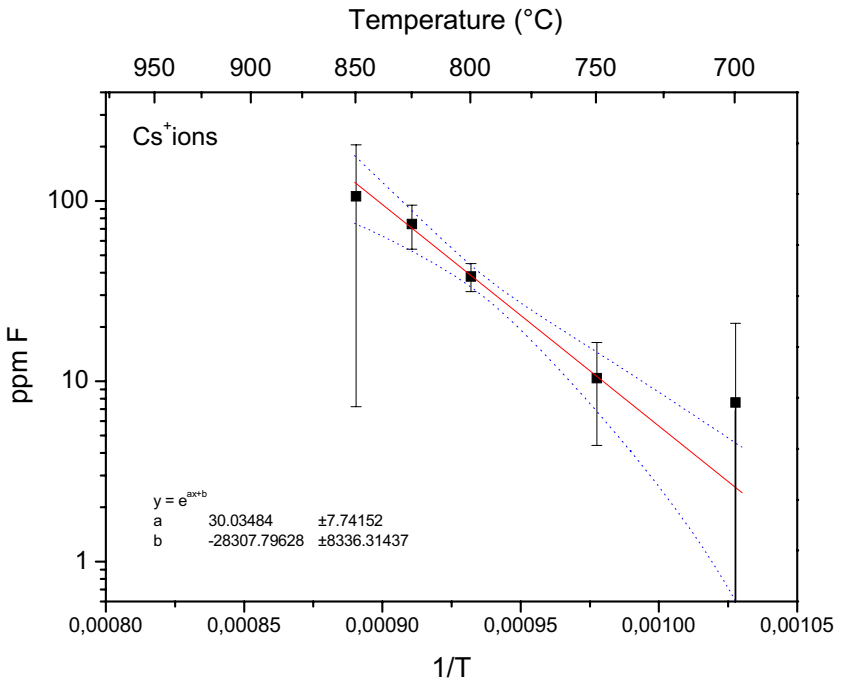

Figure 4.8 Solubility of fluorine in molten magnesium in equilibrium with MgF_2 as a function of temperature measured with Secondary Ions Mass Spectrometry (SIMS) using Cs^+ ions.

Particles were found in the samples taken at 850 and 700°C.

The Cs^+ data are used to calculate the ΔG^o value:

$$\Delta G^o = (470\ 700 \pm 130\ 600) - (346 \pm 128)\ T \qquad (4.7)$$

and for the reaction F_2 (g) = 2F (in mass%):

$$\Delta G°_3 = (- 658\,000 \pm 130\,600) - (165 \pm 128)T \qquad (4.8)$$

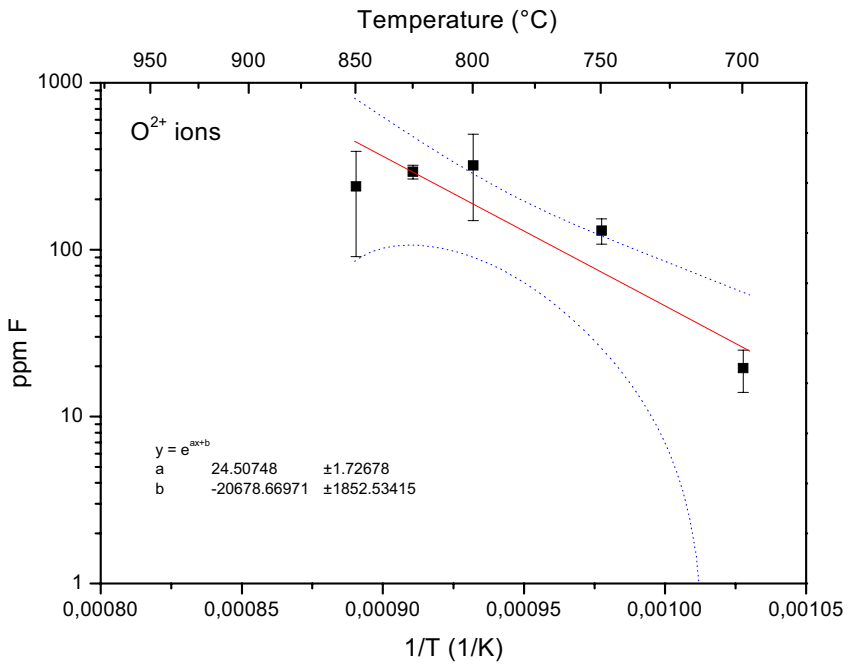

Figure 4.9 Solubility of fluorine in molten magnesium in equilibrium with MgF_2 as a function of temperature measured with SIMS using O^{2+} ions.

Solubility of fluorine in magnesium saturated with iron

The solubility of fluorine in magnesium saturated with iron as a function of temperature is plotted in Figure 4.10.

The method of analysis is GD-MS.

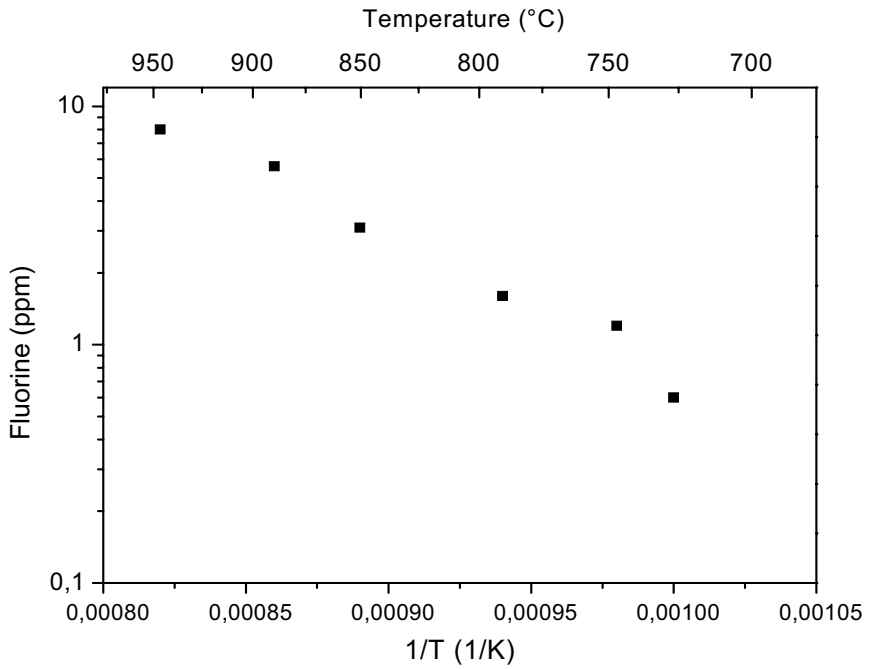

Figure 4.10 Solubility of fluorine in molten magnesium in equilibrium with MgF_2 saturated with iron, measured with GD-MS.

Using the data for the solubility, the Gibb's energy for the reaction F_2 (g) = 2F can be calculated:

$$\Delta G^\circ_3 = -899\,260 + 55.3T \text{ [J/mol]} \qquad (4.9)$$

The standard Gibb's energy for the reaction between fluorine dissolved in molten magnesium saturated with iron and solid magnesium fluoride is given as:

$$\Delta G^\circ = 229\,700 - 70.3T \text{ [J/mol]} \qquad (4.10)$$

For more details, see Eriksen [2002].

The results for the solubility of fluorine in iron saturated magnesium are compared to those for fluorine in pure magnesium in Figure 4.15. The data from

the iron saturated melt follow the other data, so one may conclude that iron does not significantly affect the solubility of fluorine on molten magnesium.

DISCUSSION

The main problem encountered during these experiments was to find suitable methods for analyzing the fluorine in magnesium. The three various analysis methods employed are compared in Figure 4.11. There are two series with Sintalyzer results. The triangles (Sintalyzer 1) indicate the three first series where the results seemed reasonable, whereas the stars (Sintalyzer 2) give the last six series with more uncertain measurements.

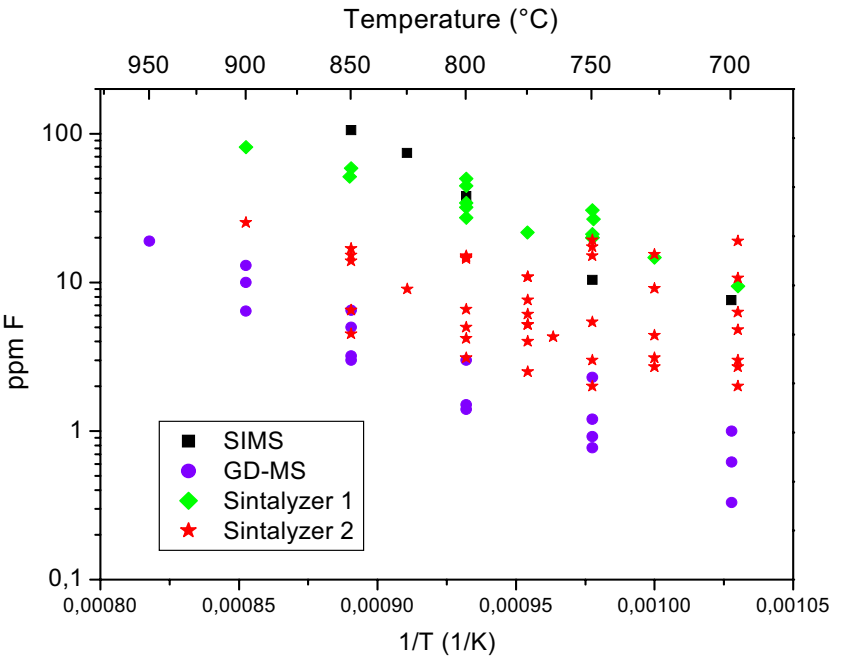

Figure 4.11 A comparison of the solubility of fluorine in equilibrium with MgF_2 for different analytical methods.

All the methods, except the six last series with the Sintalyzer, give an increasing trend for the solubility of fluorine with temperature. The three reasonable series with the Sintalyzer and the samples analyzed with SIMS lie in the same area, starting at approximately 10ppm at 700°C and going up to approximately 100

ppm at 900°C. Both the Sintalyzer method and SIMS give values of fluorine approximately ten times higher than the GD-MS method.

Even if the Sintalyzer method is rejected, there is still the question of whether the results from SIMS or the ones from GD-MS are the correct ones. SIMS has the advantage that a standard produced specially for these analysis is employed. In addition, there is some uncertainty connected to the relative uncertainty factor for the GD-MS analysis. It is therefore assumed that the results from the SIMS measurements are the correct ones. The results from both GD-MS and SIMS are compared in Figure 4.12, and it can be seen that if the fitted line for GD-MS is moved, it has approximately the same slope as the data from SIMS.

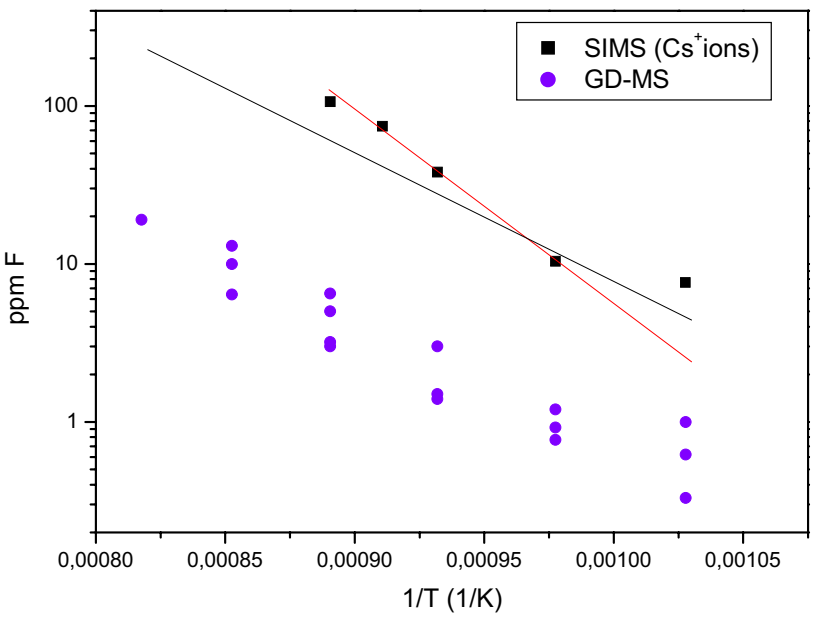

Figure 4.12 A comparison of the solubility using GD-MS and SIMS.

There is a possibility that fluorine might evaporate from the melt. The vapor pressure of fluorine can be calculated from the data in equation 4.8 at 1000K:

$$\frac{\sqrt{p_{F_2}}}{[\%\,\mathrm{F}]} = e^{\left[\left(\frac{-329000}{T} - 336\right)/(8.314)\right]} = e^{-80}$$

This shows that the vapor pressure at 1000K is so low, that it should not affect the results.

Particles in the melt

Figure 4.13 shows a crucible after the experiment is finished. There are magnesium droplets on the crucible walls and also on the metal surface. These are probably formed from magnesium vapor when the furnace is cooled. The magnesium fluoride crucible is very solid so if the metal did not adhere so well to the crucible walls, it could have been used several times.

Figure 4.13 The crucible after the experiment is completed.

Not many particles were found when the metal remaining in the crucible after the experiment was examined. However, some particles were detected at the bottom of the crucible and close to the crucible walls as can be seen in Figure 4.14. Possibly the laboratory using the Sintalyzer got samples with a high amount of particles. Particles should give a higher value of fluorine. The GD-MS analysis

did not reveal any inhomogenity in the samples. The SIMS analysis on the other hand, detected particles in two of five analyzed samples.

All the methods measure total fluorine content, both fluorine in solution and in particles. Therefore, one could argue that the method giving the lowest solubility, i.e. GD-MS would be the most correct one. The Sintalyzer dissolves the whole sample. The GD-MS method uses approximately 10 mm of the sample rod, whereas SIMS is only a surface technique, only analyzing a few microns down into the sample.

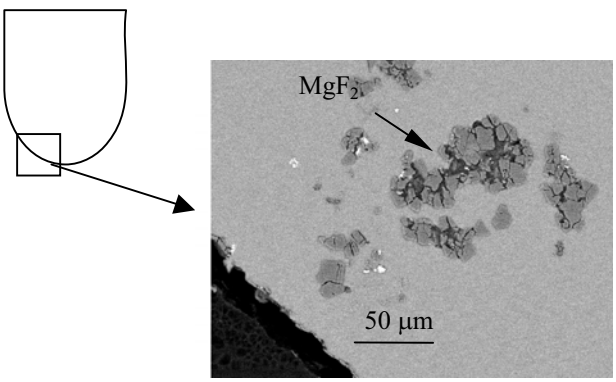

Figure 4.14 MgF_2 particles found in the melt remaining in the crucible. Picture taken close to the crucible walls and the bottom as illustrated to the left.

There is a possibility that the laboratory using GD-MS were fortunate with the samples they got, since they reported that the samples were homogenous, and the results plotted fit a straight line in a log F versus 1/T plot. Probably, the GD-MS measurements give a good estimate of the slope of the log F versus 1/T line, see Figure 4.12. It is unfortunate that a reliable relative sensitivity factor (RSF) for fluorine in magnesium is not available.

In the cases where magnesium fluoride particles actually were found with SIMS, we can see that the results then deviate from the straight line and that they have high uncertainties as was seen for the samples at 700 and 850°C in Figures 4.8 and 4.9.

The effect of iron

The addition of iron to the melt did not affect the solubility of fluorine as seen from Figure 4.15. It is not surprising that iron does not affect the solubility since the solubility of iron in magnesium is less than 0.1 at%. (See Figure 4.16)

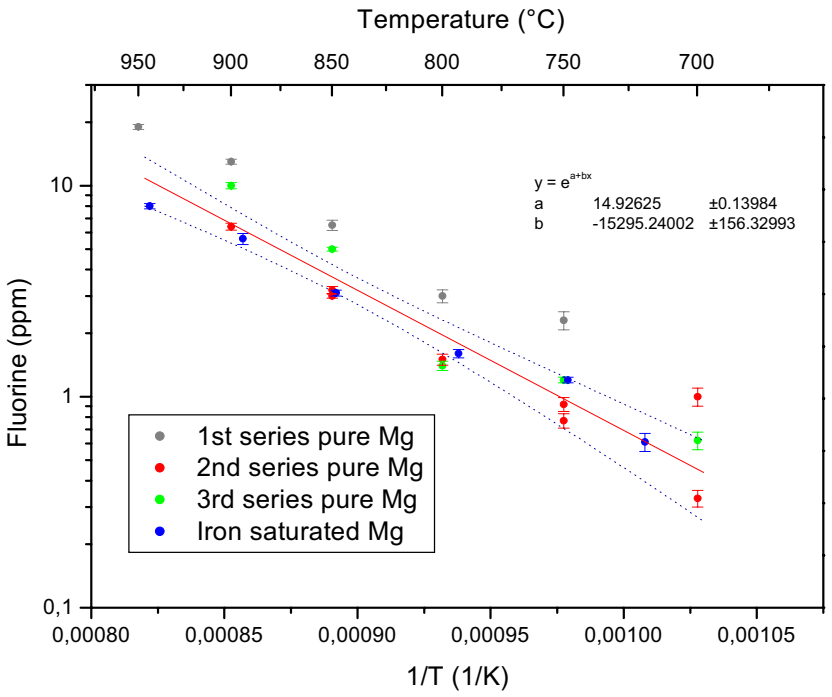

Figure 4.15 Comparison of solubility of fluorine in pure magnesium versus iron saturated magnesium. The method of analysis is GD-MS.

The GD-MS measurements with iron gave the same results as without iron.

The amount of iron in the samples was also measured at the same time as the fluorine. The solubility of iron in magnesium is well known, and by comparing our results to other works, we can see that our results fit very neatly in, Figure 4.16. This indicates that GD-MS is a method at least well suited for measuring iron in magnesium.

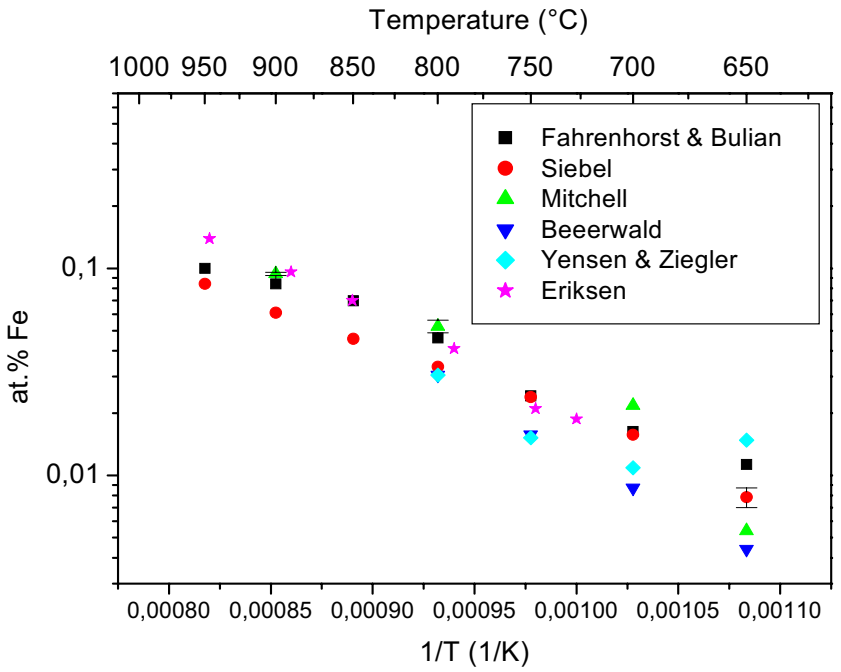

Figure 4.16 Solubility of iron in molten magnesium given in literature compared with the present study using GD-MS [Eriksen, 2002] for magnesium held in a magnesium fluoride crucible.

Protection of molten magnesium by dissolving fluorine

The main idea behind this study was to see whether it is possible to dissolve fluorine into the melt itself, and that this fluorine could help build a stable film on the melt surface. However, the solubility of fluorine in molten magnesium is so low that probably this is not an alternative. Considering a temperature of 700°C, which is a normal melt temperature in the industry, the amount of fluorine lies between 0.2 ppm (GD-MS) and 20 ppm (Sintalyzer and SIMS). This fluorine "bottleneck" would seem to be too small to supply the surface with the necessary fluorine.

CONCLUSION

Measurements of the solubility of fluorine in molten magnesium have been carried out. Various analytical methods have been applied: Sintalyzer, Glow Discharge Mass Spectrometry (GD-MS) and Secondary Ion Mass Spectrometry (SIMS). The results from the different methods may vary by a factor ten. However, it is concluded that the results from the SIMS analysis are probably the most correct ones. The $\Delta G°_3$ value for the dissolution of fluorine,
1/2 F_2 (g) = $\underline{F}$ (in mass%) is:

$\Delta G°_3/2 = (- 329\,000 \pm 65\,000) - (83 \pm 64)T$

Iron has no effect on the solubility of fluorine in molten magnesium.

For the F solubility in equilibrium with MgF_2, $MgF_2(s) = Mg\ (l) + \underline{F}$, the $\Delta G°$ is given by:

$\Delta G^o = (471\,000 \pm 131\,000) - (350 \pm 130)\ T$

It does not seem to be a viable approach to dissolve fluorine into the melt to protect the melt surface from uncontrolled oxidation.

BIBLIOGRAPHY

Aarstad, K, Syvertsen, M and Engh, T A (2002) Solubility of Fluorine in Molten Magnesium *Magnesium Technology 2002* **3**: 39-42.

Becker J.S. and Dietze H.J. (2000) Inorganic Mass Spectrometric Methods for Trace, Ultratrace, Isotope, and Surface Analysis. *International Journal of Mass Spectrometry* **197**: 1-35.

Boegaerts A. and Gijbels R. (1999) New Developments and Applications in GDMS. *Fresenius Journal of Analytical Chemistry* **364**: 367-375.

Engh, T A (1992) Principles of Metal Refining Oxford: Oxford University Press: 407-425

Eriksen, J M (2002) Solubility of Fluorine in Molten Magnesium Saturated with Iron. Project in Process Metallurgy. Norwegian University of Science and Technology.

King, F L, Teng J. and Steiner R.E. (1995) Glow Discharge Mass Spectrometry: Trace Element Determinations in Solid Samples. *Journal of Mass Spectrometry* **30**: 1061-1075.

Katz W. (1993) Secondary-Ion Mass Spectrometry. In Concise Encyclopedia of Materials Characterization. Edited by Cahn Frs R.W. and Lifshin E. Pergamon Press, Oxford. 438-445.

Press, W. H. et al. (1992) Numerical Recipes in C: The Art of Scientific Computing (2nd ed.) Cambridge: Cambridge University Press, Chapter 15.

Shiva Technologies home page http://www.shivatec.com/new/gdmsdesc.php4 Accessed May 15th 2003.

Wilson R.G., Stevie F.A. and Magee C.W. (1989) Secondary Ion Mass Spectrometry. John Wiley & Sons, Chichester.

Chapter 5 .
Discussion and Further Work

A table of the Pilling-Bedworth ratios of compounds mentioned here was presented in Table 1.2.

It is documented in this work that magnesium fluoride forms when magnesium is exposed to SF_6. With CO_2, magnesium carbonate was not detected in these samples, neither in Chapter 2 with the Kanthal furnace or in Chapter 3 with the hot stage, which is in accordance with the thermodynamic calculations. Various explanations as to why CO_2 protects be suggested:
-The CO_2 is adsorbed at the melt surface and prevents oxygen from reaching the metal
-The magnesium oxidizes according to the reaction $2\ Mg + CO_2 = 2\ MgO + C$. This reaction is much slower than oxidation of Mg in air [Aleksandrova and Roshchina, 1977] and atoms in the surface have time to realign.
-The exothermic heat generation is lower than when magnesium reacts with oxygen. This reaction takes place in the gas phase and the heat generated is dissipated in the gas so that the surface is not heated up.

For SO_2, sulphide is most likely to form thermodynamically. Sulphur is found in considerable amounts in some samples.

Calcium has a preventive effect on the ignition of magnesium [Chang et al, 1998 and Sakamoto, Akiyama and Ogi, 1997]. Aluminum and beryllium are known to have preventive effects on the oxidation of the melt. However, there are limits of

how much of such elements that can be added to melt without affecting the physical properties of the metal.

It may therefore be favorable to add a protective element as a gas if possible. This of course limits the options.

In addition, it is required that the gas should not be harmful to either people or environment, or decompose to such gases, and unwanted elements must not be introduced into the melt. Concern might also have to be taken regarding the surface finish. Customers may not like the black surfaces that occur when CO_2 is employed. All these factors narrows down the gases that can be used.

It may be that when a phase with a high volume forms at the surface, the film has to "wrinkle up" to be able to fit the surface. This concept could be applied to the samples in Chapter 2. It should be kept in mind though, that the experimental set-up is relatively crude for these experiments. For example, in Figure 2.12, a surface exposed to SO_2 in air is seen. This surface seems to be very wrinkled. The samples in CO_2 in Figures 2.23, 2.27 and 2.28 are not very wrinkled compared to the sample in SO_2.

SF_6

This work confirms that fluorine is the active element in SF_6, and that it is necessary to have oxygen present to build a strong surface film. As was seen here, the surfaces exposed to SF_6 contained large amounts of fluorine.

According to the thermodynamic calculations performed with FactSage, the reaction products between molten magnesium and SF_6 in air should be magnesium fluoride and magnesium sulphide. The presence of fluoride is well established, but no sulphide is revealed. This is the same experience as Pettersen at al.[2002] and Cashion[1998] had.

A protective gas must be able to deliver enough fluorine to the magnesium surface, but must not contain or decompose to any harmful products. This is a problem since most fluorine containing gases have disadvantages.

It is suggested in this work that, at least as a partial explanation, that the protective effect of SF_6 is due to the formation of a second phase, MgF_2, in addition to the magnesium oxide. To understand this, one may refer to the Pilling-Bedworth ratio. Using fluorine containing gases, magnesium fluoride forms and may give a Pilling-Bedworth ratio close to one. This is a simple explanation, but should not be rejected.

The assumption that the only two phases found in the films containing fluorine are MgF_2 and MgO may be questioned as was discussed in chapter 3. However, publications found on the topic both conclude that there is no mutual solubility, and that there is a separation into the two primary phases [Sharma, 1988 and Putz, Schön and Jansen, 1998].

CO_2

Carbon dioxide is an alternative that should be considered more closely. There are two major problems using CO_2: The surfaces may turn black, and carbon may be introduced into the metal which is harmful for the corrosion resistance. Although the black surfaces look as they are covered with soot, they do not contain more than approximately 1% C. Also, the black color may not be caused by soot, but may be due to a certain modification of the oxide as has been seen with aluminum. It is seen that the gas distribution system becomes more critical when using CO_2. There has to be enough CO_2, and the gas has to circulate sufficiently.

It was seen that when the furnace in Chapter 2 was contaminated with fluorine, magnesium samples exposed to CO_2 were well protected and shiny. Possibly one could dissolve fluorine in the melt in addition to using CO_2 as a protective atmosphere. The small amount of fluorine present in the molten metal might be sufficient when combined with CO_2 in the gas.

SO_2

Sample FA in Chapter 3 shows a wrinkled surface in Figure 3.32, even with the sample held below the melting point at 635°C. Probably the surface gets wrinkled when a volumnious phase forms as was proposed above. This would suggest that the protective effect is due to the formation of MgS. However, 30% of the oxide film has to consist of MgS in order to achieve an average Pilling Bedworth ratio of 1. The experiments indicated that the film consisted of 7 “parts” MgS and 40 “parts” MgO (see Table 3.14), which equals approximately 15% magnesium sulphide.

EXPERIMENTAL METHODS

Regarding experimental equipment, the hot stage provided samples that were very well suited for further studies with for example TEM, X-ray, microprobe and FE-SEM. The experiments could be repeated with other gas mixtures than SF_6 in air, e.g. the gas mixtures that were tested in Chapter 2. It would be interesting to compare these films to the ones produced with SF_6. The hot stage should also be

suitable to test “new” gases that are suggested for magnesium melt protection. This would be a fast and easy-to-handle way of doing initial experiments before testing on a larger scale is carried out.

It should be kept in mind that fluorine contaminates the equipment once it has been introduced. It would be advantageous if the hot stage could be evacuated so that the atmosphere could be better controlled, and that it is vacuum tight so that air does not leak into the chamber.

One disadvantage using the hot stage described here is that the film forms as the sample is heated up to the experimental temperature. It does not seem to be possible to start with a “fresh” molten magnesium surface as was the case with the Kanthal furnace in Chapter 2. However, the Kanthal furnace, which made a fresh surface possible, did not provide a smooth surfaces. Smooth surfaces are required for most analytical methods to give reliable results.

It was seen in this work that there is no difference in the films whether they form just below or above the melting point, except for the thickness of the films. This means that you really do not have to melt the metal to produce a film for further studies. Therefore, one may conclude that if you want to produce a film for academic studies, it is not necessary to cross the melting point. However, there may be other effects that are enhanced with increasing temperature, as suggested here, the decomposition of the gas and reaction rates. If the aim is to test a gas mixture for industrial use, the temperature of the sample should - at least eventually - be the same as the melt temperature in real life.

The microprobe is commonly used as an analysis tool in these experiments. It is important to be aware that a volume is being analyzed. In Figure 5.1, a typical analysis volume is illustrated. Signals are received from the volume illustrated. However, the film will in may cases only be a small part of the analysis volume, depending on the acceleration voltage which determines the depth of the analysis volume, and the thickness of the film. The depth of the analysis volume is typically 3-5 μm for these kinds of samples. This means that if the film is 0.1-1 mm, only a part of the signal will originate from the film.

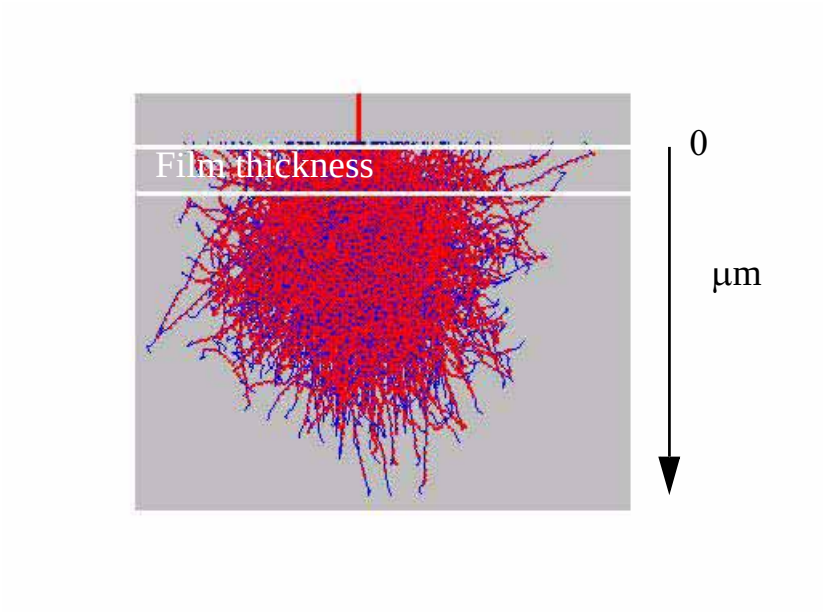

Figure 5.1 The microprobe analysis volume of a sample with an imaginary film.

INDUSTRY

There have been a few suggestions by commercial companies for alternatives to SF_6 the last couple of years, but none of them seem to be very promising so far. Replacing SF_6 with for example HFC-134a, which has a GWP of 1500, would only be a short-term solution since this gas probably also will be forbidden in the nearest future. A problem with new suggestions for melt protection gases, is that initially one does not know if other harmful gases are produced during use.

It is also a problem that commercial companies have an economic incentive to take over the research and development of new protective gas systems. Thus, commercial considerations complicate cooperation with academic communities and between companies.

FUTURE WORK

From an academic point of view, it would be very interesting to understand the kinetics governing Equation 3.1.

More experiments should be performed with SO_2 and CO_2. Cross sections of films could hopefully tell more about the formation and composition of these

films. It would be a step forward if one was able to confirm the presence of other phases such as magnesium sulphide/sulphate and carbonate if this is the case.

Methods for the effect of direct addition of fluorine to the molten metal should be studied.

It would be advantageous, when melting magnesium with various gas atmospheres, to be able to measure the off-gases produced. This could be used both to make sure that no harmful gases form, and to study the kinetics. For instance, a mass spectrometer could be employed.

The Mg-O-F, Mg-O-S and Mg-O-C systems at temperatures around 1000K should be studied further. Perhaps X-ray diffraction studies would be useful. For instance, the solubilities of F in MgO and O in MgF_2 and diffusivities of Mg^{2+}, O^{2-} and F^- should be determined. It would be interesting to find the conditions for the formation of one or several phases.

The mechanisms for CO_2 protection of magnesium should be studied in depth. Such understanding might allow us to find a gas or a gas mixture that does not deposit carbon.

Since one of the arguments against using CO_2 is that it may affect the corrosion resistance, this problem should be investigated more thoroughly. Carbon may also affect other mechanical properties, but this should be looked into. The cause of “blackening” should be studied. The possibility of using CO_2 in industry should seriously be considered by doing experiments with CO_2, also on a larger scale.

BIBLIOGRAPHY

Aleksandrova Y.P. and Roshchina I.N. (1977) Interaction of Magnesium with Gases. *Metallovedenie i Termicheskaya Obrabotka Metallov* **3:**218-221.

Cashion, S.P. (1998) The Use of Sulphur Hexafluoride for Protecting Molten Magnesium PhD-thesis The University of Queensland, Australia.

Chang S.-Y., Matsushita M., Tezuka H. and Kamio A. (1998) Ignition Prevention of Magnesium by Simultaneous Addition of Calcium and Zirconium. International *Journal of Cast Metals Research* **10**: 345-351.

Pettersen G., Øvrelid E., Tranell G., Fenstad J. and Gjestland H. (2002) Characterization of the Surface Films Formed on Molten Magnesium. *Materials Science and Engineering A* **332**: 285-294.

Putz H., Schön J.C. and Jansen M. (1998) Investigation of the Energy Landscape of Mg_2OF_2. *Computational Materials Science* **11**: 309-322.

Sakamoto M., Akiyama S. and Ogi K. (1997) Suppression of Ignition and burning of Molten Mg Alloys by Ca bearing stable oxide film. *Journal of Materials Science Letters* **16**: 1048-1050.

Sharma R.A. (1988) Phase Equilibria and Structural Species in MgF_2-MgO, MgF_2-CaO, and MgF_2-$Al2O_3$ Systems. *Journal of the American Ceramic Society* **71** (4): 272-276.

Chapter 6 . Summary

As is well known, it is found that SF_6 in air protects molten magnesium from uncontrolled oxidation. Inert carrier gases, like nitrogen and argon, for SF_6 or SO_2 do not build protective films that will prevent evaporation of magnesium.

High amounts of magnesium fluoride are seen in the protective film which forms when magnesium is exposed to SF_6 in air. The fluorine is distributed in various ways, see Figure 3.34:
-Magnesium fluoride particles underneath a continuous film
-Both as magnesium fluoride particles underneath the film and as a fluorine rich matrix in the film
-Fluorine is found in what seems to be a continuous film.
-As a fluorine rich matrix phase between oxide grains.

When 5% SF_6 is used in the gas mixture, a fine structure with a fluorine rich matrix phase and oxide grains were formed.

SF_6 in CO_2 as carrier gas did not provide a satisfying result in this work.

It is suggested that this magnesium fluoride gives a favorable Pilling-Bedworth ratio, and therefore the metal is covered completely by the film.

The thickness, L, of the film is found to be proportional to the square root of time:

$L^2 = k \cdot \text{time}$

The thickness also depends on the temperature and the partial pressure of SF_6 in the gas, expressed with k:

$$k(T, p_{SF_6}) = 0.009 \cdot \left(\frac{p_{SF_6}}{1\%}\right)^{0.6} \cdot e^{-2600\left(\frac{1}{T} - \frac{1}{973}\right)}$$

The best suitable methods to measure film thickness were the Auger Electron Spectroscopy, transmission electron microscope (TEM) and field emission scanning electron microscope (FE-SEM).

With SO_2 in air as a protective gas, sulphur is found in the film. It has not been possible to tell experimentally whether this sulphur is found as magnesium sulphide, magnesium sulphate or dissolved in MgO. Sulphide is the most thermodynamically stable, while sulphate has the most favorable Pilling Bedworth ratio. There seems to be a separation into two phases with grains in a matrix. The difference in sulphur content is small. 0.2% SO_2 in air seems to be the limit of how low the SO_2 content can go to still protect the magnesium satisfactorily. SO_2 in CO_2 as carrier gas provided good protection, but resulted in a discolored surface.

Pure CO_2 prevents both oxidation and evaporation, but gives a discolored surface, and problems with C in the metal may be encountered. Films built with CO_2 do not seem to be as strong as films formed with SF_6. Formation of magnesium carbonate has not been observed in the samples exposed to CO_2.

The dissolution of fluorine in molten magnesium, 1/2 $F_2(g)$ = $\underline{F}$ (in mass%) is found to have the following $\Delta G°_3/2$ value:

$\Delta G°_3/2$ = (- 329 000 $\pm$ 65 000) - (83$\pm$64)T

For the solubility of fluorine in equilibrium with magnesium fluoride,
MgF_2 = Mg (l) + 2$\underline{F}$, the ΔG^o value is presented below:

ΔG^o = (471 000 ± 130 600) - (350±130) T

These calculation are based on the results from the Secondary Ion Mass Spectrometry (SIMS) measurements since these are believed to be more reliable than the measurements with the Sintalyzer and Glow Discharge-Mass Spectrometry (GD-MS).

Molten magnesium in equilibrium with magnesium fluoride, is found to have a solubility of 20 ppm at 700°C. This “bottleneck” seems to be to small to supply the metal surface with enough fluorine to give a protective film.

Iron did not affect the solubility of fluorine in magnesium.

Appendix 1

For the reaction MgO=Mg(l)+1/2O_2, ΔG° equals 496 333 J at 700°C [Data from FactSage].

$$\Delta G^\circ = -RT\ln K = -8.314 \cdot 973 \cdot \ln\sqrt{p_{O_2}}$$

$$p_{O_2} = 5 \cdot 10^{-54}\text{bar}$$

This means that for pressures above $5 \cdot 10^{-54}$ bar, under equilibrium conditions, magnesium oxide will start forming.

Appendix 2

Average size and number of spots within one area of sample I which is held at 665°C in 1% SF_6 in air.

Time (hour)	Average size (μm)	# spots
1	7,0278	764
1,5	9,01	751
2	9,5506	679
2,5	12,2536	550
3,5	17,8398	495
4	18,02	619
6,5	30,4538	428
10,5	29,733	308
23	32,2558	412
24	34,238	331
26	36,2202	404
30	34,5984	390
48	33,6974	332
53	34,5984	373

Appendix 3
Criteria for a good calibration standard:

1. The compound should have a sharp melting point. There will, however, always be impurities in the compound which give a melting range instead of a melting point. The melting of the last crystal is closer to the real melting point than the beginning of the melting.
2. The standard should have a known melting point. Melting points given in the literature may vary with several degrees.
3. The melting should be easily observed. If the refraction index of the crystal is close to that of the liquid, the melting of the last crystal may be difficult to observe.
4. Reproducibility. The calibrations may be difficult to reproduce if the impurities are unevenly distributed since very small amounts of standards are used.
5. The standard has to fall in to the desired temperature range.
6. Some standards have sharp melting points, but decompose during the run.
7. Surface oxide on metal chips may prevent the metal from coalescing into a ball at the melting point.
8. Reusability. Metals that form a ball upon melting can not be used again as melting of a crystalline ball not is very obvious.
9. If the standard sublimes rapidly, nothing of the standard will be left when the melting point is reached.
10. Transparency is not a necessity.
11. The standard should not be toxic, although very small amounts are used.

[Roedder, 1984]

Appendix 4
Comparison of thickness of films derived with various analytical methods.

The thickness is given as a function of holding time on a double logarithmic plot. The holding temperature for the samples analyzed with TEM and SEM varied within the samples between 635°C 700°C. No temperature is given for these methods in the figure.

Since the results achieved with Monte Carlo simulations seemed to be 2.7 times too high, the values given here have been divided by this factor.

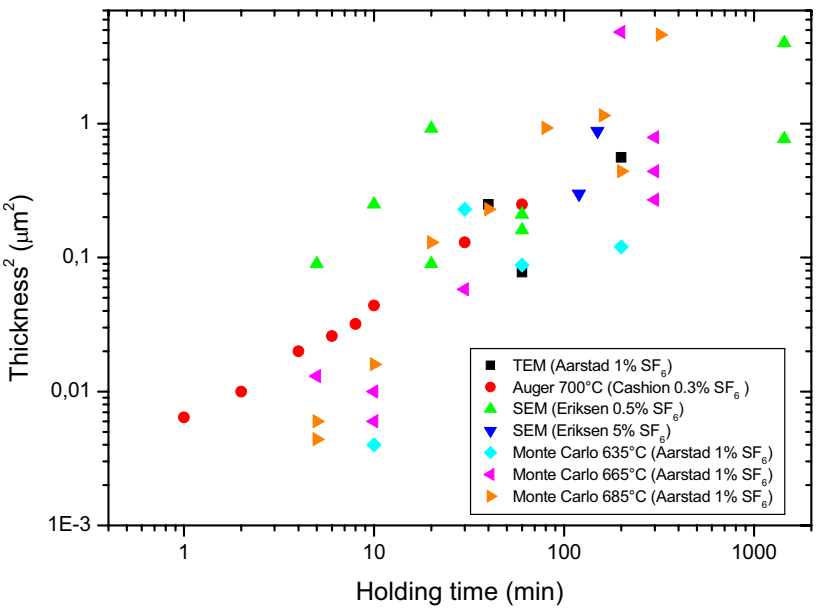

Appendix 5
Calculation of $k^*_{700,}$ E and n

The slope of the three points from the TEM measurement is determined to be:
k_{635}=0.0013
k_{665}=0.0028
k_{685}=0.0063

The slope of Cashion's data is determined to be:
k_{700}=0.0042

Assuming the following relations:
$k_{700}=0.3^n \cdot k^*_0$

$$k_{635}= \left(k^*_0 \cdot e^{-\frac{E}{R \cdot 908}+\frac{E}{R \cdot 973}} \right)$$

$$k_{665}= \left(k^*_0 \cdot e^{-\frac{E}{R \cdot 938}+\frac{E}{R \cdot 973}} \right)$$

$$k_{685}= \left(k^*_0 \cdot e^{-\frac{E}{R \cdot 958}+\frac{E}{R \cdot 973}} \right)$$

where k^*_0 is the slope at 700°C and with 1% SF6
E = temperature dependence

Using the relationships

$$\frac{k_{635}}{k_{665}} = e^{-\frac{E}{R \cdot 908}+\frac{E}{R \cdot 938}}$$

which gives $E=0.18 \cdot 10^6$

$$\frac{k_{685}}{k_{665}} = e^{-\frac{E}{R \cdot 958} + \frac{E}{R \cdot 938}}$$

which gives $E=0.30 \cdot 10^6$

Taking the average of these two values, $E=0.24 \cdot 10^6$ which will be used in the calculations from now on.

Using the expressions for k_{635}, k_{665} and k_{685}, k^*_0 can be calculated from each of the three expressions:

$$k_{635} = \left(k^*_0 \cdot e^{-\frac{E}{R \cdot 908} + \frac{E}{R \cdot 973}} \right)$$

giving $k^*_0 = 0.011$

$$k_{665} = \left(k^*_0 \cdot e^{-\frac{E}{R \cdot 938} + \frac{E}{R \cdot 973}} \right)$$

giving $k^*_0 = 0.0085$

$$k_{685} = \left(k^*_0 \cdot e^{-\frac{E}{R \cdot 958} + \frac{E}{R \cdot 973}} \right)$$

giving $k^*_0 = 0.010$

Taking the average of the three k^*_0 values gives $k^*_0 = 0.010$

Using $k_{700}=0.3^n \cdot k^*_0$
gives n=0.72

The expression for k as a function of temperature and partial pressure of SF_6 will then be as follows:

$$k(T, p_{SF_6}) = k^*_0 \cdot e^{-\frac{E}{RT} + \frac{E}{R \cdot 973}} \cdot \left(\frac{p_{SF_6}}{1\%}\right)^{0.72}$$

Inserting values for k^*_{700}, E and R, we end up with

$$\frac{k(T, p_{SF_6})}{k^*_0} = e^{0.03 \cdot (T - 973)}$$

Appendix 6

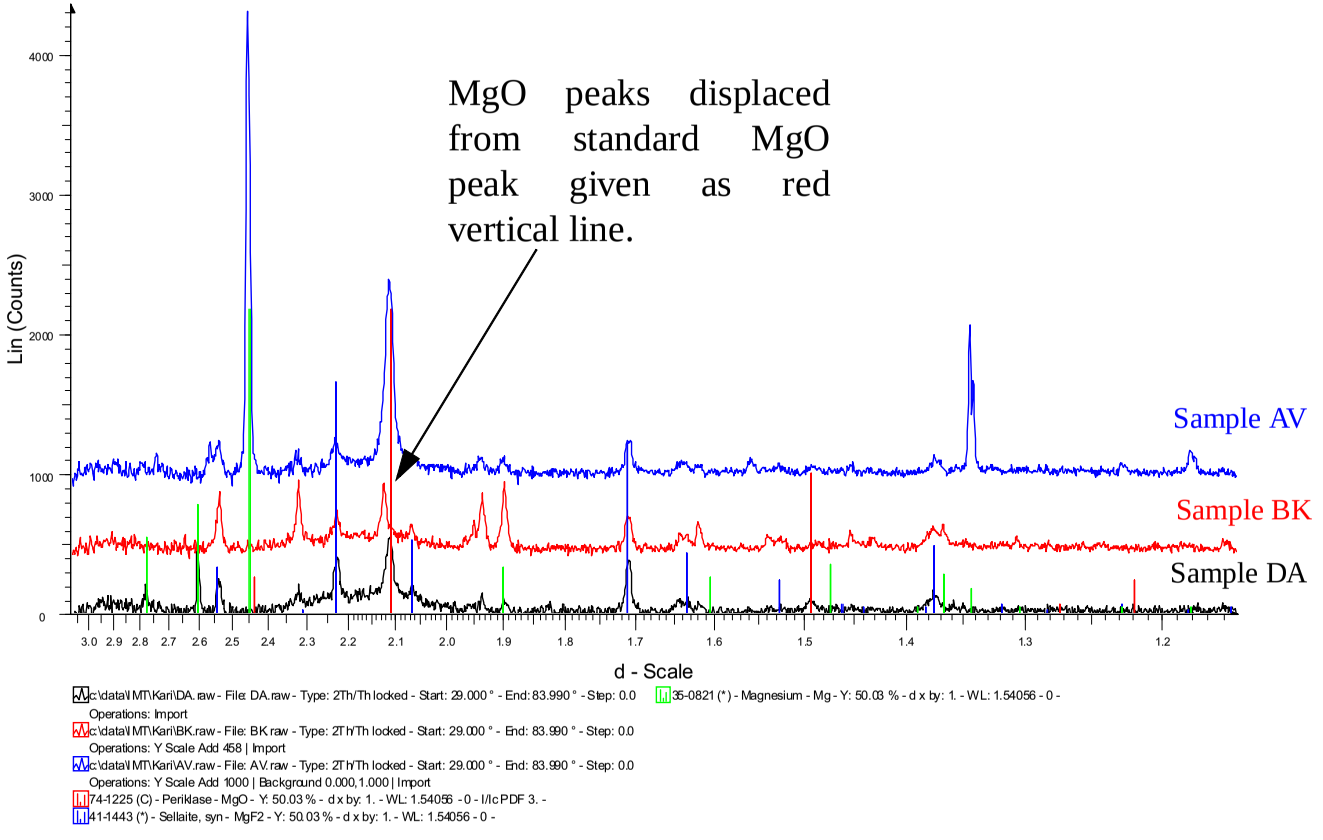

X-ray diffraction of samples DA, BK and AV in Chapter 3.

Appendix 7
Composition of surfaces measured with the microprobe with varying acceleration voltages.

Sample	3 kV			5 kV			10 kV			15 kV			20 kV		
	F	O	Mg	F	O	Mg	F	O	Mg	F	O	Mg	F	O	Mg
AQ	64	5	31	48	17	34	28	25	47	22	19	59	17	16	66
AU	11	43	47	11	44	45	12	41	47	13	35	52	13	30	58
BA	55	12	34	57	9	34	58	3	39	45	2	53	34	2	64
AV	23	33	44	24	34	42	25	34	41	25	33	42	23	31	46
BH	46	14	40	44	8	48	35	3	62	25	2	73	19	2	79
BF	47	17	36	42	21	37	53	12	36	57	7	36	52	6	42
BE	48	17	35	44	20	36	54	11	34	59	7	34	56	6	38
AR	58	9	33	54	12	33	33	22	45	24	18	58	19	16	65
BC	54	12	34	47	17	36	51	8	41	46	5	48	38	5	58
BI	59	8	33	58	6	36	57	2	41	50	1	48	41	1	58
AT	18	38	44	20	37	43	25	33	42	26	31	43	24	29	47
BG	44	19	37	50	15	35	60	5	35	50	3	46	40	3	57
BD	51	14	35	44	19	37	45	9	46	38	6	56	30	5	64
AS	52	13	35	41	22	37	34	26	41	30	22	48	26	19	55
BJ	54	12	34	56	10	34	60	4	36	54	3	43	45	2	53
BK	43	21	36	41	22	37	54	12	34	57	8	35	53	7	39
Æ	11	31	58	6	18	76	2	8	90	1	6	93	1	5	94
R	12	41	47	10	41	50	5	22	74	3	15	82	2	13	85
Ø	53	13	33	32	27	41	16	19	66	10	13	76	7	11	83
T	13	40	47	13	43	44	16	40	45	15	32	52	12	28	60
W	12	42	46	12	39	49	8	20	73	5	14	81	3	13	83

J	62	7	31	45	21	34	26	26	48	19	20	61	17	18	65
V	15	39	46	13	43	44	9	29	62	6	22	72	4	19	77
I	9	44	47	8	48	44	10	48	43	10	47	43	9	46	45
AD	13	41	47	12	43	44	9	26	64	6	20	74	4	17	78
AK	57	10	33	50	16	34	30	24	46	22	19	59	16	17	67
AH	28	32	41	29	34	38	29	33	38	27	27	46	23	24	53
AL	13	43	44	13	48	39	18	46	36	20	42	38	18	39	44
AC	12	40	48	11	44	45	13	43	44	12	35	53	13	31	57
AB	11	41	48	9	43	48	5	26	69	3	18	79	2	16	82
X	32	27	41	19	38	43	15	24	61	10	17	74	8	15	77
AE	14	39	47	11	44	45	9	37	54	6	29	65	6	27	68
AG	10	42	48	9	45	45	9	33	59	6	23	71	5	21	75
N	11	43	46	10	47	43	7	31	62	4	22	74	4	20	77
AJ	39	22	39	21	37	42	9	30	61	10	23	67	8	20	72
AA	13	39	48	11	44	45	9	31	60	6	22	73	4	19	76
Y	10	41	49	8	37	55	4	17	79	2	12	86	2	11	87
AP	28	29	43	20	37	43	16	40	44	14	34	52	13	30	57
AI	16	37	47	15	41	44	15	42	43	14	37	49	14	33	53
AM	10	42	48	12	44	44	17	40	43	14	34	52	12	30	57
AO	9	43	47	13	44	44	14	43	43	11	36	53	10	32	58
AN	41	20	39	43	19	38	34	21	44	24	17	59	20	15	65
Sample	3 kV			5 kV			10 kV			15 kV			20 kV		

Appendix 8

Samples from one series from the solubility experiments were split into two pieces, one piece sent to be analyzed with the Sintalyzer, the other part with GD-MS. The GD-MS results showed stability while the Sintalyzer results were more unstable.

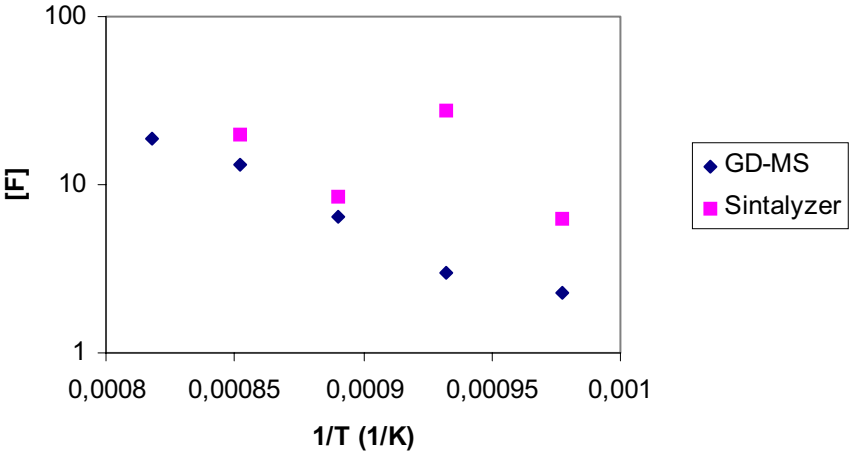

Appendix 8